Adriano Salgado Ribeiro

Production of Decyl Acetate by Enzymatic Catalysis

Dissertation presented for the degree of

Ph.D. in Chemical and Biological Engineering

by

University of Porto

Supervisors:

Maria Eugénia Rebello de Almeida Macedo

José Miguel Loureiro

Universidade do Porto
FEUP Faculdade de Engenharia

LABORATÓRIO ASSOCIADO
LSRE Laboratory of Separation and Reaction Engineering
Laboratório de catálise e materiais lcm

Porto, July 2009

Ciência.Inovação 2010
Programa Operacional Ciência e Inovação 2010
MINISTÉRIO DA CIÊNCIA, TECNOLOGIA E ENSINO SUPERIOR
FCT Fundação para a Ciência e a Tecnologia
MINISTÉRIO DA CIÊNCIA, TECNOLOGIA E ENSINO SUPERIOR

Financial support for this work was in part provided by national research grant FCT/POCTI/EQU/56732/2004, by LSRE financing by FEDER/POCI/2010 and Ph.D. scholarship by FCT (SFRH/BD/13084/2003).









O que é bonito neste mundo, e anima,
É ver que na vindima
De cada sonho
Fica a cepa a sonhar outra aventura...
E que a doçura
Que se não prova
Se transfigura
Numa doçura
Muito mais pura
E muito mais nova...

Miguel Torga in Diário VIII

AGRADECIMENTOS/ACKNOWLEDGEMENTS

Aqui é o espaço para agradecer a todos os que contribuíram, directa ou indirectamente, para este trabalho. Tradicionalmente esta é a página mais lida duma dissertação e com as maiores expectativas. Espero conseguir encontrar as palavras certas para todos e espero que se encontrem aqui todos os que se vierem procurar! Se por lapso omitir alguém, espero que compreendam; afinal, após a escrita de uma tese a sanidade mental do candidato já terá visto melhores dias.

Aos meus orientadores por me terem dado todo o apoio do mundo, espaço para crescer e liberdade para o fazer à minha maneira. À Olga por tudo! À Manela que, para além do apoio, tão bem tem continuado esta área de trabalho. À Professora Susana Barreiros, por tão bem me ter recebido em sua "casa" e ao Pedro Vidinha pela colaboração e por ser o Pedro Vidinha!

Aos meus pais por me terem ensinado que só não sou capaz de fazer aquilo que não tentar a sério, aos meus avós por me terem mostrado o que é ser genuinamente bom, ao meu irmão por ser o meu melhor Amigo desde o minuto zero e à Teresa pelos novos pontos de vista que trouxe com ela. À minha segunda família, Lamas, da qual desde cedo me senti parte.

Aos meus CAPPPs, Isabel, João, Eduardo, Maria João, Ricardo e Nuno. Vocês são os meus amigos mais antigos e a prova de que o que é bom na vida permanece.

Ao Eduardo e ao Davide. A Licenciatura não teria tido metade da piada! ALT Rules!

À Ana Alexandra, ao Afonso, à Filipa, à Manuela, ao Tiago, à Inês, ao Ratola, à Olga (mais uma vez, e bem merece!), à Roxane, à Isabel, à Mónica e ao Miguel. Vocês foram a minha tribo durante o tempo todo que passei na FEUP e continuam a sê-lo.

À Luísa, ao Pedro, ao Óscar, à Mafalda, à Maria e à Sílvia com quem partilhei o material de laboratório, alguns cafés, crises, preocupações e alegrias. Ao Carlos pelo pragmatismo contagiante.

À Alejandro, mi segundo Hermano, aunque guevon, como todos los hermanos!

Ao Vale, ao Tiago e ao Portilho, pela amizade, por me deixarem ir para casa trabalhar na dissertação, e por me permitirem desligar do trabalho mesmo no local de trabalho.

To Catarina and Din, who (together with Filipa) greatly contributed for me having written the last 30 pages of this dissertation on schedule. Life has brought me to the most amazing people along the way. You two are the latest ones.

Finalmente, a ti, Susana, que vieste dar sentido a tudo isto. A tudo.

ABSTRACT

The aim of this work was to study the production of long chain esters by enzymaticaly catalyzed transesterification reactions in organic media, a step towards the development of more sustainable alternatives to the traditional chemical processes for ester production.

Decyl acetate, a long-chain ester used in the perfumery and food industries, was produced by the transesterification reaction between vinyl acetate and decanol catalyzed by an immobilized lipase.

A preliminary enzyme screening was made by performing the transesterification reaction in a batch reactor with 40 mL reaction volume, at 30 ºC, with hexane as the solvent, using several commercial enzymes from two major biocatalyst suppliers. Novozym 435 was the most active catalyst for the transesterification of vinyl acetate and decanol and was chosen to perform all subsequent work. The enzyme content was determined for different particle sizes, showing that smaller particles present higher enzyme content ($g_{Enzyme}/g_{Particle}$). Furthermore, the specific enzyme loadings are consistent with an egg-shell intraparticle enzyme distribution, with an enzyme outer layer of c.a. 80 μm.

Diffusion limitations were shown to exist. The egg-shell intraparticle distribution of the enzyme seems to influence the results obtained with different particle sizes, but evidence of internal diffusion limitations is particularly visible as the enzyme distribution appears to become homogeneous (by sufficiently decreasing the particle size) or the particles are crushed.

The intrinsic kinetic parameters of the reaction were calculated, according to a Ping-pong bi-bi kinetic model with competitive inhibition by the alcohol. The determination was performed in the absence of diffusion limitations, which was accomplished by crushing the catalyst particles. The rate equation typically used for initial reaction rates was found to describe the complete reaction as long as an activity based rate equation was used, as the activity coefficients of the reactants vary significantly with the composition of the reaction mixture.

A model for a batch reactor performing transesterification reactions was developed. The model included the effect of internal and external mass transfer resistances, the heterogeneous intraparticle distribution of the enzyme and the thermodynamic non-ideality of the reaction mixture, by using an activity coefficient based kinetic equation. The model successfully predicted several sets of experimental data obtained with catalyst particles of different

sizes and different initial concentrations of each reagent. All parameters used in the simulations were either estimated or experimentally measured.

A steady state model based on the same assumptions of the previous one was developed and used to analyze the influence of the model parameters and of different enzyme distributions. It was shown that for the transesterification of vinyl acetate and decanol, the observable reaction rate is favored by distributions that place the enzyme closer to the surface.

A model for a packed bed reactor performing transesterification reactions was developed. The model includes the effect of internal and external mass transfer resistances, the heterogeneous intraparticle distribution of the enzyme and the thermodynamic non-ideality of the reaction mixture, by using an activity coefficient based kinetic equation. The model does not account for axial and radial dispersion, and pressure drop along the reactor and the plug flow mechanism is assumed. Several experiments were performed in a packed reactor which was operated for 26 consecutive hours without any measurable loss in enzyme activity. The steady state conversion was measured for different flow rates and was in good agreement with the model's predictions. Contrary to the case of the batch reactor, where agitation is simple to induce, external diffusion limitations were present in the packed bed reactor due to the low flow rates used.

Additional experiments were performed in a batch reactor with an equimolar mixture of vinyl acetate and decanol, without solvent. There were no evidences of reduction in enzyme activity in the absence of hexane but a temperature increase of 10ºC was obtained in the initial stage of the reaction, caused by its exothermic nature. Internal diffusion limitations were shown to exist in the solvent free system as well.

In terms or reactor modeling, the applicability of the developed model was limited by the temperature increase verified due to the exothermic nature of the reaction. The model was nevertheless able to describe the reaction course once the temperature of the reaction medium returned to values close to 30 ºC showing that the activity based kinetic equation used is applicable in the absence of hexane. Since the activity coefficients of vinyl acetate and decanol are lower than the ones obtained in hexane, a concentration based kinetic equation with kinetic parameters determined in hexane would fail to describe the solvent free system, further confirming the potential of this approach.

RESUMO

O objectivo deste trabalho foi o estudo da produção de ésteres de cadeia longa por transesterificação, catalisada por enzimas, em meio orgânico, um passo na direcção do desenvolvimento de processos mais sustentáveis, alternativos aos processos químicos tradicionais.

O acetato de decilo, um éster de cadeia longa usado nas indústrias alimentar e dos perfumes, foi produzido através da reacção de transesterificação entre acetato de vinilo e decanol, catalisada por uma lipase imobilizada em suporte sólido.

Foi efectuada uma triagem preliminar, efectuando a reacção de transesterificação em estudo num reactor fechado, com um volume reaccional de 40 mL, à temperatura de 30 ºC, usando hexano como solvente. Foram testados vários produtos disponibilizados por dois dos maiores fornecedores mundiais de enzimas sendo a Novozym 435 a enzima que permitiu obter maiores velocidades reaccionais. Assim, a Novozym 435 foi usada em todas as experiências no decurso deste trabalho. O conteúdo enzimático foi determinado para partículas de diferentes tamanhos, revelando que o conteúdo enzimático ($g_{Enzima}/g_{Partícula}$) aumenta com a diminuição do tamanho de partícula. Os valores obtidos para o conteúdo enzimático são consistentes com uma distribuição intraparticular do tipo casca-de-ovo, com uma espessura de cerca de 80 μm.

Foram detectadas limitações difusionais internas. A distribuição intraparticular do tipo casca-de-ovo, parece influenciar os resultados obtidos com partículas de diferentes tamanhos, mas as limitações difusionais tornam-se evidentes quando o tamanho de partícula se aproxima do tamanho da casca ou quando as partículas são esmagadas.

Foram determinados os parâmetros cinéticos intrínsecos, de acordo com o modelo Ping-pong bi-bi, com inibição competitiva por parte do álcool. A determinação foi efectuada na ausência de limitações difusionais, esmagando previamente as partículas de catalisador. A equação de velocidade de reacção tipicamente aplicada para descrever velocidades iniciais foi capaz de descrever a reacção até ao final, desde que a equação usada seja baseada nas actividades dos substratos e não nas suas concentrações, uma vez que os coeficientes de actividade das espécies em solução variam significativamente com a composição do meio.

Foi desenvolvido um modelo para reacções de transesterificação catalisadas por enzimas em reactor fechado. O modelo inclui o efeito de resistências difusionais internas e externas, a distribuição heterogénea da enzima no suporte e a não idealidade termodinâmica do meio

reaccional. O modelo foi capaz de prever os resultados experimentais obtidos com partículas de catalisador de diferentes tamanhos e diferentes concentrações iniciais dos substratos. Todos os parâmetros do modelo foram estimados ou determinados nas experiências anteriores.

Foi desenvolvido um modelo de estado estacionário, baseado nos mesmos pressupostos, que foi usado para analisar a influência dos parâmetros do modelo e de diferentes distribuições intraparticulares de enzima. Distribuições que colocam a enzima mais perto da superfície favorecem a velocidade observável da reacção em estudo.

Foi desenvolvido um modelo para reacções de transesterificação catalisadas por enzimas em reactor de leito fixo. O modelo inclui a influência de resistências difusionais internas e externas, a distribuição heterogénea da enzima no suporte e a não idealidade termodinâmica do meio reaccional. O modelo não contabiliza os fenómenos de dispersão axial e radial, a queda de pressão ao longo do reactor e foi assumido fluxo pistão. Foram efectuadas várias experiências em reactor de leito fixo, que operou durante 26h consecutivas sem perda de actividade mensurável do catalisador. Foi determinada a conversão de estado estacionário para diferentes caudais de alimentação e os resultados experimentais obtidos encontram-se de acordo com as previsões do modelo. Contrariamente ao reactor fechado, verificou-se a existência de resistências difusionais externas, devido aos caudais reduzidos que foram usados nas experiências.

Foram efectuadas experiências adicionais em reactor fechado, com uma mistura equimolar de acetato de vinilo e decanol, sem solvente. Não foram encontradas evidências de redução de actividade da enzima na ausência de hexano mas verificou-se um aumento de temperatura do meio reaccional de 10 °C no início da reacção, devido à sua natureza exotérmica. Tal como em hexano, verificaram-se evidências de resistências difusionais internas no sistema sem solvente.

Em termos de modelação, a aplicação do modelo desenvolvido ao sistema sem solvente encontra-se limitada pela variação de temperatura verificada ao longo da reacção. No entanto, o modelo foi capaz de descrever o decurso da reacção após a temperatura se aproximar novamente de valores próximos de 30°C, indicando que a equação de velocidade de reacção baseada em actividades pode, neste caso, ser aplicável na ausência do solvente. Uma vez que os coeficientes de actividade dos substratos são inferiores aos obtidos em hexano, uma equação baseada em concentrações, com os parâmetros cinéticos determinados em hexano não seria aplicável ao sistema sem solvente, ilustrando o potencial desta abordagem.

RESUME

L'objectif de ce travail était celui d'étudier la production d'esters de chaîne longue par transestérification, catalysée par enzymes, en milieu organique, une étape dans la direction du développement de procédés plus soutenables, alternatifs aux procédés chimiques traditionnels.

L'acétate de décile, un ester de chaîne longue utilisé dans les industries alimentaire et des parfums, était produit par la réaction de transestérification entre l'acétate de vinyle et le décanol, catalysée par une lipase immobilisée en support solide.

Un triage préliminaire était effectué, conduisant la réaction de transestérification en étude dans un réacteur fermé, avec un volume réactionnel de 40 mL, à la température de 30 ºC, en utilisant l'hexane comme solvant. Plusieurs produits, mis à la disposition par deux des plus grands fournisseurs mondiales d'enzymes, étaient testés. La Novozym 435 était la plus active, raison pour laquelle elle était utilisée dans toutes les essais décrits dans ce travail. Le contenu enzymatique était déterminé pour des particules de différentes tailles, montrant que le contenu enzymatique ($g_{enzyme}/g_{particule}$) augmente avec la diminution de la taille des particules. Les valeurs obtenues du contenu enzymatique sont consistants avec une distribution intraparticulaire du type coquille d'œuf, avec une épaisseur de 80 μm environ.

Des limitations diffusionelles internes étaient détectées. La distribution intraparticulaire du type coquille d'œuf apparemment influence les résultats obtenus avec des particules de différentes tailles, mais les limitations diffusionelles deviennent plus importantes lorsque la taille approche celle de la coquille ou quand les particules sont écrasées.

Les paramètres cinétiques intrinsèques étaient déterminés suivant le modèle Ping-pong bi-bi avec inhibition compétitive de la part de l'alcool. La détermination était effectuée en l'absence de limitations diffusionelles, écrasant préalablement les particules de catalyseur. L'équation de vitesse de réaction typiquement appliquée pour décrire les vitesses initiales était capable de décrire la réaction jusqu'au bout, dès que l'équation utilisée soit écrite en fonction des activités des substrats mais non en fonction de leurs concentrations, une fois que les coefficients d'activité des espèces en solution varient significativement avec la composition du milieu.

Un modèle pour les réactions de transestérification catalysés par enzymes en réacteur fermé était développé. Le modèle inclut l'effet de résistances internes et externes à la diffusion, la distribution hétérogène d'enzyme sur le support et la non idéalité thermodynamique du milieu réactionnel. Le modèle était capable de prévoir les résultats expérimentales obtenus

avec des particules de catalyseur de différentes tailles et différentes concentrations initiales de substrats. Tous les paramètres du modèle étaient estimés ou déterminés en expériences précédentes.

Un modèle d'état stationnaire basé sur les mêmes principes était développé; il était utilisé pour analyser l'influence des paramètres du modèle et de différentes distributions intraparticulaires d'enzyme. Les distributions qui placent l'enzyme plus proche de la surface favorisent la vitesse observable de la réaction en étude.

Un modèle d'état stationnaire pour des réactions de transestérification catalysées par enzymes en réacteur de lit fixe était aussi développé. Le modèle inclut l'influence de résistances internes et externes à la diffusion, la distribution hétérogène d'enzyme sur le support et la non idéalité thermodynamique du milieu réactionnel. Le modèle ne tient pas compte des phénomènes de dispersion axiale et radiale et de la chute de pression au long du réacteur et considère l'écoulement piston de la phase mobile. Plusieurs expériences étaient effectuées en réacteur de lit fixe, qui a opéré pendant 26h consécutives sans perte de l'activité mesurable du catalyseur. La conversion d'état stationnaire pour différents débits d'alimentation était déterminée et les résultats expérimentales obtenus sont d'accord avec les prévisions du modèle. Contrairement au réacteur fermé, on observe l'existence de résistances externes à la diffusion, à cause des débits réduits utilisés dans les expériences.

Des expériences additionnelles en réacteur fermé étaient effectuées, avec un mélange equimolaire d'acétate de vinyle et décanol, sans solvant. Aucunes évidences de réduction d'activité de l'enzyme en l'absence d'hexane n'étaient observées, mais on a vérifié une élévation de la température du milieu réactionnel de 10 ºC au début de la réaction, du au fait qu'elle est exothermique. Aussi bien qu'en hexane, on a observé des évidences de la présence de résistances internes à la diffusion dans ce système sans solvant.

En termes de modélisation, l'application du modèle développé au système sans solvant est limitée par la variation de température observé au cours de la réaction. Néanmoins, le modèle était capable de décrire le cours de la réaction après que la température retourne à des valeurs proches de 30ºC, montrant que l'équation de vitesse de réaction basée en activités peut être, dans ce cas, appliquée en l'absence de solvant. Une fois que les coefficients d'activité des substrats sont inférieurs aux obtenus en hexane, une équation basée en concentrations, avec les paramètres cinétiques déterminées en hexane ne serait pas applicable au système sans solvant, montrant le potentiel de cette approche.

TABLE OF CONTENTS

1. INTRODUCTION 1

1.1 Esters 1

1.2 Decyl acetate 2

1.3 Ester production 2

1.4 Enzyme catalysis and ester production 5

1.5 Enzyme immobilization and mass transfer 7

1.6 Enzyme reactor modeling 9

1.7 Thermodynamic activity based kinetic equations 10

1.8 Purpose and outline of the work 11

1.9 Bibliography 12

2. KINETIC MODELING OF THE ENZYME CATALYZED PRODUCTION OF DECYL ACETATE 17

2.1 Reactive system 17

2.2 Experimental method 18

2.2.1 Enzymes and chemicals 18

2.2.2 Experiments in batch reactor 18

2.2.3 Analytical methods 19

2.2.4 Determination of the protein content 19

2.3 Results and discussion 19

2.3.1 Enzyme screening 19

2.3.2 External mass transfer studies 22

2.3.3 Internal mass transfer studies 24

2.3.4 Kinetic modeling and kinetic parameter determination 31

2.4 Conclusions 47

2.5 Nomenclature 48

2.6 Bibliography 50

3. PRODUCTION OF DECYL ACETATE IN A BATCH REACTOR: MODELING AND SIMULATION 53

3.1 Experimental methods 53

3.1.1 Enzymes and chemicals 53

3.1.2 General method for experiments in batch reactor 53

3.1.3 Analytical methods 54

3.2 Batch reactor model development 54

3.2.1 Kinetic mechanism 54

3.2.2 Intraparticle material balance 55

3.2.3 Bulk phase mass balance 56

3.2.4 Complete model 57

3.2.5 Intraparticle distribution and definition of E(r) 61

3.3 Effectiveness factor and steady state model development 64

3.3.1 Steady state model development 64

3.3.2 Effectiveness factor calculation 65

3.4 Model numerical solution 66

3.5 Results and discussion 66

3.5.1 parameters used for the simulation of the experimental data - Physical characterization of the catalyst particles and diffusion coefficients 66

3.5.2 Model validation 68

3.5.3 Effect of the parameters of the model 74

3.6 Conclusions 86

3.7 Nomenclature 88

3.8 Bibliography 90

4. PRODUCTION OF DECYL ACETATE IN A PACKED BED REACTOR: MODELING AND SIMULATION 92

4.1 Experimental methods 92
4.1.1 Enzymes and chemicals 92
4.1.2 Experimental setup 92
4.1.3 Analytical methods 93

4.2 Dimensional analysis of the reactor 93
4.2.1 Estimation of preassure drop 95
4.2.2 Influence of axial dispersion 96
4.2.3 radial concentration profiles 97
4.2.4 Influence of external diffusion 98

4.3 Packed bed reactor model development 99
4.3.1 Intraparticle material balance 99
4.3.2 Bulk phase material balance 100
4.3.3 Complete model 101

4.4 Results and Discussion 103

4.5 Conclusions 115

4.6 Nomenclature 117

4.7 Bibliography 119

5. CONCLUSIONS AND FUTURE WORK 122

APPENDIXES 126

A. Modified Lowry method for the determination of the content of adsorbed proteins 126

B. Modified UNIFAC Model of Dortmund 128

C. Calculation of the diffusion coefficients by the Wilke-Chang method 133

FIGURE CAPTIONS

Figure 1.1. Batch production process for butyl acetate (Aslam et al. 2001) 3

Figure 1.2. Continuous production process for methyl acetate (Aslam et al. 2001). 4

Figure 1.3. Representation of the action of a catalyst in the activation energy of the reaction (Levenspiel 1999). 5

Figure 1.4. Growth of biocatalytic processes operated at industrial scale (Straathof et al. 2002). 6

Figure 1.5. Illustration of the path of the reactants and scale in heterogeneous catalysis (Schmidt 1998). 8

Figure 2.1. Initial reaction rates obtained with several commercial enzymes for the reaction of vinyl acetate with decanol (0.1M: 0.1M) in hexane at 30ºC 21

Figure 2.2. Effect of particle diameter on the reactants conversion as a function of time. Reaction conditions: [A]=[B]=0.1 M, W_S=0.56 mg/mL and T=30 ºC for all assays. 25

Figure 2.3. Effect of padding the magnetic bar used for stirring, when using 240μm particles. Reaction conditions: [A]=[B]=0.1 M; T=30 ºC. 25

Figure 2.4. Effect of particle diameter on the reactants conversion as a function of time. [A]=[B]=0.1 M, W_{Enzyme}=0.069 mg_{Enzyme}/mL and T=30 ºC for all assays. 27

Figure 2.5. Effect of particle diameter on the reactants conversion as a function of time. [A]=[B]=0.1 M, W_{Enzyme}=0.069 mg_{Enzyme}/mL and T=30 ºC for all assays. 28

Figure 2.6. Ping-pong bi-bi kinetic mechanism 32

Figure 2.7. Effect of the initial concentrations of vinyl acetate (red triangles) and decanol (green circles). T=30 ºC and crushed Novozym 435 particles used for all essays. 37

Figure 2.8. Effect of the initial concentration of decyl acetate. T=30 ºC, C_A=C_B=0.1 M, W_S=0.4 mg/mL and crushed Novozym 435 particles used for all essays. 37

Figure 2.9. Experimental *vs.* simulated results for different initial concentrations of vinyl acetate and decanol. T=30 ºC and crushed Novozym 435 particles used for all essays.....39

Figure 2.10. Experimental *vs.* Simulated results for equimolar initial concentrations of vinyl acetate and decanol. T=30 ºC and crushed particles used for all essays. 40

Figure 2.11. Activity coefficients of all species in solution throughout the reaction. **(a)** [A]=[B]=0.1 M, W_S=0.5 mg/mL **(b)** [A]= 1 M, [B]=0.1 M, W_S=0.4 mg/mL. 42

Figure 2.12. Initial and final activity coefficient (bars) and percentage variation (■) throughout the reaction for several sets of initial conditions **(a)** vinyl acetate **(b)** decanol **(c)** decyl acetate **(d)** hexane. 45

Figure 2.13. Experimental *vs.* simulated results using the activity based kinetic equation for different initial concentrations of vinyl acetate and decanol. T=30 ºC and crushed particles used for all essays. 46

Figure 2.14. Experimental vs. simulated results using the activity based kinetic equation for equimolar initial concentrations of vinyl acetate and decanol. T=30 ºC and crushed particles used for all essays. 46

Figure 3.1. Visible light image (left) of the Novozym 435 bead embedded in paraffin and cross-sectioned. The right panel shows the enzyme distribution throughout the center section of the Novozym 435 bead (Mei et al. 2003). 61

Figure 3.2. Experimental data (▲, ●, ▼) and model predictions (─, ---, ···) for different particle sizes. Reaction conditions: [A]=[B]=0.1 M, W_S=0.56 mg/mL and T=30 ºC for all assays. 69

Figure 3.3. Experimental data (▲, ○, ▼, □) and model predictions (─, ---, ···, -·-) for different particle sizes. [A]=[B]=0.1 M, W_{Enzyme}=0.069 mg_{Enzyme}/mL and T=30 ºC for all assays. 69

Figure 3.4. Model predictions for different particle sizes, [A]=[B]=0.1M, W_{Enzyme}=0.069 mg_{Enzyme}/mL and T=30 ºC, assuming: (a) Homogeneous enzyme distribution (b) Egg-shell distribution with shell thickness independent of the particle size (c) Shell thickness dependent of particle size, considering 240μm particles present a homogeneous distribution. 71

Figure 3.5. Experimental results (symbols) and model predictions (lines) for different initial concentrations of vinyl acetate. d_P=460 μm, W_S=0.76 mg/mL and T=30 ºC..... 72

Figure 3.6. Experimental results (symbols) and model predictions (lines) for different initial concentrations of vinyl acetate. d_P=360 μm, W_S=0.64 mg/mL and T=30 ºC..... 73

Figure 3.7. Experimental results (symbols) and model predictions (lines) for different initial concentrations of decanol. d_P=240 μm, W_S=0.64 mg/mL and T=30 ºC..... 73

Figure 3.8. Experimental results (symbols) and model predictions (lines) for different initial concentrations of decanol. d_P=240 μm, W_S=0.64 mg/mL and T=30 ºC..... 74

Figure 3.9. Effect of the kinetic parameters and Thiele modulus on the effectiveness factor (a) K_{I0}/K_{M0}=0.156 (b) K_{I0}/K_{M0}=1.56 (c) K_{I0}/K_{M0}=15.6..... 76

Figure 3.10. Simulations obtained with different values of ϕ_1 and ϕ_2. —ϕ_1=1; ··· ϕ_1=10; --- ϕ_1=100. ■ K_{I0}/K_{MA0}=0.156; ○ K_{I0}/K_{MA0}=1.56; ▲ K_{I0}/K_{MA0}=15.6. 79

Figure 3.11. Effectiveness factor vs. Thiele modulus for different intraparticle enzyme distributions (K_{I0}/K_{MA0}=1.56, $K_{MA0}=K_{MB0}$=1). 81

Figure 3.12. Intraparticle dimensionless concentration profiles for different enzyme distributions (ϕ=5, K_{I0}/K_{MA0}=1.56, $K_{MA0}=K_{MB0}$=1)..... 84

Figure 3.13. Effect of Bim on effectiveness factor (K_{M0}=1) (a) K_{I0}/K_{M0}=0.156 (b) K_{I0}/K_{M0}=1.56. 85

Figure 4.1. Reynolds number as a function of the flow rate, for different bulk porosities. d_p=460μm, T=30 ºC. 94

Figure 4.2. Pressure drop across the packed bed reactor as a function of the flow rate, for different bulk porosities. d_p=460 μm, d_T=6.6 mm, L=55 mm, T=30ºC. 95

Figure 4.3. Biot number as a function of the flow rate. d_p=460 μm, T=30 ºC. 99

Figure 4.4. Effect of flow rate on the steady state conversion and space time. Feed composition: [A]=[B]=0.1 M; Reactor: L=55 mm, d=6.6 mm, ε_B=0.56; catalyst: d_p=460 μm. T=30 ºC for all essays. 103

Figure 4.5. Steady state conversion as function of time. Feed composition: [A]=[B]=0.08 M; Reactor: L=55 mm, d=6.6 mm, ε_B=0.56; catalyst: d_p=460 μm. T=30 ºC..... 105

Figure 4.6. Volumetric productivity and steady state conversion as a function of the flow rate. Feed composition: [A]=[B]=0.1 M; Reactor: L=55 mm, d=6.6 mm, ε_B=0.56; catalyst: d_p=460 μm. T=30 ºC for all essays. 106

Figure 4.7. Initial and final activity coefficient (bars) and percentage variation (■) throughout the reaction for several sets of initial conditions **(a)** vinyl acetate **(b)** decanol **(c)** decyl acetate. 109

Figure 4.8. Conversion and temperature as a function of time. [A]=[B]=3.4 M, W_{Enzyme}=0.15 mg_{Enzyme}/mL and d_p=463 μm for all essays. Simulation 1: simulation with internal diffusion limitations; Simulation 2: simulation without internal diffusion limitations; Simulation 3: partial simulation starting at 69.5% conversion. 112

Figure 4.9. Effect of particle diameter on the reactants conversion as a function of time. Reaction conditions: [A]=[B]=3.4 M, W_{Enzyme}=0.15 mg_{Enzyme}/mL and $T_{initial}$=30 ºC for all assays. 114

Figure 4.10. Effect of particle diameter on the initial reaction rate. Reaction conditions: [A]=[B]=3.4 M, W_{Enzyme}=0.15 mg_{Enzyme}/mL and $T_{initial}$=30 ºC for all assays..... 115

TABLE CAPTIONS

Table 2.1. Specific enzyme content for the several available catalysts. 20

Table 2.2. Specific enzyme content for Novozym 435 particles of different sizes. 26

Table 2.3. Fraction of particle that contains enzyme for each particle size, assuming a shell of 77μm. 30

Table 2.4. Parameters of the Ping-pong bi-bi rate equation..... 32

Table 2.5. Kinetic constants for the Novozym 435 catalysed transesterification reaction of vinyl acetate with decanol in hexane at 30ºC. 38

Table 2.6. Activity based kinetic constants for the Novozym 435 catalyzed transesterification reaction of vinyl acetate with decanol in hexane at 30 ºC. 44

Table 3.1. Dimensionless parameters and variables of the model. 58

Table 3.2. Parameters used in the simulations. 67

Table 3.3. Thickness of the enzyme shell for Novozym 435 particles of different sizes, assuming that the thickness of the shell is dependent of the particle size and the 240 μm particles are homogeneous. 71

Table 3.4. Effectiveness factor for different K_{M0} while keeping all other parameters constant 77

Table 4.1. Dimensionless numbers present in the Ranz-Marshall correlation..... 98

Table 4.2. Dimensionless parameters and variables of the packed bed reactor model. 102

Table 4.3. Parameters used in the simulations 104

Table 4.4. Diffusion coefficients of the reactants in solvent free operation and in decyl acetate 110

Table 4.5. Specific enzyme content for Novozym 435 particles of different sizes. 111

1. INTRODUCTION

1.1 ESTERS

Organic esters are generally defined as the product of the condensation between an acid and an alcohol or phenol (Sakamuri 2001):

$$R_1COOH + R_2OH \leftrightarrow R_1COOR_2 + H_2O \quad (1.1)$$

where R_1 and R_2 represent hydrocarbon chains that can be identical or not.

Esters can be found in nature, in large amounts, mostly in oils, fats and waxes and find widespread application in a variety of fields. In today's technologies, esters find innumerous application as solvents, for paints and adhesives, as processing aids for rubbers and plastics, as synthetic lubricants, surfactants, pharmaceuticals or as monomers for the production of several polymers. Esters are also used extensively in the flavors and fragrances industries (Fahlbusch et al. 2005), where they are included in the composition of perfumes, flavors, cosmetics, soaps and air fresheners. Aliphatic esters are present in nearly all fruits and many

flowers and contribute to their characteristic scent, being therefore useful in many flavor and fragrance formulations. In perfumery, as in nature, acetates are more prevalent due to their stability. Acetates of alcohols with up to 6 carbon atoms are often employed for fruity notes whereas longer chained ones (C_8, C_{10} and C_{12}) are used for blossom fragrances.

1.2 DECYL ACETATE

Decyl acetate is a long-chain ester that has a floral, orange-rose odor and a characteristic flavor. At high dilution it has a sweet flavor with a pineapple-like undertone (Burdock, 2004). These characteristics clearly define the two main fields where this high added value product finds applications: in the food and in the fragrance/cosmetic industries. In the perfumery industry, Decyl acetate is used in the creation and/or manufacturing of fragrance concentrates of all types and, in addition to its floral, orange-rose odor, its odor is also described as "floral clean waxy fresh laundered clothes" (TheGoodScentsCompany 2008). As decyl acetate is reported to have been found in orange, lemon, melon, apple, citrus peel oils, orange juice, strawberry fruit, blue cheese, cognac, plums and cardamom (Burdock 2004), it is classified as a nature-identical substance (and not as artificial) by the International Organization of the Flavor Industry (IOFI), i.e., a naturally occurring substance that is produced by synthetic means (InternationalOrganizationOfTheFlavorIndustry 2008). It is also recognized and registered by the Joint Expert Committee on Food Additives (JECFA) under nr. 132, the American Food and Drug Administration (FDA) under 21 CFR 172.515, the Council of Europe (CoE) under nr. 199 and the Flavor and Extract Manufacturers Association (FEMA) under nr. 2367 (Burdock 2004). In the food industry there are several examples of decyl acetate usage as a flavoring agent: alcoholic and non-alcoholic beverages, gelatins, puddings, baked goods, hard and soft candy, chewing gum and frozen dairy (Burdock 2004).

1.3 ESTER PRODUCTION

Although esters are present in nature, synthetic esters are more commonly employed in commercial applications, in order to fulfill the market demands. Esters are most commonly produced by conducting the correspondent esterification reaction – Equation (1.1) – in a batch reactor, at temperatures of around 100°C, using strong mineral acids, such as sulphuric

or hydrochloric acids, as catalysts, but cation-exchange resins might also be employed. Since the esterification is an equilibrium reaction, distillation is usually employed to push the reaction towards completion, by removing the water or the ester from the reaction system (Aslam et al. 2001).

Alternatively, the esterification can be performed in a continuous reactive distillation process, in which the reaction is conducted directly in a distillation column (Duarte and Loureiro 2004).

Figure 1.1 and Figure 1.2 illustrate a possible layout of the batch and the continuous processes, respectively.

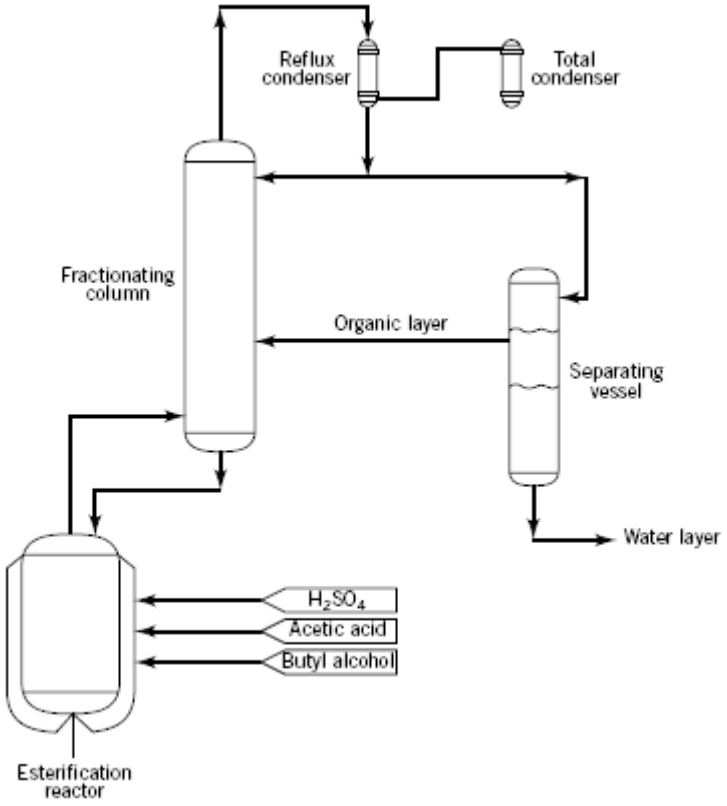


Figure 1.1. Batch production process for butyl acetate (Aslam et al. 2001)

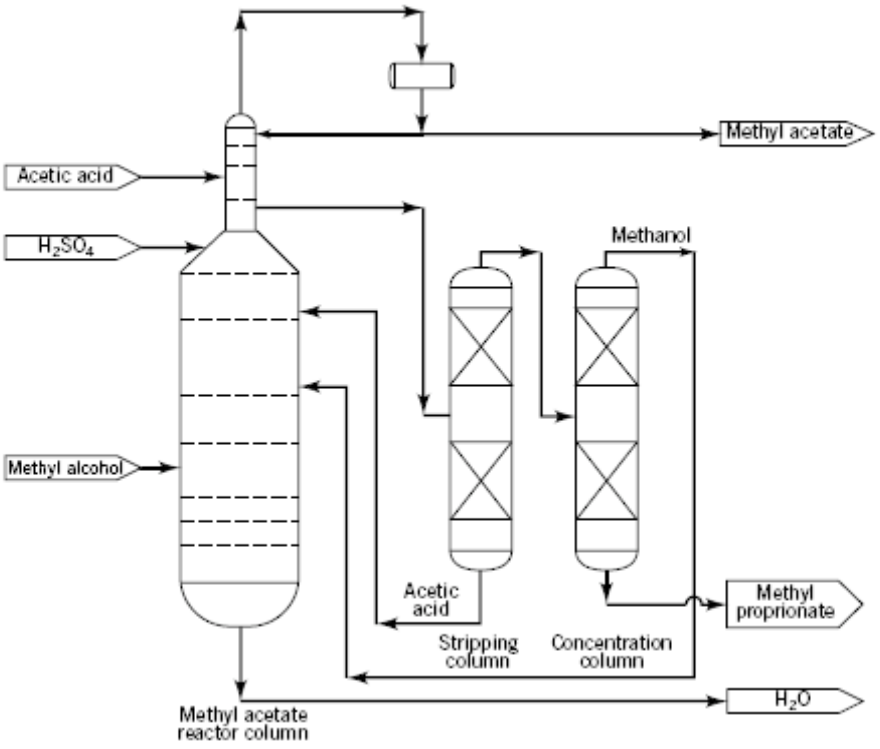


Figure 1.2. Continuous production process for methyl acetate (Aslam et al. 2001).

A transesterification reaction can also be employed for the production of esters. In this case an ester reacts with an alcohol, an acid or another ester and there is an exchange of the alkoxy group(s):

$$R_1COOR_2 + R_3OH \leftrightarrow R_1COOR_3 + R_2OH \quad (1.2)$$

$$R_1COOR_2 + R_3COOH \leftrightarrow R_1COOH + R_3COOR_2 \quad (1.3)$$

$$R_1COOR_2 + R_3COOR_4 \leftrightarrow R_1COOR_3 + R_3COOR_2 \quad (1.4)$$

Of the three possibilities, alcoholysis is most commonly applied (Aslam et al. 2001). In this case, besides the acid catalysts, with process conditions similar to the ones employed to perform the esterification reaction, alkaline catalysts (alkali metal alkoxides) may also be

used to perform the reaction at room temperature. A process layout similar to the one used for esterification can also be applied for alcoholysis.

1.4 ENZYME CATALYSIS AND ESTER PRODUCTION

Enzymes are biological catalysts. They are present in nature in many different forms of life where they are responsible for catalyzing reactions which are essential to life itself, such as the transformation of Carbon dioxide into Carbonic acid, in human red blood cells, catalyzed by Carbonic anhydrase, that enables the removal of CO_2 from the tissues and its transportation to the lungs. As any catalyst, enzymes act by lowering the activation energy of specific reactions, thus increasing the reaction rate, as illustrated in the well known Figure 1.4. (Levenspiel 1999).

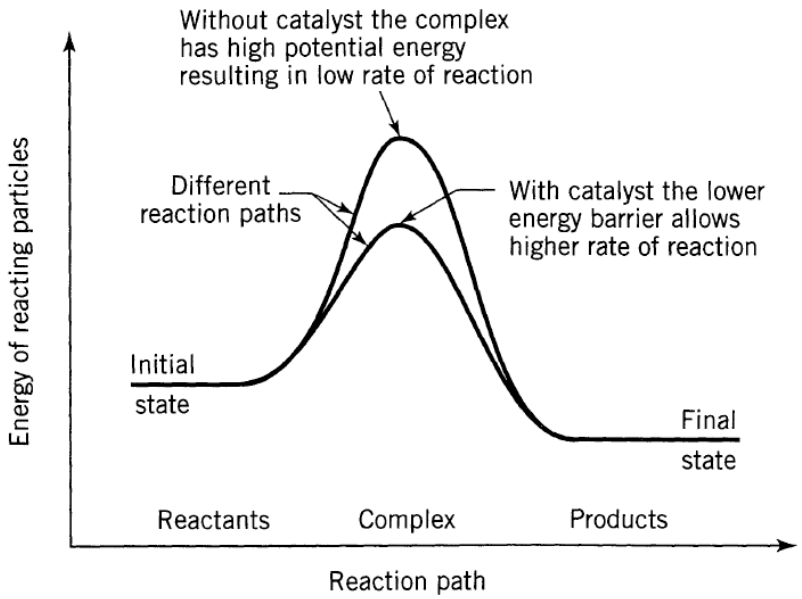


Figure 1.3. Representation of the action of a catalyst in the activation energy of the reaction (Levenspiel 1999).

The first reference to the word *enzyme* dates back to 1878 by Wilhelm Kühne, German physiologist. Since then developments have succeeded and enzymes are no longer *only* nature's catalysts but have been integrated in many processes and everyday products,

representing in 2008 an estimated €3.4 Billion market with an annual growth of 6.5-10% (Tramoy 2008). Some examples of the widespread application of enzymes are the production of starch-derived syrups, such as high-fructose corn syrup (amylases), lactose free dairy products (lactases), laundry detergents (proteases, lipases) or contact lens cleaners (proteases).

Another field of great potential is the synthesis of chemicals, where the growing need for the development of sustainable processes that use renewable raw materials and minimize chemical and energetic waste is nowadays widely recognized (Sheldon 2005) and major enzyme producers such as Novozymes are investing strongly on the development of this field (Tramoy 2008). Here the use of biocatalysts can also constitute a more sustainable alternative to some traditional chemical processes. Additionally, high regioselectivity and stereoselectivity constitute attractive and useful features of these biocatalysts and are mainly responsible for the rapid growth of the number of biocatalytic industrial processes for the production of chemicals, where using an enzyme as catalyst reduces or eliminates unwanted side-reactions; the number of biotransformations already operated at an industrial scale had already grown above 100 in 2002 (Straathof et al. 2002), and nearly 90% of the products involved chirality.

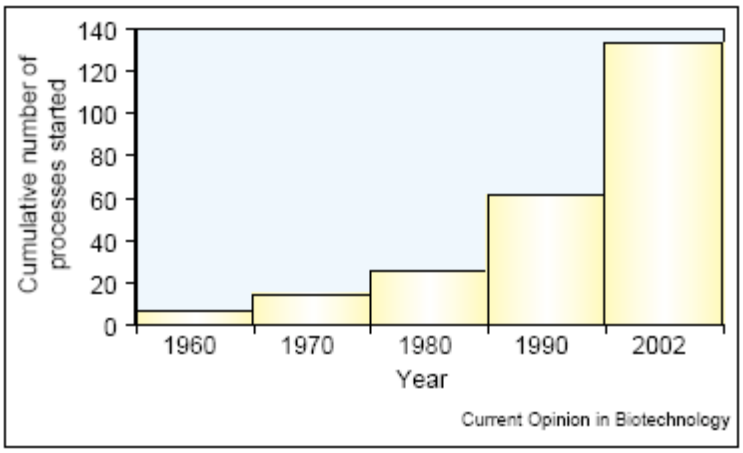


Figure 1.4. Growth of biocatalytic processes operated at industrial scale (Straathof et al. 2002).

The majority of industrially established biocatalytic processes for the production of organic chemicals involve hydrolases (Straathof et al. 2002). Among this group of enzymes, Lipases are commonly employed and great attention has been paid to lipase-catalyzed reactions in the research world (Gandhi et al. 2000; Davis and Boyer 2001).

Although in nature enzymes typically operate in aqueous media, it is well established, since the late eighties, that enzymes are active in organic media as well (Zaks and Klibanov 1984; Klibanov 1986). Furthermore, enzymes are capable of catalyzing reactions that would not be possible to perform in water and key properties such as regioselectivity, stereoselectivity and stability can be markedly affected by the choice of solvent (Klibanov 2001).

The natural ability of lipases to catalyze the hydrolysis of ester bonds in aqueous environment, has leaded to well established commercial applications. In organic media, however, lipases are capable of catalyzing the reverse reaction (esterification) and can furthermore be applied to transesterification reactions (Yahya et al. 1998; Yadav and Devi 2004; Zhang et al. 2004; Zhang et al. 2005). In this field, besides potentially constituting an energetically more efficient route to ester production, as most lipases are active at mild temperatures, lipases exhibit high regioselectivity and stereoselectivity while showing great versatility, by accepting a wide range of substrates (Gandhi et al. 2000). Lipases thus show great potential for the production of esters, eliminating the use of strong acids as catalysts and significantly reducing energy costs, by operating at milder temperatures.

1.5 ENZYME IMMOBILIZATION AND MASS TRANSFER

When enzymes are used in organic chemical synthesis, the cost of the biocatalyst can be, in many cases, a fairly important part of the overall production process cost (van Roon et al. 2006). This is one of the driving forces that led to a rapid growth in the development of immobilization techniques and processes with the purpose of creating more stable, active and easily reusable biocatalysts (Petkar et al. 2006; Vidinha et al. 2006). Additionally, the usage of immobilized enzymes facilitate their separation from the reaction medium, hence reducing the cost of the downstream processing, making immobilized enzymes one of the most suitable forms for application in enzymatic reactors.

Immobilization introduces additional challenges and opportunities. Aspects such as enzyme-support interactions, pore and particle size and the types of forces involved in the attachment of the enzyme to the surface of the support were shown to affect enzyme activity and selectivity (Vidinha et al. 2004; Park et al. 2006; Petkar et al. 2006; Vidinha et al. 2006; van Roon et al. 2007) and can all be tuned to optimize the performance of the enzyme making this a challenging and multidisciplinary field of research.

With the immobilization, the enzyme activity becomes a function of the micro-environment that surrounds it, inside the support, rather than the bulk conditions of the reaction medium. The reactants need to diffuse from the bulk medium to the external surface of the support and then, in the case of porous particles, along the pores where most of the immobilized enzyme will be and where the reaction will take place. Depending on the velocity of these transport phenomena when compared to the reaction rate, mass transfer can become an important part of the overall reaction processes (Engasser and Hisland 1979; Bódalo et al. 1986; Palazzi and Converti 2001; Zhang et al. 2005) affecting both the apparent reaction rate and, in the case of multiple reactions, the selectivity (Xiu et al. 2000; van Roon et al. 2006). Several experimental works have been reported in this area (Yahya et al. 1998; Yadav and Devi 2004; Zhang et al. 2004; Zhang et al. 2005). In the studies where diffusional limitations were experimentally noticed, the classical particle size test was performed, leading in most cases to the conclusion that mass transfer resistances cannot be entirely eliminated (Palazzi and Converti 2001; Zhang et al. 2004).

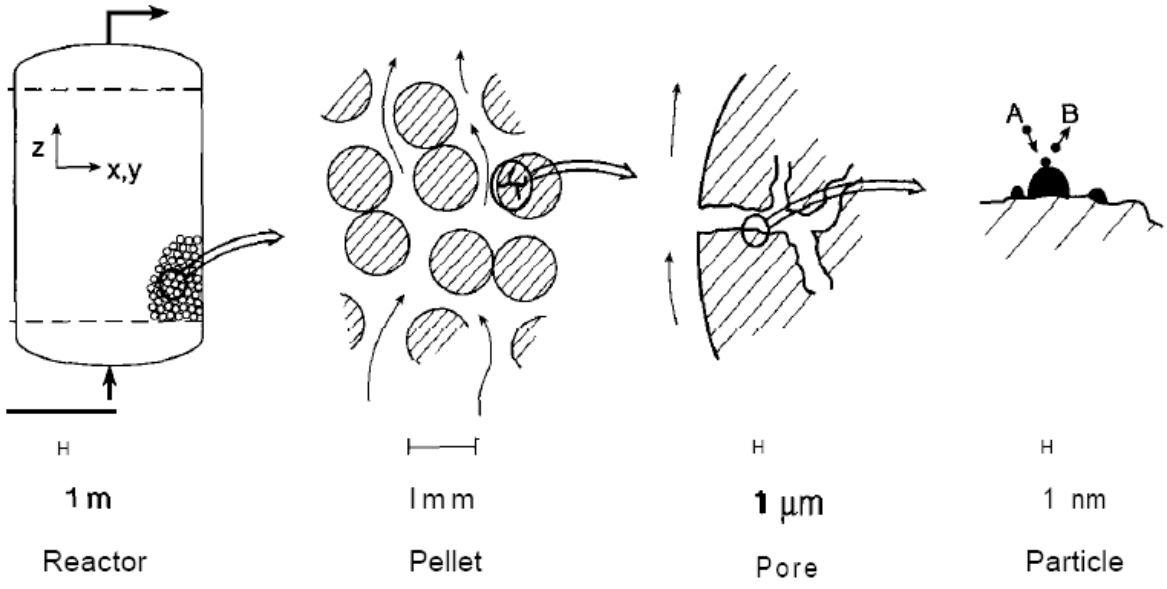


Figure 1.5. Illustration of the path of the reactants and scale in heterogeneous catalysis (Schmidt 1998).

When such diffusion limitations are present, the way the enzyme is distributed inside the support can also affect the macroscopic behavior of the catalyst (Do and Hossain 1986; Do

and Hossain 1987; Ladero et al. 2001; van Roon et al. 2006). Since the reaction rate now depends on the amount of enzyme present in each point of the support, if the enzyme distribution is heterogeneous, the reaction rate will be different for different positions inside the particle. Thus, knowledge of how different enzyme distributions will affect a specific reaction process and the development of models that can predict its influence can be a valuable tool for catalyst design (Do and Hossain 1986; Do and Hossain 1987; van Roon et al. 2006).

1.6 ENZYME REACTOR MODELING

Several reactor models have been developed and applied to describe biocatalytic immobilized enzyme reactors (Engasser and Hisland 1979; Bódalo et al. 1995; Abu-Reesh 1997; Goddard et al. 2000; Xiu et al. 2000; Al-Muftah and Abu-Reesh 2005; Al-Muftah and Abu-Reesh 2005; van Roon et al. 2006). Most of these works deal with the case of one substrate reactions following Michaelis-Menten kinetics in different types of reactors.

Additional complexity has been introduced by considering reversibility and inhibition, in several kinds of reactors. Mammarella and Rubiolo (Mammarella and Rubiolo 2006), presented a packed bed reactor model for lactose hydrolysis catalyzed by lactase, following irreversible Michaelis-Menten kinetics with competitive product inhibition, while, Bódalo et al. (Bódalo et al. 1995) added reversibility of the reaction, developing a model for a fluidized bed reactor performing monosubstrate reactions, following reversible Michaelis-Menten with competitive product inhibition.

Regarding multiple reaction systems Xiu et al. (Xiu et al. 2000) studied the kinetic resolution of racemates in a batch reactor and the influence of mass transfer limitations in the enantiomeric ratio; more recently Van Roon et al. (van Roon et al. 2006) developed a reactor model for a more complex reaction system for the synthesis of cephalexin and accounted for heterogeneous distribution of the enzyme inside the support, in which the enzyme is mostly located in the outer region of spherical particles showing a concave profile. For the case of esterification/transesterification reactions, Goddard et al. (Goddard et al. 2000) developed a model, assuming a simplified Michaelis-Menten kinetics when one of the substrates is present in excess ($C_i >> K_{Mi}$).

Al-Muftah and Abu-Reesh (Al-Muftah and Abu-Reesh 2005; Al-Muftah and Abu-Reesh 2005) presented a detailed parametric analysis of a packed bed reactor model for lactose

hydrolysis following irreversible Michaelis-Menten kinetics with competitive product inhibition

Djennard et al. (Djennad et al. 2005) studied enzymatic membrane reactors and developed a model for the hydrolysis of p-nitro phenol laurate catalyzed by *Candida rugosa* lipase immobilized in a membrane, following irreversible Michaelis-Menten kinetics.

The majority of the models deal with internal and/or external mass transfer resistances, mostly differing in the type of reactor or the kinetic mechanism. Although well established that esterification reactions follow a Ping-pong bi-bi kinetic mechanism, to the extent of our knowledge, no reactor model has been developed considering this reaction kinetics.

1.7 THERMODYNAMIC ACTIVITY BASED KINETIC EQUATIONS

Thermodynamic activity based kinetic equations for enzyme catalysis have received some attention (Straathof et al. 1992; van Tol et al. 1995a; van Tol et al. 1995b; Sandoval et al. 2001; Sandoval et al. 2002), with the purpose of calculating kinetic parameters that are independent of the solvent used to perform the reactions. This would considerably reduce the experimental work required for both solvent selection and kinetic modeling, and should be possible as long as the solvent does not interact with the active site of the enzyme and the several binding and unbinding steps do not depend on the solvent (Straathof et al. 1992; van Tol et al. 1995; Sandoval et al. 2001). It has been shown that although the kinetic parameters dependence with the solvent is significantly reduced by this approach, some deviations still occur (Sandoval et al. 2001). One solvent adapted parameter to account for the residual solvent effects was introduced by Sandoval et al. (Sandoval et al. 2001) with satisfactory results.

For a given solvent, the application of a thermodynamic activity based kinetic equation is also relevant when the reaction mixture is highly non-ideal and the activity coefficients of the substrates change significantly within the range of concentrations used.

1.8 PURPOSE AND OUTLINE OF THE WORK

In this work, with the aim of studying the production of long chain esters by transesterification reactions catalyzed by enzymes in organic media, Decyl acetate was produced through the transesterification of vinyl acetate and decanol, in hexane, catalyzed by an immobilized lipase in two different types of reactors (batch tank reactor and tubular packed bed). Besides the reaction kinetics, phenomena that affect the course of the reaction such as internal and external mass transfer resistances, intraparticle distribution of the enzyme, and the thermodynamic non-ideality of the reaction medium, were analyzed in detail and models were developed for both types of reactors.

The work is organized in 5 sections, being the first one the introductory chapter.

In Section 2, a preliminary enzyme screening is performed to choose the most suitable catalyst for the reaction. The chosen catalyst is physically characterized, as additional data is required for modeling purposes, and the influence of mass transfer limitations (internal and external) is evaluated in a batch reactor. The intrinsic kinetic parameters are then determined in the absence of diffusion limitations and the influence of the thermodynamic non-ideality of the reaction mixture in the reaction rate is analyzed in detail.

In Section 3, a batch reactor model is developed, taking into account the effect of internal and external mass transfer resistances, the heterogeneous intraparticle distribution of the enzyme and the thermodynamic non-ideality of the reaction mixture. Several experiments are performed in a batch reactor with catalyst particles of different sizes, amount of catalyst in the reactors and different initial concentrations of both substrates to test the capability of the model to predict the obtained results, without fitting any parameter. A steady-state model based on the same assumptions is also developed to perform an analysis of the influence of each of the model's parameters and different intraparticle enzyme distributions.

In Section 4, the same reaction is performed in a packed bed reactor and a reactor model is developed and tested for this system. The stability of the enzyme is also tested in continuous operation mode. Also in this section, the solvent free production of decyl acetate is tested in a batch reactor, the main differences in comparison to its production in hexane are ana-

lyzed and the capacity of the model presented in Section 3 to describe the solvent free system is tested.

Finally, the conclusions of the work are presented in Section 5 together with suggestions of future work.

1.9 BIBLIOGRAPHY

Abu-Reesh, I. M. (1997). Predicting the performance of immobilized enzyme reactors using reversible Michaelis–Menten kinetics. Bioprocess. Eng. 17: 131-137.

Al-Muftah, A. E. and Abu-Reesh, I. M. (2005). Effects of internal mass transfer and product inhibition on a simulated immobilized enzyme-catalyzed reactor for lactose hydrolysis. Biochemical Engineering Journal 23 (2): 139-153.

Al-Muftah, A. E. and Abu-Reesh, I. M. (2005). Effects of simultaneous internal and external mass transfer and product inhibition on immobilized enzyme-catalyzed reactor. Biochemical Engineering Journal 27 (2): 167-178.

Aslam, M., Torrence, G. P. and Zey, E. G. (2001). Esterification. Kirk-Othmer Encyclopedia of Chemical Technology, John Wiley & Sons. 10: 471-496.

Bódalo, A., Gómez, J. L., Gómez, E., Bastida, J., Iborra, J. L. and Manjón, A. (1986). analysis of diffusion effects on immobilized enzymes on porous supports with reversible Michaelis-Menten kinetics. Enzyme and Microbial Technology 8: 433-438.

Bódalo, A., Gómez, J. L., Gómez, E., Bastida, J. and Máximo, M. F. (1995). Fluidized bed reactors operating with immobilized enzyme systems: Design model and its experimental verification. Enzyme Microb. Technol. 17: 915-922.

Burdock, G. A. (2004). Fenaroli's handbook of flavor ingredients (Fifth Edition). Boca Raton, CRC Press.

Davis, B. G. and Boyer, V. (2001). Biocatalysis and enzymes in organic synthesis Nat. Prod. Rep. 18 (618-640).

Djennad, M., Benachour, D., Berger, H., Belhamiti, O. and Schomacker, R. (2005). Modeling of a catalyzed reaction using lipase immobilized in a poly(vinyl alcohol) membrane. Engineering in Life Sciences 5 (1): 29-37.

Do, D. D. and Hossain, M. M. (1986). Novel Method of determination of the internal enzyme distribution within porous solid supports and the deactivation rate constant. Biotechnology and Bioengineering 28 (4): 486-493.

Do, D. D. and Hossain, M. M. (1987). New method to determine active enzyme distribution, effective diffusivity, rate constant for main reaction and rate constant for deactivation. Biotechnology and Bioengineering 29 (5): 545-551.

Duarte, C. and Loureiro, J. M. (2004). Effect of Adsorption on Residue Curve Maps for Heterogeneous Catalytic Distillation Systems. Industrial & Engineering Chemistry Research 43: 3242-3250.

Engasser, J. M. and Hisland, P. (1979). Diffusional effects on the heterogeneous kinetics of two-substrate enzymic reactions. Journal of Theoretical Biology 77: 427-440.

Fahlbusch, K.-G., Hammerschmidt, F.-J., Panten, J., Pickenhagen, W., Schatkowski, D., Bauer, K., Garbe, D. and Surburg, H. (2005). Flavors and Fragrances. Ullmann's Encyclopedia of Chemical Technology. Wiley-VCH: 1-130.

Gandhi, N. N., Patil, N. S., Sawant, S. B. and Joshi, J. B. (2000). Lipase-catalyzed esterification. Catalysis Reviews: Science & Engineering 42: 439-480.

Goddard, E., Bosley, J. and Al-Duri, B. (2000). Lipase-catalysed esterification of oleic acid and ethanol in a continuous packed bed reactor, using supercritical CO2 as solvent: approximation of system kinetics. J. Chem. Tech. Biotechnol. 75: 715-721.

InternationalOrganizationOfTheFlavorIndustry. (2008). Retrieved November 2008, from http://www.iofi.org.

Klibanov, A. M. (1986). Enzymes that work in organic solvents. CHEMTECH 16 (6): 354-359.

Klibanov, A. M. (2001). Improving enzymes by using them in organic solvents. Nature 409: 241-246.

Ladero, M., Santos, A. and García-Ochoa, F. (2001). Diffusion and chemical reaction rates with nonuniform enzyme distribution: an experimental approach. Biotechnology and Bioengineering 72 (4): 458-467.

Levenspiel, O. (1999). Chemical Reaction Engineering (Third Edition). John Wiley and Sons.

Mammarella, E. J. and Rubiolo, A. C. (2006). Predicting the packed-bed reactor performance with immobilized microbial lactase. Process Biochemistry 41 (7): 1627-1636.

Palazzi, P. and Converti, A. (2001). Evaluation of diffusional resistances in the process of glucose isomerization to fructose by immobilized glucose isomerase. Enzyme and Microbial Technology 28: 246-252.

Park, E. Y., Sato, M. and Kojima, S. (2006). Fatty acid methyl ester production using lipase-immobilizing silica particles with different particle sizes and different specific surface areas. Enzyme and Microbial Technology 39 (4): 889-896.

Petkar, M., Lali, A., Caimi, P. and Daminati, M. (2006). Immobilization of lipases for non-aqueous synthesis. Journal of Molecular Catalysis B: Enzymatic 39 (1-4): 83-90.

Sakamuri, R. (2001). Esters, Organic. Kirk-Othmer Encyclopedia of Chemical Technology, John Wiley & Sons. 10: 497-526.

Sandoval, G., Condoret, J. S., Monsan, P. and Marty, A. (2002). Esterification by immobilized lipase in solvent-free media: Kinetic and thermodynamic arguments. Biotechnology and Bioengineering 78 (3): 313-320.

Sandoval, G. C., Marty, A. and Condoret, J.-S. (2001). Thermodynamic activity-based enzyme kinetics: Efficient tool for nonaqueous enzymology. AIChE Journal 47 (3): 718-726.

Schmidt, L. D. (1998). The Engineering of Chemical Reactions, Oxford University Press.

Sheldon, R. A. (2005). Green solvents for sustainable organic synthesis: state of the art. Green Chemistry 7 (5): 267-278.

Straathof, A. J. J., Panke, S. and Schmid, A. (2002). The production of fine chemicals by biotransformations. Current Opinion in Biotechnology 13 (6): 548-556.

Straathof, A. J. J., Rakels, J. L. L. and Heijnen, J. J. (1992). Enzyme kinetics in monophasic and biphasic aqueous-organic systems, in J. Tramper, Vermue, M. H., Beeftink, H. H. and Stockar, U. v., Eds. Enzyme kinetics in monophasic and biphasic aqueous-organic systems. Biocatalysis in Non-Conventional Media. Amstedam, Elsevier.

TheGoodScentsCompany. (2008). Retrieved November 2008, from http://www.thegoodscentscompany.com.

Tramoy, P. (2008). "Review on the Enzyme Market." Retrieved July 2009, from http://www.lifescience-online.com/articles.html?portalPage=Lifescience+Today.Articles&a=1011.

van Roon, J. L., Arntz, M. M. H. D., Kallenberg, A. I., Paasman, M. A., Tramper, J., Schroen, C. G. P. H. and Beeftink, H. H. (2006). A multicomponent reaction-diffusion model of a heterogeneously distributed immobilized enzyme. Applied Microbiology and Biotechnology 72 (2): 263-278.

van Roon, J. L., Schroen, C. G. P. H., Tramper, J. and Beeftink, H. H. (2007). Biocatalysts: Measurement, modelling and design of heterogeneity. Biotechnology Advances 25 (2): 137-147.

van Tol, J. B. A., Jongejan, J. A., Duine, J. A., Kierkels, H. G. T., Gelade, E. F. T., Mosterd, F., van der Tweel, J. J. and Kamphuis, J. (1995). Thermodynamic and kinetic parameters of lipase-catalyzed eater hydrolysis in biphasic systems with varying organic solvents. Biotechnology and Bioengineering 48 (3): 179-189.

van Tol, J. B. A., Stevens, R. M. M., Veldhuizen, W. J., Jongejan, J. A. and Duine, J. A. (1995). Do organic solvents affect the catalytic properties of lipase? Intrinsic kinetic parameters of lipases in ester hydrolysis and formation in various organic solvents. Biotechnology and Bioengineering 47 (1): 71-81.

Vidinha, P., Augusto, V., Almeida, M., Fonseca, I., Fidalgo, A., Ilharco, L., S. Cabral, J. M. and Barreiros, S. (2006). Sol-gel encapsulation: An efficient and versatile immobilization technique for cutinase in non-aqueous media. Journal of Biotechnology 121 (1): 23-33.

Vidinha, P., Harper, N., Micaelo, N. M., Lourenco, N. M. T., Gomes Da Silva, M. D. R., Cabral, J., Afonso, C. A. M., Soares, C. M. and Barreiros, S. (2004). Effect of immobilization

support, water activity, and enzyme ionization state on cutinase activity and enantioselectivity in organic media. Biotechnology and Bioengineering 85 (4): 442-449.

Xiu, G.-H., Jiang, L. and Li, P. (2000). Mass-transfer limitations for immobilized enzyme-catalyzed kinetic resolution of racemate in a batch reactor. Ind. Eng. Chem. Res. 39: 4054-4062.

Yadav, G. D. and Devi, K. M. (2004). Immobilized lipase-catalysed esterification and transesterification reactions in non-aqueous media for the synthesis of tetrahydrofurfuryl butyrate: comparison and kinetic modeling. Chemical Engineering Science 59: 373-383.

Yahya, A. R. M., Anderson, W. A. and Moo-Young, M. (1998). Ester synthesis in lipase-catalyzed reactions. Enzyme and Microbial Technology 23: 438-450.

Zaks, A. and Klibanov, A. M. (1984). Enzymatic catalysis in organic media at 100ºC. Science 224: 1249-1251.

Zhang, J., Wu, J. and Yang, L. (2004). The kinetic study on lipase-catalyzed asymmetric alcoholysis of a-cyano-benzyl acetate in organic media. J. Mol. Catal. B: Enzym. 31: 67-72.

Zhang, T., Yang, L. and Zhu, Z. (2005). Determination of internal diffusion limitation and its macroscopic kinetics of the transesterification of CPB alcohol catalyzed by immobilized lipase in organic media. Enzyme and Microbial Technology 36 (2-3): 203-209.

2. KINETIC MODELING OF THE ENZYME CATALYZED PRODUCTION OF DECYL ACETATE

In this section, a preliminary enzyme screening is performed to choose the most suitable catalyst for the reaction. The chosen catalyst is physically characterized, as additional data is required for modeling purposes, and the influence of mass transfer limitations (internal and external) is evaluated in a batch reactor. The intrinsic kinetic parameters are then determined in the absence of diffusion limitations and the influence of the thermodynamic non-ideality of the reaction mixture in the reaction rate is analyzed in detail.

2.1 REACTIVE SYSTEM

Decyl acetate can generally be produced by one of two routes: esterification or trans-esterification. The first one is basically the reverse of the hydrolysis of an ester and consists in the reaction of an alcohol with an acid:

$$\text{Acid} + \text{Alcohol} \leftrightarrow \text{Ester} + \text{Water} \tag{2.1}$$

In a transesterification, the acid is replaced by an ester:

$$\text{Ester 1} + \text{Alcohol 1} \leftrightarrow \text{Ester 2} + \text{Alcohol 2} \tag{2.2}$$

Both types of reactions can be catalyzed enzymaticaly, using lipases.

For decyl acetate, the esterification route would consist in:

$$\text{Acetic acid} + \text{Decanol} \leftrightarrow \text{Decyl Acetate} + \text{Water} \quad (2.3)$$

Acetic acid however is known to have an inhibitory effect on enzymes such as lipases which can be avoided by replacing it with an acetate. Vinyl esters are often chosen to play this role as the byproduct of the reaction conveniently tautomerizes to acetaldehyde (Yadav and Trivedi 2003), displacing the equilibrium in favor of the production of the ester. If vinyl acetate is chosen, the reaction becomes:

$$\text{Vinyl Acetate} + \text{Decanol} \rightarrow \text{Decyl Acetate} + \text{Acetaldehyde} \quad (2.4)$$

All subsequent studies were performed using as reactants vinyl acetate + decanol, with hexane as the solvent.

2.2 EXPERIMENTAL METHOD

2.2.1 ENZYMES AND CHEMICALS

Vinyl acetate, decanol and decyl acetate were obtained from Sigma-Aldrich (>99%). Hexane was purchased from Merck (pro-analysis). Novozym 435, Lipozym TL-IM and Lipozym RM-IM were gently provided by Novozymes. Amano PSC-I, Amano PSC-II, Amano PSD, Amano F-AP 15, Amano AYS and Amano AK-20 were kindly provided by Amano Enzyme Inc.

2.2.2 EXPERIMENTS IN BATCH REACTOR

All reactions were performed in magnetically stirred jacketed reactors with 100 mL capacity, at 30 ºC, with reaction volume of 40 mL and with hexane as the solvent. When relevant to the analysis, the magnetic bars were padded with soft paper to ensure that the particle size was maintained constant throughout the reaction.

Novozym 435 particles were separated in groups of different sizes through sieving. When particle crushing was necessary, it was either performed with a pestle (for small quantities) or by means of a magnetic stirrer bar.

To assess if the reaction could proceed in the absence of the catalyst, blank runs were also performed during 24 hours, at the same operational conditions but without any catalyst and no conversion was detected.

The occurrence of side reactions was not considered since no additional peaks were detected in the chromatographic analysis and the amount of decyl acetate formed was always consistent with the decrease in concentration of the limiting reactant.

2.2.3 ANALYTICAL METHODS

Several 200 μL samples were withdrawn throughout the reactions and analyzed by gas chromatography in a Varian CP-3800 GC equipped with a TCD detector and auto sampler. A 25 m x 0.53 mm WCOT column was used in the analysis and the calibration was made with synthetic mixtures of the pure components. The operating temperatures were 270 ºC for the injector, 165 ºC for the column oven and 340 ºC for the TCD filament and helium was used as the carrier gas. All data presented are the average of three measurements.

2.2.4 DETERMINATION OF THE PROTEIN CONTENT

The enzyme content of the Novozym 435 particles was determined at Faculdade de Ciências e Tecnologia Universidade Nova de Lisboa by a modified Lowry method (Lowry et al. 1951), as described in Appendix A.

2.3 RESULTS AND DISCUSSION

2.3.1 ENZYME SCREENING

There are numerous enzymes on the market capable of catalyzing the reaction between vinyl acetate and decanol. Novozymes and Amano Enzyme Inc., two world leading enzyme suppliers, gently provided a reasonable group of immobilized lipases for a preliminary enzyme screening. These are the enzymes that the suppliers recommended for the chosen type of reaction system. To better characterize these catalysts and analyze the subsequent

results, the amount of enzyme per mass of catalyst particle, W_E, was determined. The results obtained are shown in Table 2.1.

The specific enzyme content of the catalysts Amano PSC II and Amano PSD could not be determined by the adopted modified Lowry method as the enzyme is covalently attached to the support. It is worth noting that, when compared to Novozymes, immobilized lipases from Amano present larger enzyme contents.

Table 2.1. Specific enzyme content for the several available catalysts.

Enzyme	W_E ($g_{Enzyme}/g_{Particle}$)
Amano AK-20	0.139
Amano AYS	0.184
Amano F-AP 15	0.239
Amano PSC-I	0.237
Amano PSC-II	-
Amano PSD	-
Lipozym RM-IM	0.058
Lipozym TL-IM	0.078
Novozym 435	0.090

For the screening itself, the initial reaction rate, R^0, obtained for the reaction of vinyl acetate and decanol in hexane at 30 ºC at an equimolar initial concentration of 0.1M of each reagent, was used as a measure of the catalytic activity of the available enzymes. The initial reaction rate was calculated from the linear part of the concentration vs. time curve, which, in this case, can safely be assumed as such below 15% conversion. The results obtained are shown in Figure 2.1.

In terms of the production process, the key parameter is R^0 in mol/L.g_{Part}.min rather than mol/L.g_{Enzyme}.min, since it reflects the behavior of the catalyst rather than the activity of the enzyme alone. Clearly, Novozym 435 is the most active catalyst towards the reaction of vinyl acetate with decanol; the initial reaction rate obtained with Novozym 435 is almost three-fold higher than the one obtained with Amano PSC-II, the second most active catalyst. *Candida antarctica* lipase B, immobilized in the Novozym particles, is also the most active enzyme from the ones for which the specific enzyme content could be determined, with the remark that no data could be obtained for Amano PSC-II and Amano PSD.

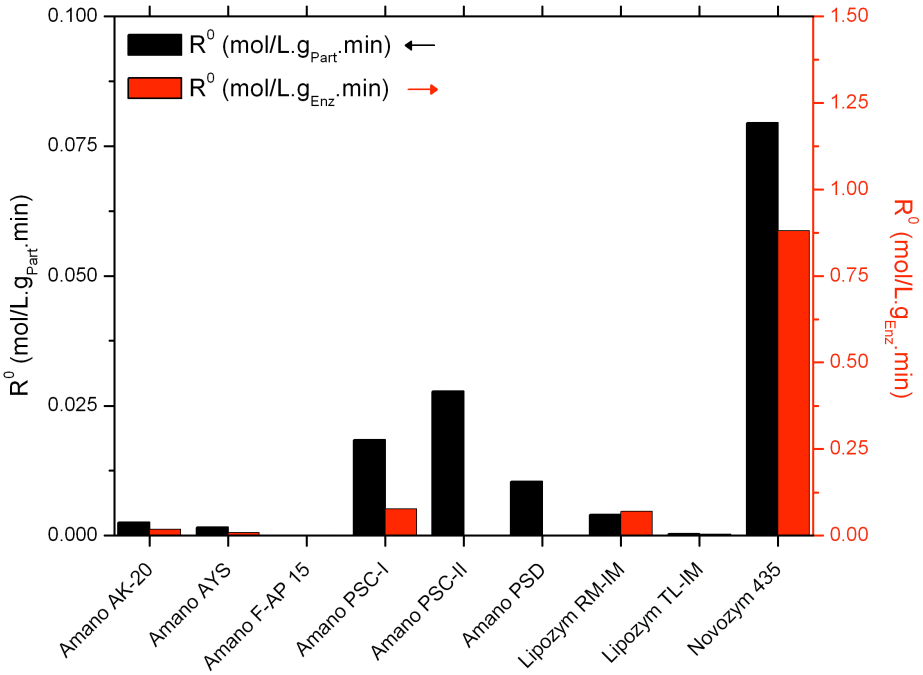


Figure 2.1. Initial reaction rates obtained with several commercial enzymes for the reaction of vinyl acetate with decanol (0.1M: 0.1M) in hexane at 30ºC

Novozym 435 is also the most expensive catalyst tested (€1440/kg, bulk quote; the least expensive enzyme that showed more than just residual activity being Lipozym RM-IM at €525/kg), but it still appears to be the best option, since it nevertheless provides the lowest cost of catalyst per mol of decyl acetate produced per hour.

Besides appearing to be the most active and cost effective enzyme, Novozym 435 presents several features which are convenient for reactor modeling works:

- It is a well characterized enzyme (Hari Krishna and Karanth 2001; Kirk and Christensen 2002; Yadav and Devi 2004; Yadav and Lathi 2004);

- It is a stable and robust enzyme: its catalytic activity does not depend on the water activity, in the case of transesterification reactions, as strongly as other enzymes (Almeida et al. 1998).

Amano PSC-I and Lipozym RM-IM provide an interesting comparison; although the catalytic activity of Lipozym RM-IM is only 20% of the Amano PSC-I, the activity of the corresponding immobilized enzymes is very similar. The increase in catalytic activity of Amano PSC-I towards vinyl acetate and decanol, when compared to Lipozym RM-IM, is a result of a higher yield of immobilization rather than the usage of a more active enzyme.

Novozym 435 was thus selected for all subsequent work. The first step for studying a reactive system is the determination/construction of a kinetic model that describes its behavior and the estimation of the corresponding kinetic parameters; however, as an immobilized enzyme is being used as the catalyst, to assess the intrinsic kinetic parameters it is convenient to eliminate the influence of other competing phenomena such as external and internal diffusion. The other option would be to correctly account for the influence of these phenomena, increasing the complexity of the models and possible sources of error.

2.3.2 EXTERNAL MASS TRANSFER STUDIES

When working with enzymes immobilized in porous particles, as with any other supported catalysts, in order to reach the enzyme molecules, the reactants must firstly diffuse from the bulk liquid to the surface of the particles, across a stagnant layer of fluid, and then inside its pores, where the enzyme is immobilized. In a batch reactor, the thickness of the stagnant film can generally be reduced by stirring the reaction mixture, minimizing, if not eliminating, the influence of external mass transport in the overall reaction process.

To ensure the absence of external diffusion limitations in all experiments, the stirring speed was gradually increased until it had no influence in the evolution of the observed concentrations of the reacting components, which occurred for an agitation speed of around 350 rpm (results not shown here). This test was performed at 30 ºC with a 0.1 M concentration of each reactant and 240 μm particles (the smallest particle size used). Similar values have been reported previously by other authors (Yadav and Trivedi 2003; Trubiano et al. 2007). To ensure a safety margin, all subsequent experiments were performed at 500 rpm.

The Biot number for mass transfer, Bi_m, is a dimensionless parameter that compares the internal and external diffusion rates or time constants (Froment and Bischoff 1990) and is given by:

$$Bi_m = \frac{\tau_D}{\tau_f} = \frac{k_f R_p}{De} \tag{2.5}$$

where τ_D represents the internal diffusion time constant, τ_f the film diffusion time constant, k_f the mass transfer coefficient between the liquid and the catalyst surface, *De* the effective diffusivity and R_P the particle radius

In general, external mass transfer limitations can be neglected for $Bi_m>10$. From commonly used correlations it is possible to determine the influence of the particle size of the catalyst in the mass transfer coefficient between the liquid and the catalyst surface. Using, for example, the Ranz-Marshall correlation (Ranz and Marshall 1952) – Equation (2.6) – it can be shown that the mass transfer coefficient between the liquid and the catalyst surface increases as the particle size decreases.

$$Sh=2+0.6Re^{1/2}Sc^{1/3} \tag{2.6}$$

where *Sh* represents the Sherwood number, *Re* the Reynolds number and *Sc* the Schmidt number.

The proportionality of k_f with the Reynolds number depends of the flow regime, as follows:

$$\begin{aligned} k_f \ \alpha \frac{1}{d_p}, &\quad \text{for laminar flow} \\ k_f \ \alpha \frac{1}{d_p^{1/2}}, &\quad \text{for turbulent flow} \end{aligned} \tag{2.7}$$

Nevertheless, for high Reynolds numbers, the Biot number for mass transfer for smaller particles will ultimately be smaller as well, due to the more significant decrease in the internal diffusion path, as obtained by combining equations (2.5) and (2.7):

$$\begin{aligned} Bim \ \alpha \frac{1}{De}, &\quad \text{for laminar flow} \\ Bim \ \alpha \frac{d_p^{1/2}}{De}, &\quad \text{for turbulent flow} \end{aligned} \tag{2.8}$$

Therefore, the smallest particle size, 240 μm, was used to determine the adequate stirring speed, since it is the case where the strongest agitation is required. If the external diffusion limitations are negligible for the smallest particle size, it is assured that they will also be negligible for larger particles, when the same stirring speed is used.

2.3.3 INTERNAL MASS TRANSFER STUDIES

The influence of internal mass transfer in a given heterogeneous catalytic process can be minimized by reducing the particle size and hence, shortening the diffusion path. If catalyst particles of different sizes are available, they can be used to assess the relative influence of internal diffusion in the overall process. Whenever internal diffusion limitations are present, a reduction in the particle size, usually leads to an enhancement of the reaction rate. When reducing the particle size has no further influence in the reaction rate, internal diffusion is fast enough to be considered negligible and the process is controlled by the chemical reaction.

In order to assess the influence of internal diffusion, the same reaction conditions were used for different particle sizes of the catalyst ([A]=[B]=0.1 M, W_S=0.56 mg/mL, where [A] represents the concentration of vinyl acetate, [B] the concentration of decanol and W_S, the amount of catalyst inside the reactor). The results obtained, in terms of the reactants conversion as a function of time, are presented in Figure 2.2.

To perform these reactions, the magnetic bar used for the stirring was padded with soft paper in order to prevent the otherwise observed crushing of the particles as a result of the repeated shear from the bar. The resulting change in particle size would largely affect the results of the experiments, as can be seen in Figure 2.3, which compares results obtained with and without the paper padding. The data obtained without padding from 40min forward (red open triangles in Figure 2.3) was the result of the paper padding accidentally detaching from the magnetic bar. To ensure that the paper did not affect the reaction, a blank run was performed with the same conditions stated above but without the enzyme and no conversion was detected. The enhancement of the reaction rate due the crushing of the particles is clear and can, by itself, indicate the presence of internal diffusion limitations.

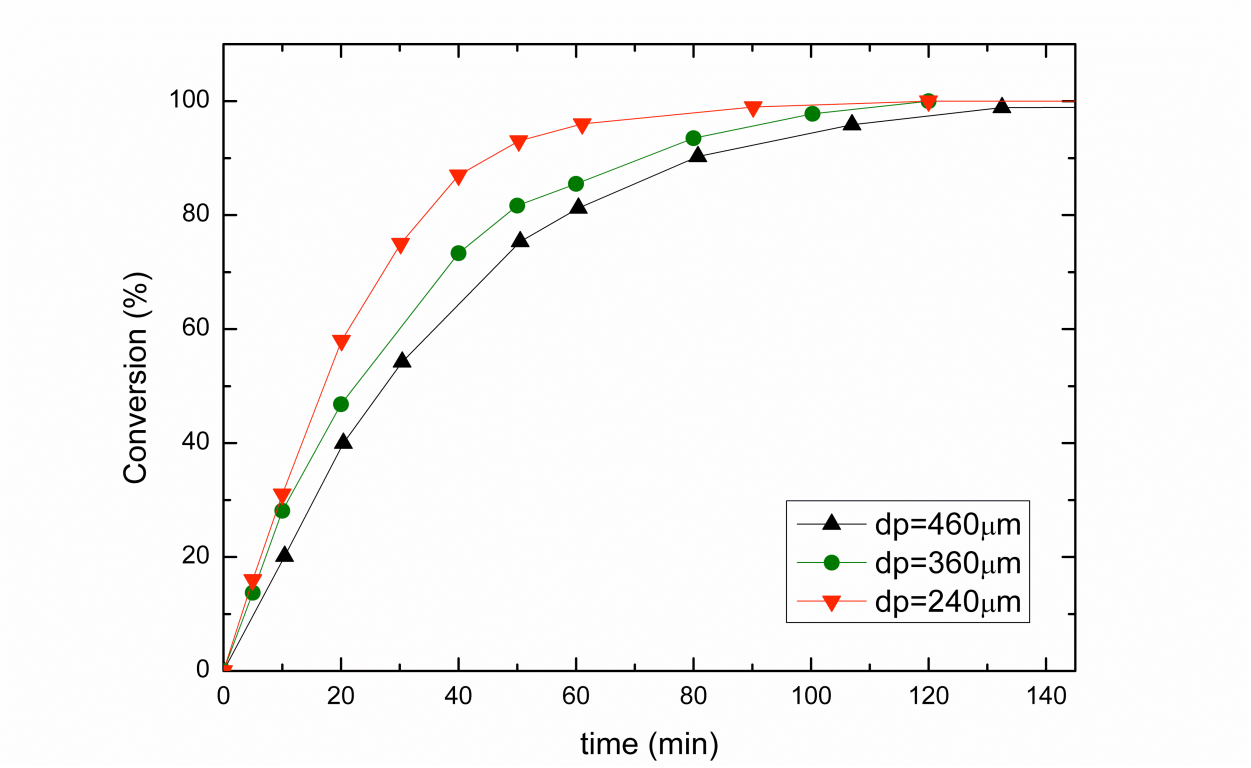


Figure 2.2. Effect of particle diameter on the reactants conversion as a function of time. Reaction conditions: [A]=[B]=0.1 M, W_S=0.56 mg/mL and T=30 ºC for all assays.

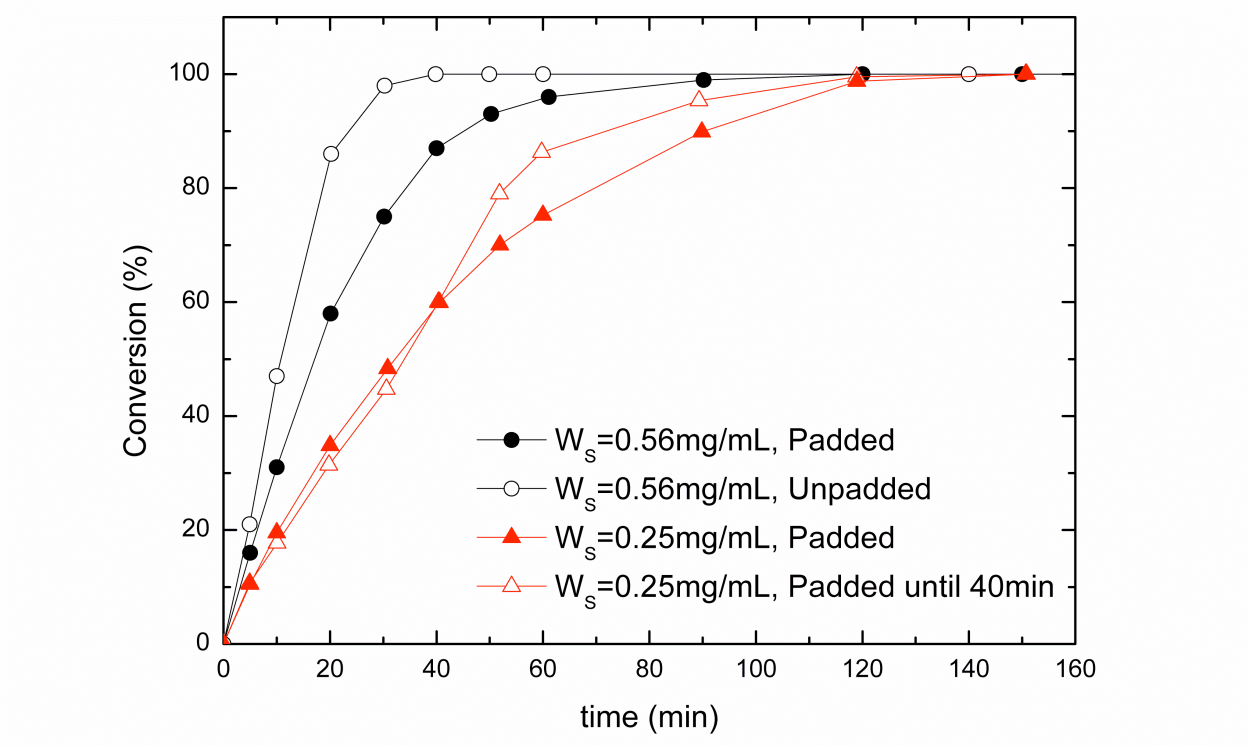


Figure 2.3. Effect of padding the magnetic bar used for stirring, when using 240µm particles. Reaction conditions: [A]=[B]=0.1 M; T=30 ºC.

The results shown in Figure 2.2 seem to indicate the presence of mass transfer limitations as well; however, the larger leap observed between the curves corresponding to 360μm and 240μm particles appears comparatively excessive. Typically, the curves tend to approach as the particle size becomes smaller, and the internal diffusion limitations lose relevance, until they overlap, in the limiting case of a reaction controlled process.

For this reason, the enzyme content was then determined for each particle size. The results are shown in Table 2.2.

Table 2.2. Specific enzyme content for Novozym 435 particles of different sizes.

Average Particle Size (μm)	**Enzyme Load ($g_{enzyme}/g_{particle}$)**
460	0.092
360	0.108
240	0.125

The values obtained for the enzyme content show that the specific enzyme loading (mass of enzyme/mass of particle) depends on the particle size; smaller particles have a larger specific enzyme loading than the larger ones. Garcia-Alles and Gotor (Garcia-Alles and Gotor 1998) already presented some experimental evidence suggesting that the specific enzyme loading varies with the particle size, being larger for smaller particles. A similar correlation was reported by van Roon et al. (van Roon et al. 2003) for immobilized Penicilin-G Acylase and such dependence of the specific enzyme loading with the particle size could be related to internal mass transfer limitations during the enzyme immobilization process. This is supported by the results obtained more recently by Chen et al. (Chen et al. 2007) stating that, although the maximum attainable specific enzyme loading (saturation) is independent of the particle size, smaller particles will saturate with enzyme faster.

When using the same amount of catalyst particles in all experiments we are actually performing the reactions with different amounts of enzyme. As the particle size decreases, the amount of enzyme in the reactors will be larger, contributing to an enhancement in the reaction rate that is not directly related to the reduction of diffusion limitations. This suggests that part of the behavior shown in Figure 2.2 is a result of the different enzyme amount used in each experiment, and not entirely due to internal diffusion limitations.

In order to correctly account for the different specific enzyme loadings, the same experiment was repeated, but now with a constant enzyme amount fed to the reactor, instead of a constant mass of catalyst particles. The results are presented in Figure 2.4.

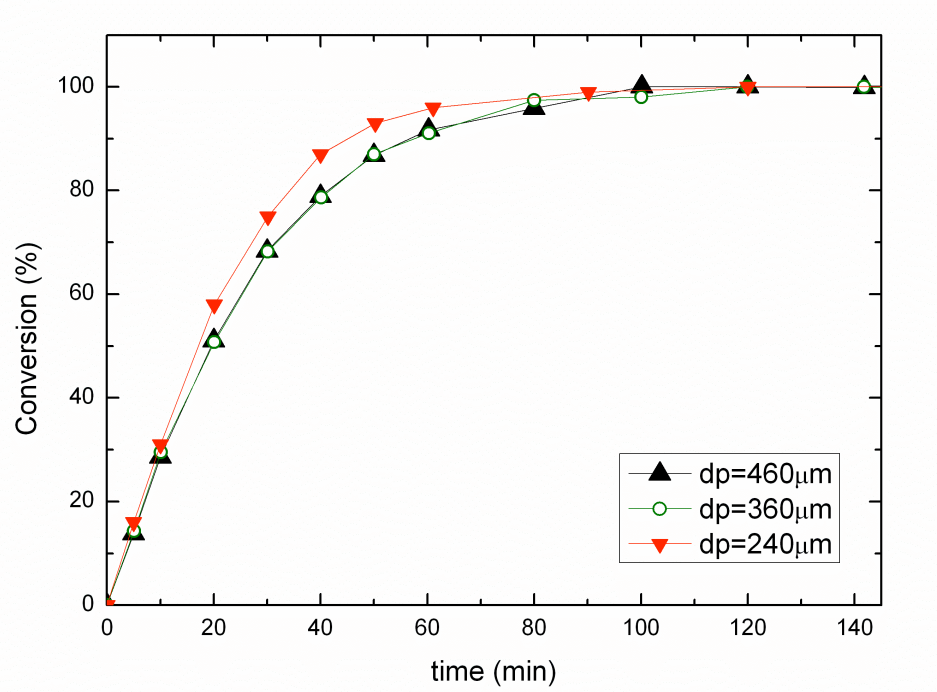


Figure 2.4. Effect of particle diameter on the reactants conversion as a function of time. [A]=[B]=0.1 M, W_{Enzyme}=0.069 mg_{Enzyme}/mL and T=30 ºC for all assays.

In this new set of experiments, for the 460 μm and 360 μm particles the conversion curves overlap (which is the classical behavior of a kinetically controlled reaction process) but an even more atypical increase in the reaction rate is still observed for the smaller 240 μm particles. Two consecutive sets of particles behave as if internal diffusion is negligible, but the reaction rate is then enhanced by further reducing the particle diameter.

To further study this behavior, and continue testing for the presence of internal diffusion limitations, a reasonable amount of particles of each size was crushed into a fine powder and new reactions were performed with the same experimental conditions. The results obtained are shown in Figure 2.5 along with the results obtained with intact particles already presented in Figure 2.4. When crushing the 240 μm particles the reaction rate was consistently higher, confirming the presence of internal diffusion limitations, even for the smallest particle size used. Full conversion was reached in less than half the time necessary when using intact

particles. For 360 µm and 460 µm particles, however, no reproducible results (not shown here) were achieved with this method (the results shown in Figure 2.5 for crushed 360 µm particles were obtained through a different crushing method, described next)

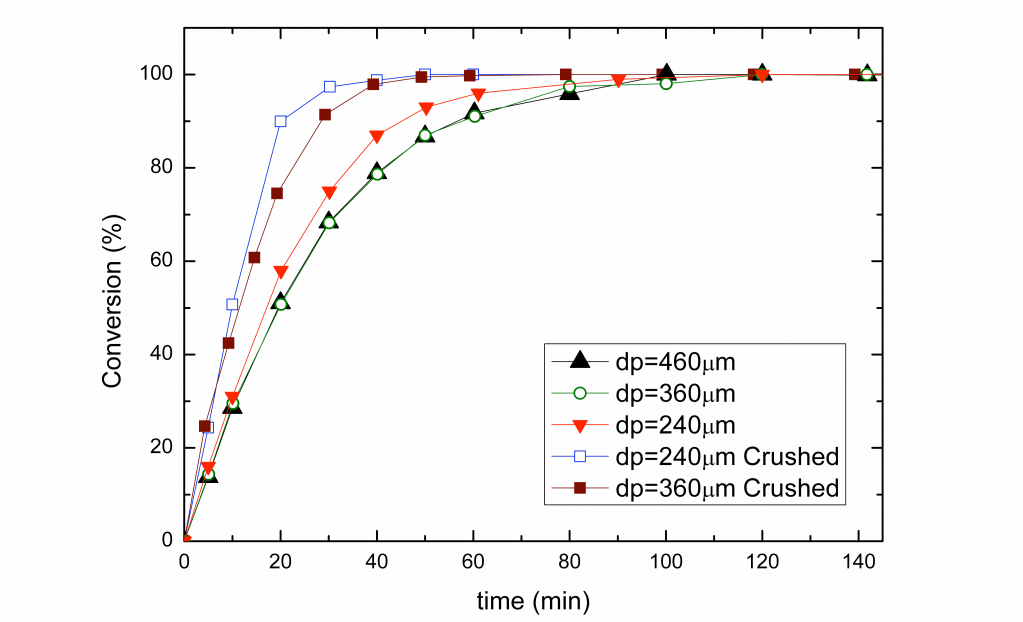


Figure 2.5. Effect of particle diameter on the reactants conversion as a function of time. [A]=[B]=0.1 M, W_{Enzyme}=0.069 mg_{Enzyme}/mL and T=30 ºC for all assays.

It has been shown that Novozym 435 has an egg-shell intraparticle distribution (Mei et al. 2003). In their work, Mei et al. (2003) studied the internal distribution of Novozym 435 using synchrotron infrared microspectroscopy, showing that for a particle size around 600 µm there is only an approximately 100 µm thick enzyme layer in the outer portion of the particle. Several modeling studies were done in the eighties (Clark et al. 1985; Hossain et al. 1986) that associated this kind of intraparticle distribution with restricted diffusion conditions during the immobilization process since, as the immobilization proceeds, the pore size will be reduced by the adsorbed enzyme. More recently, Mei et al. (2003) suggested that restricted diffusion during the immobilization process is unlikely for Novozym 435 since the enzyme molecules are ten times smaller than the average pore size of the support and proposed that protein-protein interactions coupled with a high affinity for the support could block the enzyme from reaching the central part of the particles. When crushing a particle, given the heterogeneous distribution of the enzyme inside the support, the obtained powder will be

heterogeneous as well; it will be composed of active fragments that contain immobilized enzyme, which come from the outer region, and inert fragments that come from the core. When crushing an excessive amount of particles and then using only a smaller amount, it cannot be ensured that the proportion of enzyme/support is maintained. In fact, the lack of reproducible results described above for the 460 μm and 360 μm sets demonstrate that this was probably the case in our experiments.

The 240 μm particles, however, did not exhibit this behavior, as reproducible results were consistently obtained (shown in Figure 2.5). This shows that the enzyme must either be homogeneously distributed throughout the entire particle or at least that the volume of the shell is much larger than the volume of the inert core. For this to be the case, the thickness of the enzyme outer shell should be of the same order of magnitude of the radius of the particles. In fact, the average radius of these particles, 120 μm, is very close to the thickness of the layer determined by Mei et al. (2003) for particles of 600 μm. An outer shell of 100 μm would represent more than 99.5% of the volume of the 240 μm particles.

It is possible to estimate the thickness of the enzyme layer for the production lot used in the experiments from the specific enzyme loading data, presented in Table 2.2. Assuming that:

- The amount of immobilized enzyme is constant throughout the shell;
- Locally, the amount of enzyme per volume of support is the same, regardless of the particle size;

Regardless of the particle size, the mass of enzyme per volume of shell is constant and the following equation applies:

$$W_{E1}\rho_{app1}\frac{V_{particle1}}{V_{Shell1}} = \text{Const.}, \quad \forall\ \text{Particle size} \tag{2.9}$$

where ρ_{app} represents the apparent density, $V_{particle}$ the total volume of a Novozym 435 particle and V_{Shell} the volume of the outer region where the enzyme is immobilized.

Assuming that the apparent density does not depend on the particle size and that the particles are spherical, Equation (2.9) yields:

$$W_{E1}\frac{1}{1-\left(\frac{R_{i1}}{R_{P1}}\right)^3}=\text{Const.},\quad \forall\ \text{Particle size} \tag{2.10}$$

Where R_P represents the particle radius and R_i, the radial position of the boundary between the enzyme shell and the inert core, i.e.:

$$R_i = R_P - [\text{Shell Thickness}] \tag{2.11}$$

Writing Equation (2.10) for the three different sets of particles and solving for an equal shell length:

- Const.≈ 130 mg/μm^3, with a sum of relative deviations of 2%
- Shell Thickness = 77.6 μm

Based on a 77.6μm shell, Table 2.3 presents, for each particle size, the volume occupied by the enzyme shell. For 240 μm particles, the volume of the shell represents more than 95% of the total volume of the particle; this can reasonably be assumed enough to ensure that, for this particle size, the amount of catalyst withdrawn to perform the reactions is representative of the composition of the entire crushed sample.

Table 2.3. Fraction of particle that contains enzyme for each particle size, assuming a shell of 77μm.

Average Particle Size (μm)	Fraction of support that contains enzyme (%v/v)
460	70.9
360	81.6
240	95.6

In the case of the 360 μm particles, to ensure that the proportion of enzyme/support is the same in each experiment, only the required amount of catalyst that was going to be used in each reaction was crushed and fed to the reactor. The results obtained in this way are also shown in Figure 2.5 and indicate a large enhancement of the reaction rate due to the conse-

quent reduction of the particle size. The results of the experiments with crushed particles should be independent of the particle size; the slight differences in the reaction rate obtained with 240 μm particles when compared with 360 μm particles could be associated with the experimental procedure as some catalyst is always lost during the crushing/reactor feeding procedure.

The results obtained from the experiments with crushed particles indicate that diffusion limitations exist, despite the fact that the curves obtained for the two sets of larger particles overlap. Full conversion for the reactions performed using crushed Novozym 435 particles was attained in less than half the time necessary when using the intact particles. The results obtained by crushing a large amount of particles seem to indicate that while the larger particles exhibit an egg-shell distribution, the smaller ones appear to be homogeneous. This observation is consistent with the fact that in the latter case, the dimensions of the enzyme outer shell reported by other authors (Mei et al. 2003) are of the same order of magnitude of the particle radius. Additionally, from a rough calculation it was possible to estimate that, in the case of 240 μm particles, the outer shell represents more than 95% of the total volume of the particle.

Although the curves presented for the 360 μm and 460 μm particles overlap, despite the existence of internal mass transfer resistances, the results obtained with 240 μm particles already indicate an increase in the reaction rate. This behavior may then be associated with the internal distribution of the enzyme, since a change occurs when the particle radius becomes of the same order of magnitude of the enzyme outer shell and thus, the enzyme distribution apparently becomes homogeneous.

2.3.4 KINETIC MODELING AND KINETIC PARAMETER DETERMINATION

2.3.4.1 KINETIC MODEL

The Ping-pong bi-bi model is widely used to describe the kinetics of transesterification reactions (Yahya et al. 1998; Yadav and Devi 2004; Zhang et al. 2004; Zhang et al. 2005). According to this ordered mechanism (Figure 2.6), the ester firstly binds to the active site of the enzyme, and the first product is released (bi-product), leading to the formation of a substrate altered enzyme complex. The alcohol then binds to this complex and the second product (main product) is formed and released, returning the enzyme to its native state.

Considering this mechanism, the reaction rate, *R*, can be described by Equation (2.12). The equation parameters are described in Table 2.4.

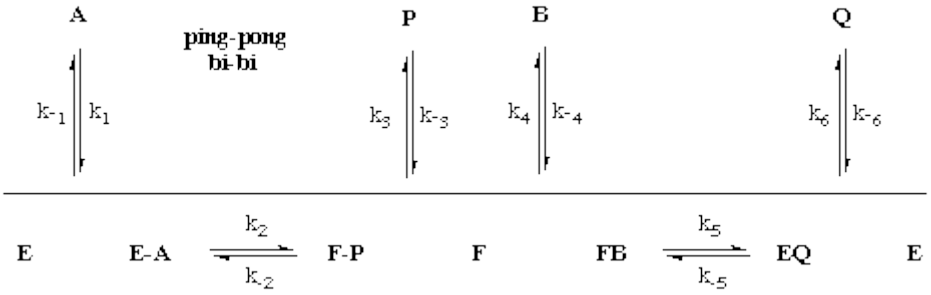


Figure 2.6. Ping-pong bi-bi kinetic mechanism

$$R = \frac{V_{\max f} V_{\max r} \left([A][B] - \frac{[P][Q]}{K_{eq}} \right)}{V_{\max r} K_{MB} [A] + V_r K_{MA} [B] + \frac{V_{\max f} K_{MQ} [P]}{K_{eq}} + \frac{V_{\max f} K_{MP} [Q]}{K_{eq}} + V_r [A][B] + \frac{V_{\max f} K_{MQ} [A][P]}{K_{eq} K_{iA}} + \frac{V_{\max f} [P][Q]}{K_{eq}} + \frac{V_{\max r} K_{MA} [P][Q]}{K_{iq}}} \quad (2.12)$$

Table 2.4. Parameters of the Ping-pong bi-bi rate equation.

Parameter	Designation	Physical meaning
$V_{max\ f}$	Maximum forward reaction rate	Limiting rate of the forward reaction
$V_{max\ r}$	Maximum reverse reaction rate	Limiting rate of the reverse reaction
K_{eq}	Equilibrium constant	$\frac{[P][Q]}{[A][B]}$
K_{MA}	Michaelis constant for component A	Concentration of A such that R = $V_{max\ f}/2$ at saturating B and zero P and Q
K_{MB}	Michaelis constant for component B	Concentration of B such that R = $V_{max\ f}/2$ at saturating A and zero P and Q
K_{MP}	Michaelis constant for component P	Concentration of P such that R = $-V_{max\ r}/2$ at zero A and B and saturating Q

K_{MQ}	Michaelis constant for component Q	Concentration of Q such that R = $-V_{max\ r}/2$ at zero A and B and saturating P
K_{iA}	Inhibition constant for component A	Inhibition const. of A acting on the reverse reaction (Competition with P and Q)
K_{iQ}	Inhibition constant for component Q	Inhibition const. of Q acting on the forward reaction (Competition with A and B).

Although there are 9 parameters on the Ping-pong bi-bi reaction rate equation, some of them can usually be neglected if the enzyme has significantly higher affinity for some of the components or if there are large differences in their concentrations. In the simplest case, when the affinity of the enzyme for the substrates is much higher than the affinity for the products, the following simplified equation can be used instead to describe the reaction rate:

$$R = \frac{V_{\max}\left([A][B] - \frac{[P][Q]}{K_{eq}}\right)}{K_{MB}[A] + K_{MA}[B] + [A][B]} \tag{2.13}$$

Equation (2.13) can be further simplified if the concentration of the reactants is much higher than the concentration of the products, *i.e.* at the beginning of the reaction; in this case, Equation (2.13) is reduced to the initial reaction rate, R^0:

$$R^0 = \frac{V_{max}}{\frac{K_{MA}}{[A]} + \frac{K_{MB}}{[B]} + 1} \tag{2.14}$$

For esterifications/transesterifications, an additional competitive inhibition step is usually added to the ping-pong bi-bi kinetic mechanism since the alcohol can also compete with the acid/ester in binding to the enzyme in its native state but no product is formed:

$$R^0 = \frac{V_{max}}{\frac{K_{MA}}{[A]}\left(1 + \frac{[B]}{K_I}\right) + \frac{K_{MB}}{[B]} + 1} \tag{2.15}$$

where K_I represents the competitive inhibition constant.

When vinyl acetate is used as a reactant, the first product formed is vinyl alcohol that quickly tautomerizes to acetaldehyde, making the overall transesterification irreversible (Yadav and Trivedi 2003). This is consistent with the experimental results shown in Section 2.3.3 above, where full conversions were always obtained. Hence, in this case the reversibility term, $\frac{[P][Q]}{K_{eq}}$, is always negligible. Regarding the other terms, they will only be negligible if the affinity of the enzyme towards the substrates is sufficiently higher than towards the products. If this assumption is fully verified, Equation (2.15) might not be limited to the initial period of the reaction and successfully describe the entire reaction process. As a first approach, the capacity of Equation (2.15) to describe the reaction process will be tested; if this equation fails, additional terms will be introduced based on the obtained results.

2.3.4.2 DETERMINATION OF THE CONCENTRATION BASED INTRINSIC KINETIC PARAMETERS

To determine the reaction kinetics and its kinetic parameters several reactions were performed with different initial reactant concentrations. To avoid the influence of internal mass transfer all experiments were performed using crushed particles, obtained from the 240μm group.

Equation (2.15) presents 4 parameters: the maximum forward reaction rate, V_{max}, the Michaelis constants, K_{MA} and K_{MB}, and the competitive inhibition constant K_I. With 4 parameters, it is common to find several sets of parameters that satisfactorily describe the reaction process in the studied range of concentrations. Most of these sets, however, will be of limited applicability outside the range of concentrations over which they were determined. To ensure a broader applicability it is useful, when possible, to create conditions to determine the kinetic parameters independently, by analyzing specific limiting cases in the equation of the reaction rate.

Equation (2.15) can be further simplified by raising the concentration of one of the reactants, possibly eliminating its influence and also the influence of part of the kinetic parameters. If the concentration of vinyl acetate is much larger than the concentration of decanol, Equation (2.15) simplifies to:

$$R = \frac{V_{max}}{\frac{K_{MB}}{[B]} + 1} \qquad [A] >> [B] \tag{2.16}$$

From Equation (2.16), provided that the concentration of vinyl acetate is sufficiently larger than the concentration of decanol, the reaction rate becomes independent of the concentration of the reacting ester, depending only on two parameters: V_{max} and K_{MB}. It is worth noting that if $\frac{K_{MB}}{[B]}$ is much larger than 1, then V_{max} and K_{MB} cannot be determined independently, since Equation (2.16) becomes a first order reaction rate equation on decanol with reaction constant $\frac{V_{max}}{K_{MB}}$:

$$R = \frac{V_{max}}{K_{MB}}[B] \qquad \text{and} \qquad [A] >> [B] \qquad K_{MB} >> [B] \tag{2.17}$$

On the other hand, if the concentration of decanol is much larger than the concentration of vinyl acetate, Equation (2.15) becomes:

$$R = \frac{V_{max}}{\frac{K_{MA}}{[A]} + \frac{K_{MA}}{K_I}\frac{[B]}{[A]} + 1} \qquad [B] >> [A] \tag{2.18}$$

In this case, however, unless inhibition by decanol is negligible, the reaction rate will still depend on the concentration of both reactants, and on three parameters: K_{MA}, K_I and V_{max}. Again, it is possible that V_{max} and, in this case, K_{MA} might not be independently determined; if $\frac{K_{MA}}{[A]} + \frac{K_{MA}}{K_I}\frac{[B]}{[A]}$ is much larger than 1, Equation (2.18) becomes:

$$R = \frac{V_{max}}{\frac{K_{MA}}{[A]} + \frac{K_{MA}}{K_I}\frac{[B]}{[A]}} \quad \text{and} \quad [B] >> [A] \quad \text{and} \quad K_{MA} + \frac{K_{MA}}{K_I}[B] >> [A] \tag{2.19}$$

and only the lumped parameter K_{MA}/V_{max} can be obtained.

The experimental results obtained while varying the concentration of each reactant individually (shown in Figure 2.7) were qualitatively consistent with this model, since the reaction is inhibited by larger concentrations of the alcohol and enhanced by higher concentrations of vinyl acetate. Moreover, when fixing the initial concentration of decanol and increasing the initial concentration of vinyl acetate, the conversion curves practically overlapped, indicating that the concentration of vinyl acetate no longer influenced the reaction rate, as predicted by Equations (2.16) or (2.17). The curve obtained with an initial concentration of vinyl acetate of 1.2 M appears to be slightly slower than the curve obtained with 1M, which could be associated to small experimental deviations. As a result of the competitive inhibition by decanol, fixing the concentration of vinyl acetate and increasing decanol has an adverse effect in the reaction rate; in this case, as predicted by Equations (2.18) or (2.19), the reaction rate remains a function of the concentration of decanol.

The validity of Equation (2.15) also depends on the enzyme having a significantly larger affinity for the reactants than for the products, or in this particular case, given the tautomerization of vinyl alcohol to acetaldehyde, for decyl acetate. To test this hypothesis, two reactions were performed with an initial amount of decyl acetate in the reaction medium, in order to amplify its possible effect. The results obtained, shown in Figure 2.8, do not indicate any significant detectable influence of decyl acetate in the reaction rate.

As it was previously shown, the specific enzyme loading depends of the particle size. Additionally it is possible that the amount of immobilized enzyme also depends on the commercial lot used. To ensure that the kinetic parameters obtained were independent of the particle size and could be used for Novozym 435 particles with different specific enzyme loadings, care was taken to express the reaction rate in terms of the mass of enzyme instead of the total mass of the catalyst particles.

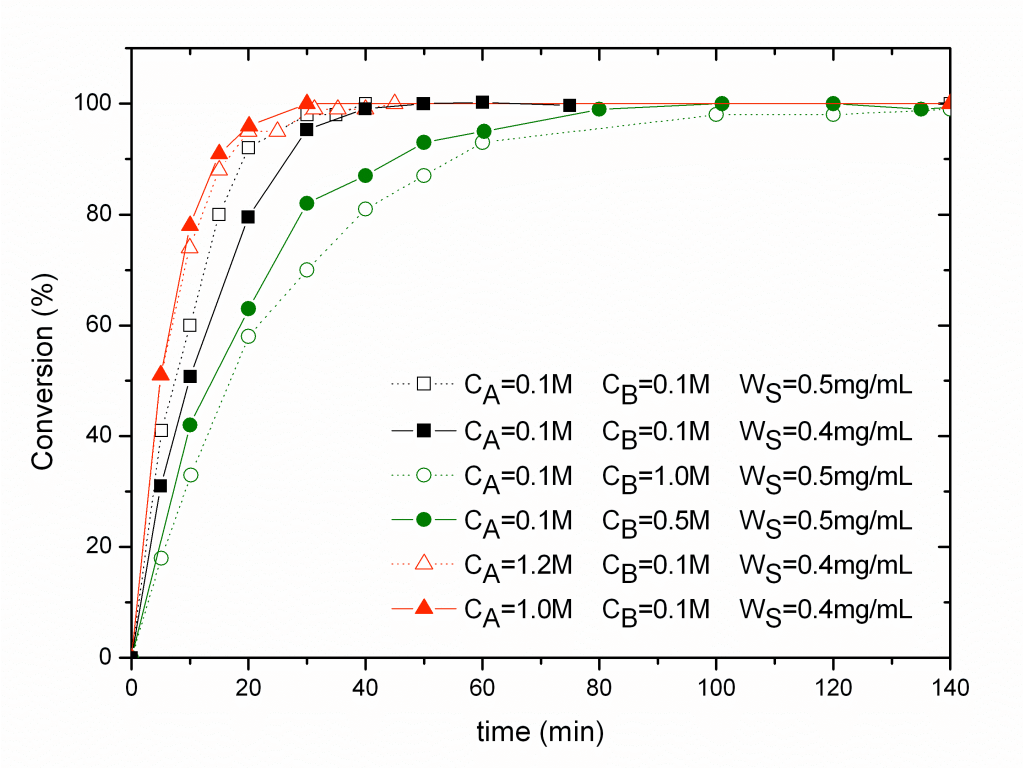


Figure 2.7. Effect of the initial concentrations of vinyl acetate (red triangles) and decanol (green circles). T=30 ºC and crushed Novozym 435 particles used for all essays.

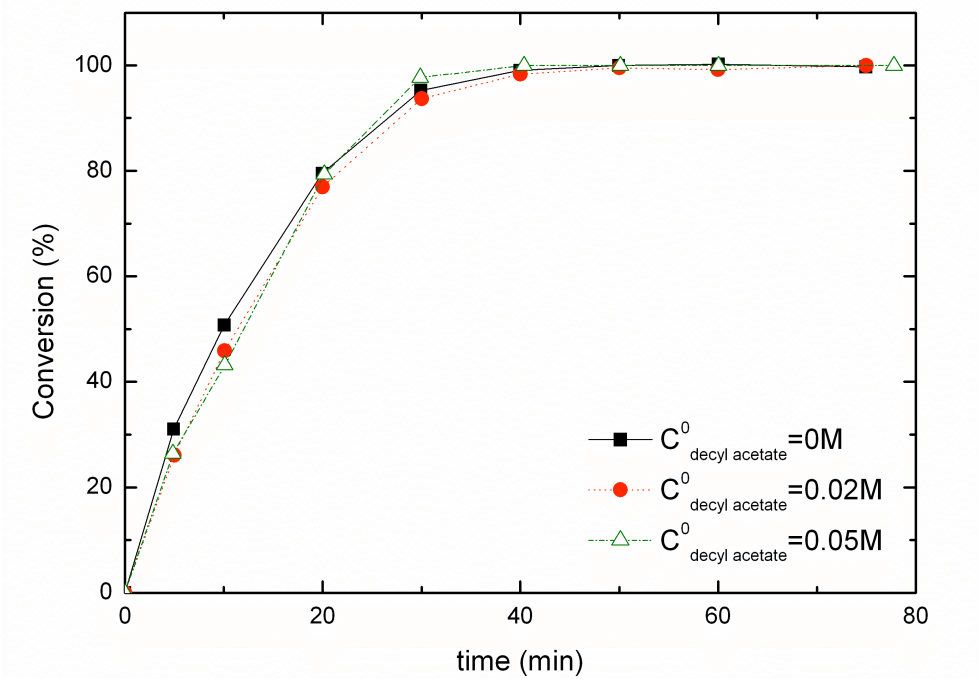


Figure 2.8. Effect of the initial concentration of decyl acetate. T=30 ºC, C_A=C_B=0.1 M, W_S=0.4 mg/mL and crushed Novozym 435 particles used for all essays.

The kinetic parameters can then be determined by fitting this model to the experimental data, through minimization of the sum of the squared residues (SSQ):

$$SSQ = \left(\frac{C_{EXP} - C_{CALC}}{C_{EXP}} \right)^2 \qquad (2.20)$$

An adaptive random search optimization algorithm was used (Salcedo et al. 1990; Salcedo 1992). More than 100 data points were used in the optimization, covering a range from 0.1 M until 1.25 M initial concentrations of each reactant.

To reduce the number of parameters to be fitted simultaneously, the optimization was started by fitting the limiting cases when the concentration of one of the reactants is much larger than the concentration of the other, represented by Equations (2.16) ([A]>>[B]) and (2.18) ([B]>>[A]).

As shown in Figure 2.7, for an initial concentration of decanol of 0.1 M, an initial concentration of vinyl acetate ten times larger is enough to ensure that the reaction rate is apparently independent of this substrate. This type of data was firstly used to estimate V_{max} and K_{MB} (Equation (2.16)).

Data from experiments where the initial concentration of decanol was larger than the initial concentration of vinyl acetate were then used to estimate K_{MA} and K_I (Equation (2.18)).

The parameters obtained as described above were then applied as initial guesses for the complete estimating procedure. The parameters did not vary considerably from their initial guesses. The parameters obtained in this way are presented in Table 2.5.

Table 2.5. Kinetic constants for the Novozym 435 catalysed transesterification reaction of vinyl acetate with decanol in hexane at 30ºC.

Parameter	Value*
V_{max} (mol/g_{Enz}.min)	0.909
K_{MA} (M)	0.604
K_{MB} (M)	0.195
K_I (M)	0.912
SSQ/N_{points} (M^2)	3.6×10^{-2}

*Cases where $[A]^0=[B]^0$ were not included in the optimization because of the findings described below. In this case, no set of parameters was found that could describe all the experiments performed.

Figure 2.9 and Figure 2.10 compare the experimental results with the calculated values given by Equation **Error! Reference source not found.**, using the concentration based kinetic parameters presented in Table 2.5.

Using Equation (2.15), a concentration based kinetic equation, good results were obtained in the range of initial concentrations between 0.1 and 1.25 M for both substrates, except for the cases where the initial concentrations of vinyl acetate and decanol are equal.

The model is in good agreement with the experimental results as long as the initial concentrations of both reactants are not the same. When the initial concentrations of vinyl acetate and decanol are both 0.1 M, the calculated results correspond to lower reaction rates than the ones observed experimentally. The reaction rates obtained experimentally would be consistent with a more concentrated reaction medium. When the initial concentrations are set at 0.5M, the model predicts the experimental results reasonably well, but some differences are observed throughout the reaction, especially between 30% and 90% conversion; the results seem to indicate a tendency for the reaction to proceed more slowly than the model predicts.

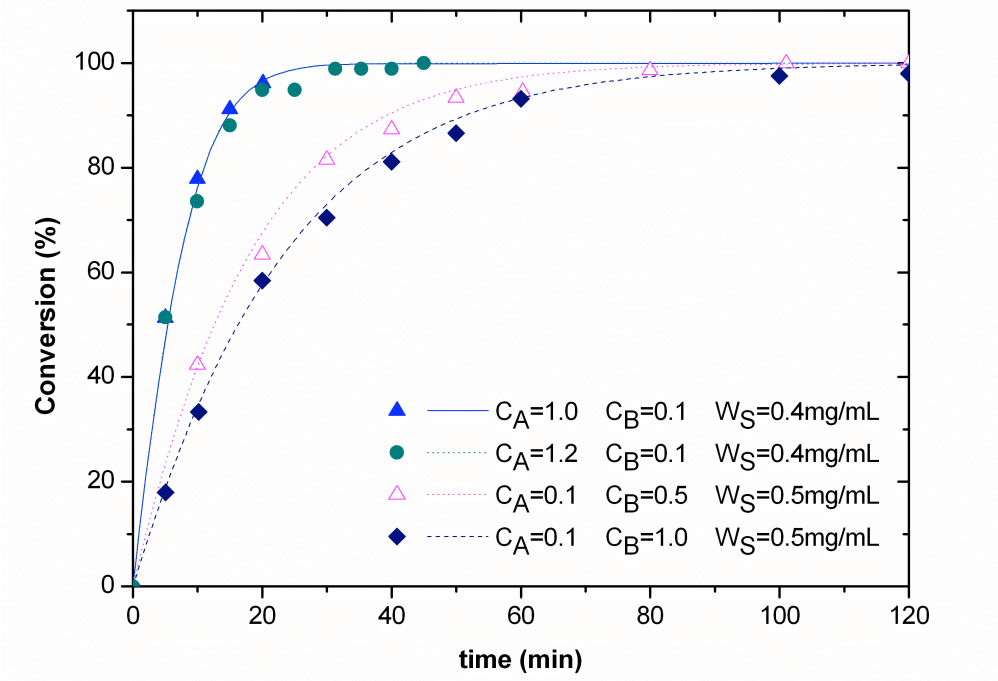


Figure 2.9. Experimental *vs.* simulated results for different initial concentrations of vinyl acetate and decanol. T=30 ºC and crushed Novozym 435 particles used for all essays.

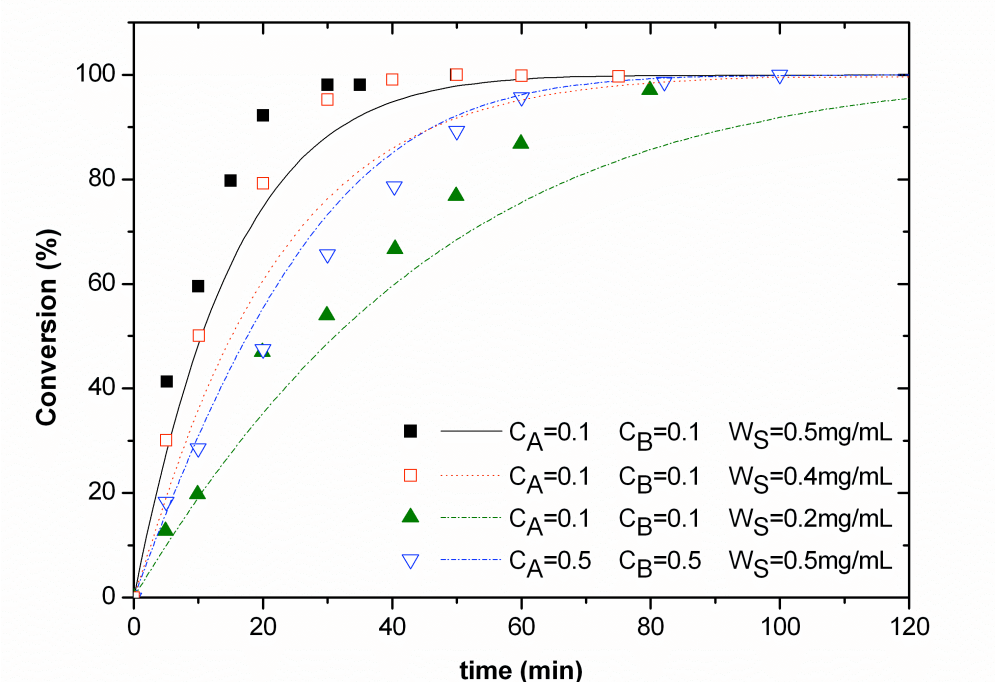


Figure 2.10. Experimental *vs.* Simulated results for equimolar initial concentrations of vinyl acetate and decanol. T=30 ºC and crushed particles used for all essays.

The difference in polarity between decanol and the other components makes the reaction mixture non-ideal. In fact, the activity coefficient of decanol is expected to be higher for more diluted solutions, which is consistent with some of the differences that were found between the experimental and predicted reaction rates for [A]=[B]=0.1 M. If the observed differences are the result of the thermodynamic non-ideality of the reaction medium, then an activity based kinetic equation would be more suitable to express the reaction rate.

2.3.4.3 DETERMINATION OF THE ACTIVITY BASED INTRINSIC KINETIC PARAMETERS

In the previous section, it was shown that the concentration based kinetic equation derived from the Ping-pong bi-bi model with competitive inhibition by the alcohol was not able to satisfactorily describe the reaction throughout the entire range of concentrations that were tested experimentally. As this might be related to the thermodynamic non-ideality of the reaction medium, Equation (2.21), the activity based version of the Ping-pong bi-bi kinetic equation with competitive inhibition by decanol, was introduced to describe the reaction rate:

$$R = \frac{V^a_{max}}{\frac{K^a_{MA}}{a_A}\left(1 + \frac{a_B}{K^a_I}\right) + \frac{K^a_B}{a_B} + 1} \tag{2.21}$$

where a_i stands for the activity of component I in the liquid phase and the superscript a indicates an activity based parameter.

This kinetic equation is valid if the activity coefficients for the enzyme, its complexes and transition states are either constant over the entire range of concentrations or if they all have similar values (Straathof et al. 1992). In the first case, as the activity coefficients might not necessarily be equal, the kinetic constants would become lumped parameters that include a ratio of the activity coefficients of either the enzyme or one of its complexes and the respective transition state.

Activities can be calculated by means of activity coefficients:

$$a_i = \gamma_i x_i \tag{2.22}$$

In turn, activity coefficients can be calculated by several methods. The modified UNIFAC method of Dortmund (Gmehling et al. 1993) was chosen for the calculations. This group contribution model allows a reliable prediction of different thermodynamic properties in wide ranges of temperature and composition. Relatively to the original UNIFAC method, this model generally improves the description of phase equilibria at lower concentrations, which is precisely the region where the concentration based kinetic model fails to predict the experimental results of this work.

Figure 2.11 shows how the calculated activity coefficients of all species evolve throughout the reaction for two different sets of initial conditions.

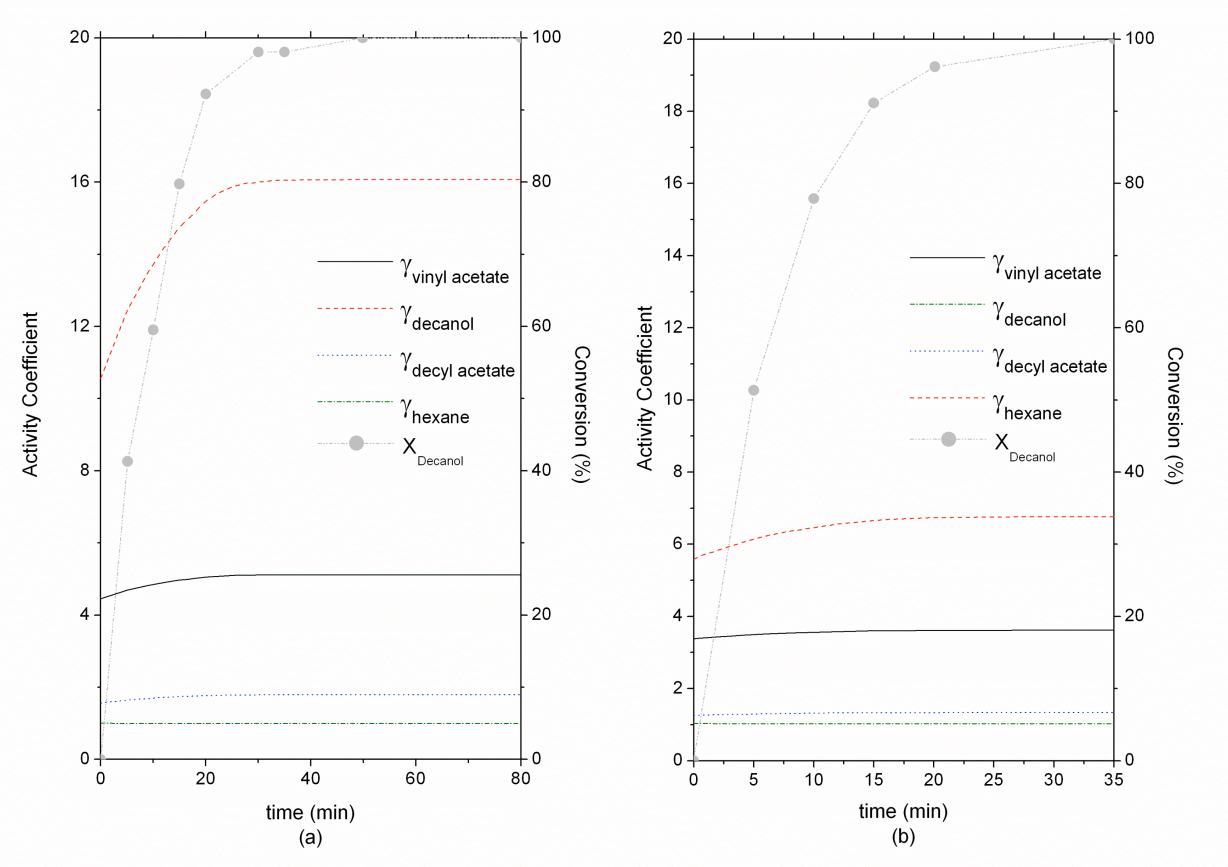


Figure 2.11. Activity coefficients of all species in solution throughout the reaction. **(a)** [A]=[B]=0.1 M, W_S=0.5 mg/mL **(b)** [A]= 1 M, [B]=0.1 M, W_S=0.4 mg/mL.

For the case with initial concentrations [A]=1 M and [B]=0.1 M, the activity coefficients of all species remain practically constant, except for decanol that increases 16%. On the other hand, for initial concentrations [A]=[B]=0.1 M, the case the concentration based model failed to describe, the variation of the activity coefficient of decanol is very accentuated, increasing 50% throughout the reaction. A similar behavior was obtained when calculating the activity coefficients for the several initial conditions presented in the previous section. Figure 2.12 illustrates the variation of the activity coefficients of all species throughout the reaction for several sets of initial conditions.

In terms of reaction rate it is only important to analyze the activity coefficients of the reactants since it was shown previously that the reaction rate can be considered, for this range of concentrations, independent of the concentration of decyl acetate. Of all the experimental conditions tested, the case [A]=[B]=0.1 M is the one where the reactants present higher activity coefficients; the activity coefficient of vinyl acetate is, in this case, nearly two times

larger than in the rest of the experiments and for decanol the difference is even higher. This behavior is expected for polar components, like alcohols or acids, when diluted in non-polar solvents like hexane.

During the three experiments with the same initial concentration of vinyl acetate and decanol the variation of the correspondent activity coefficients of both reactants is also significantly larger. For the case where [A]=[B]=0.5 M, the activity coefficient of decanol increases more than the activity coefficient of vinyl acetate; since the magnitude of the inhibitory effect depends on the ratio $\frac{a_B}{a_A}$, the inhibition will be larger as the reaction proceeds which might explain why the concentration based model seems to predict a higher reaction rate than the one observed experimentally after 30% conversion.

If there is a range of initial conditions over which the same constant activity coefficients can be assumed for each reactant, the concentration based model should be able to describe the behavior of the reaction system. For modeling purposes, in all experiments performed with excess of one of the reactants, the activity coefficient of vinyl acetate could reasonably be assumed constant. In the case of decanol, two situations can be identified:

- For [A] > [B] and [A]=0.1 M and [B]=0.5 M, the activity coefficient of decanol is similar;
- For [A]=0.1 M and [B]≥1 M, the activity coefficient of decanol is much lower; in this case, however, the dominant terms in the reaction rate would be $\frac{K_{MA}}{[A]}$ and $\frac{K_{MA}}{K_I}\frac{[B]}{[A]}$ and this variation could be lumped in the parameter K_I.

An optimization strategy similar to the one used to obtain the concentration based kinetic parameters was thus implemented to obtain the activity based kinetic constants. The values obtained in this way are presented in Table 2.6.

The activity based equation was able to satisfactorily describe the reaction process throughout the entire range of tested concentrations (0.1 M to 1.5 M), indicating that the differences between the experimental data and the predictions obtained with the concentration based rate equation can be related to the thermodynamic non-ideality of the reaction mixture. Figure 2.13 and Figure 2.14 compare the simulations with the experimental results.

Table 2.6. Activity based kinetic constants for the Novozym 435 catalyzed transesterification reaction of vinyl acetate with decanol in hexane at 30 ºC.

Parameter	Activity based value
V_{max} (mol/g_{Enz}.min)	0.542
K_{MA} (M)	0.0862
K_{MB} (M)	0.0788
K_I (M)	0.125
SSQ/N_{points} (M^2)	$3.9x10^{-2}$

Regarding the reactions performed with excess of vinyl acetate, the model predicts that for high concentrations of this substrate the reaction rate will begin to decrease slightly. For these conditions, the concentration based kinetic mechanism would simplify to Equation (2.16), predicting that the reaction rate would become independent of the concentration of vinyl acetate. Following the same approach using the activity based rate equation, for [A]>>[B] it reduces to:

$$R = \frac{V_{max}}{\frac{K_{MB}^{a}}{a_B} + 1} \qquad [A] >> [B] \tag{2.23}$$

Similarly to Equation (2.16), from Equation (2.23), increasing the concentration of vinyl acetate above a certain level would not have a direct impact in the reaction rate; however, in this case, a higher concentration of this substrate will decrease the activity coefficient of decanol, ultimately decreasing the reaction rate. Another experiment was performed to confirm this behavior with a higher concentration of vinyl acetate. The result is shown in Figure 2.13 and again, the model predicts a slightly lower reaction rate. Regarding the experimental results it is not evident given the close proximity of the data points, but the conversion curves seem to exhibit this behavior as well.

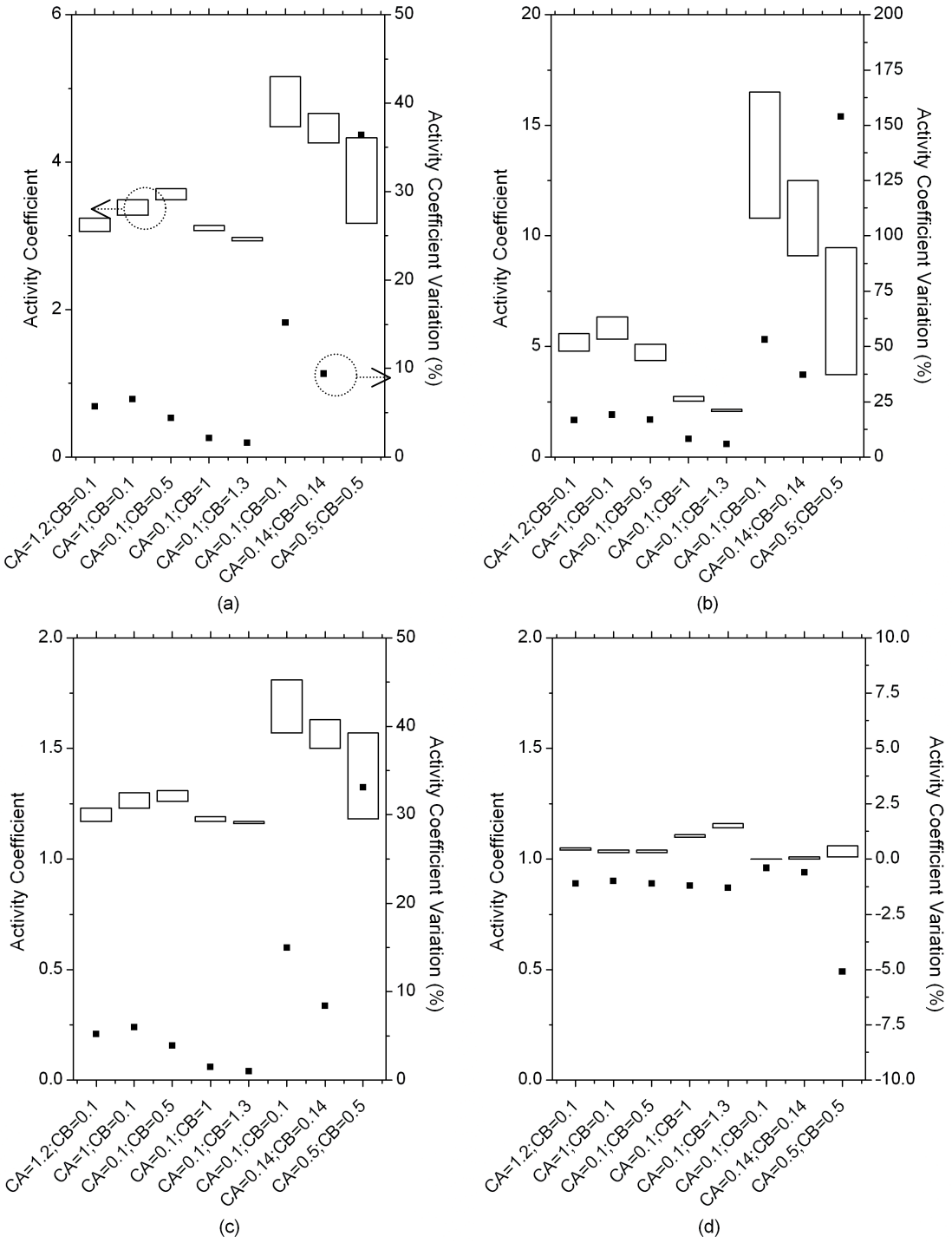


Figure 2.12. Initial and final activity coefficient (bars) and percentage variation (■) throughout the reaction for several sets of initial conditions **(a)** vinyl acetate **(b)** decanol **(c)** decyl acetate **(d)** hexane.

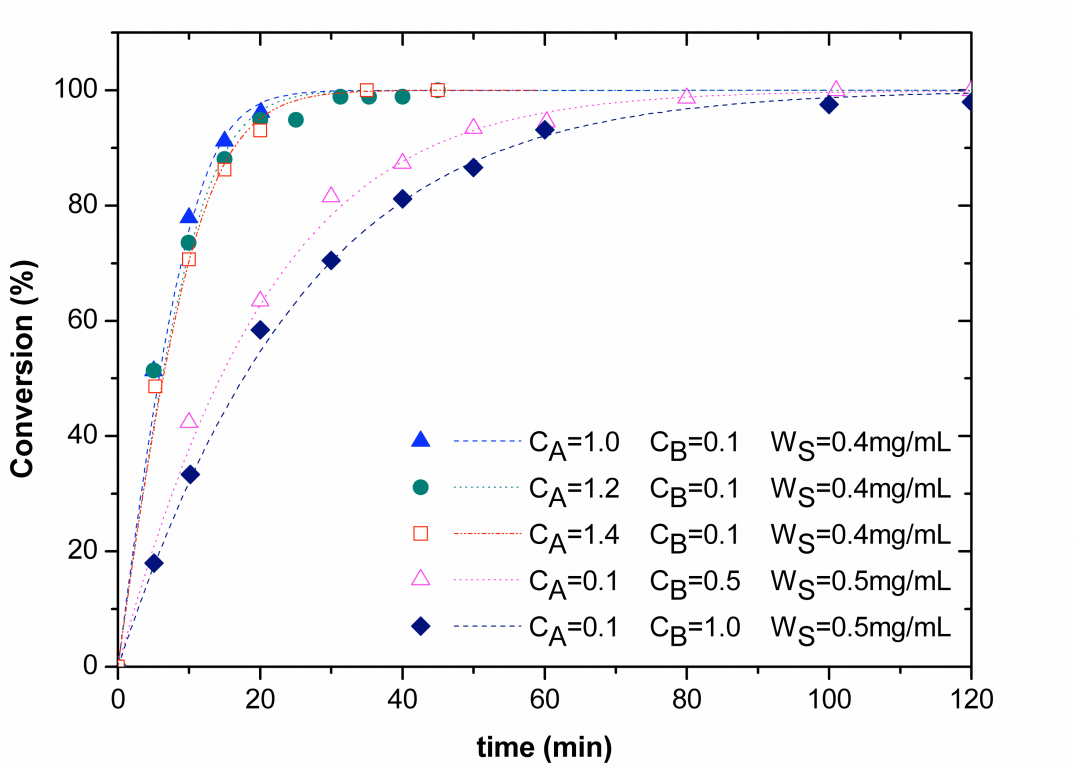


Figure 2.13. Experimental *vs.* simulated results using the activity based kinetic equation for different initial concentrations of vinyl acetate and decanol. T=30 ºC and crushed particles used for all essays.

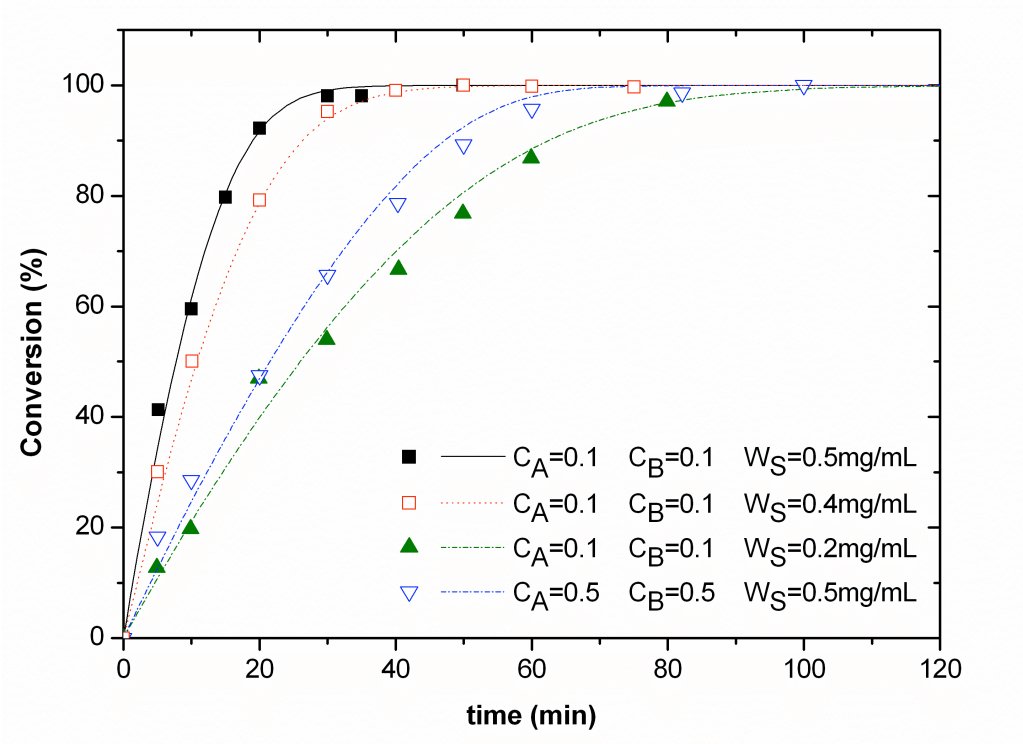


Figure 2.14. Experimental vs. simulated results using the activity based kinetic equation for equimolar initial concentrations of vinyl acetate and decanol. T=30 ºC and crushed particles used for all essays.

2.4 CONCLUSIONS

The transesterification of vinyl acetate and decanol in hexane catalyzed by Novozym 435 was studied, with particular emphasis on the influence of internal diffusion, enzyme distribution, specific enzyme loading and the determination of the intrinsic kinetic parameters.

A preliminary enzyme screening was made using several enzymes from two major biocatalyst suppliers, Amano Inc. and Novozymes. Novozym 435 was the most active catalyst for the transesterification of vinyl acetate and decanol and was chosen to perform all subsequent work.

It was shown that the specific enzyme loading of Novozym 435 increases as the particle size decreases. As a consequence, care should be taken to ensure that this does not affect mass transfer studies by using the same enzyme amount instead of the same mass of catalyst particles.

Specific enzyme loading measurements were performed for catalyst particles of different sizes, showing that smaller particles present higher enzyme content ($g_{Enzyme}/g_{Particle}$). The specific enzyme loadings are consistent with an egg-shell intraparticle enzyme distribution, with an enzyme outer layer of c.a. 80 μm.

Diffusion limitations were shown to exist but could be eliminated by reducing the particle size through crushing. The first results however could be misleading as the egg-shell distribution of the enzyme inside the particles seems to influence the results obtained with different particle sizes. Evidence of internal diffusion limitations is particularly visible as the enzyme distribution appears to become homogeneous (by sufficiently decreasing the particle size) or the particles are crushed. In the latter case, the time required to reach full conversion is reduced to less than half.

Finally, the intrinsic kinetic parameters of the reaction were calculated, according to a Ping-pong bi-bi kinetic model with competitive inhibition by the alcohol. The determination was performed in the absence of diffusion limitations, which was accomplished by crushing the catalyst particles.

The rate equation typically used for initial reaction rates was found to describe the complete reaction. This is due to the fact that when using vinyl acetate as a reactant for transesterification reactions, the tautomerization of the first product that is formed, vinyl alcohol, to acetaldehyde makes the reaction irreversible. Additionally, the enzyme presents a

higher affinity towards the reactants than towards the products, and the latter do not influence the reaction rate in the range of concentration that was used.

When using a concentration based rate equation, it was not possible to describe the reaction across the entire range of concentrations tested (0.1-1.25 M of each reactant). The model failed to describe the cases in which an equal concentration of both reactants was used. The differences were particularly notorious in the case of low concentration of both reactants (0.1 M:0.1 M), were the model predicted faster reaction rates than the ones obtained experimentally. It was shown using the Modified UNIFAC Model of Dortmund, that the activity coefficients of both species vary with the composition of the reaction mixture, for the range of concentrations experimentally used, with a significant impact in the reaction rate that was not accounted for with a concentration based rate equation. Additionally, the activity coefficients of both reactants were considerably higher in the cases the model failed to describe, which could account for the deviations. This is a typical behavior given the difference in polarity between decanol and the other components.

.The corresponding activity based kinetic equation was found to satisfactorily describe the reaction. The activity based kinetic equation correctly accounts for the thermodynamic non-ideality of the reaction mixture, which makes it more suitable to describe this reaction process due to the differences in polarity of the components.

2.5 NOMENCLATURE

[i]	Concentration of component i (M)
A	Vinyl acetate
a_i	Activity of component i
B	Decanol
Bim	Biot number for mass transfer
C_i	Concentration of component i (M)
De	Effective diffusivity (cm^2/s)
d_p	Particle diameter (μm)
K_{eq}	Equilibrium constant
k_f	Mass transfer coefficient between the liquid and the catalyst surface (cm/s)
K_I	Competitive inhibition constant (M)
K_{ii}	Inhibition constant for component i (M)
K_{Mi}	Michaelis constant for substrate i (M)
N_{Points}	Number of experimental points used in the optimization

R	Reaction rate (mol/g_{enzyme}.min or mol/$g_{catalyst}$.min)
Re	Reynolds number
R_p	Particle radius (μm)
Sc	Schmidt number
Sh	Sherwood number
SSQ	Sum of the squared residues
T	Temperature (ºC)
t	Time (min)
V_L	Volume of the liquid phase in the reactor
V_{max}	Maximum forward reaction rate (mol/g_{Enzyme}.min)
$V_{max,f}$	Maximum forward reaction rate (mol/g_{Enzym}e.min)
$V_{max,r}$	Maximum reverse reaction rate (mol/g_{Enzyme}.min)
W_E	Specific enzyme loading ($g_{Enzyme}/g_{catalyst\ particles}$)
W_{Enzyme}	Amount of enzyme within the reactor (mg/mL)
W_S	Amount of catalyst particles within the reactor (mg/mL)
X_i	Conversion of component i (%) or group mole fraction of group i
x_i	mole fraction of component i

Greek Symbols

γ_i	Activity coefficient of component i
τ_D	Internal diffusion time constant (s)
τ_F	Film diffusion time constant (s)

Subscripts

A	Vinyl Acetate
B	Decanol
P	First product of the transesterification (alcohol – vinyl acohol)
Q	Second product of the transesterification product (ester – decyl acetate)

Superscripts

0	Initial
a	Activity based

2.6 BIBLIOGRAPHY

Almeida, M. C., Ruivo, R., Maia, C., Freire, L., de Sampaio, T. C. and Barreiros, S. (1998). Novozym 435 activity in compressed gases. Water activity and temperature effects. Enzyme and Microbial Technology 22 (6): 494-499.

Chen, B., Miller, E. M., Miller, L., Maikner, J. J. and Gross, R. A. (2007). Effects of macroporous resin size on *Candida antarctica* lipase B adsorption, fraction of active molecules, and catalytic activity for polyester synthesis. Langmuir 23 (3): 1381-1387.

Clark, D. S., Bailey, J. E. and Do, D. D. (1985). Mathematical model for restricted diffusion effects on macromolecule impregnation in porous supports. Biotechnology and Bioengineering 27 (2): 208-213.

Froment, G. F. and Bischoff, K. B. (1990). Chemical reactor analysis and design (Second Edition). New York, John Wiley and Sons.

Garcia-Alles, L. F. and Gotor, V. (1998). Lipase-catalyzed transesterification in organic media: Solvent effects on equilibrium and individual rate constants. Biotechnology and Bioengineering 59 (6): 684-694.

Gmehling, J., Li, J. and Schiller, M. (1993). Modified UNIFAC model. 2. Present parameter matrix and results for different thermodynamic properties. Industrial & Engineering Chemistry Research 32 (1): 178-193.

Hari Krishna, S. and Karanth, N. G. (2001). Lipase-catalyzed synthesis of isoamyl butyrate - A kinetic study. Biochim. Biophys. Acta (BBA)/Protein Structure and Molecular Enzymology 1477 (2): 262-267.

Hossain, M. M., Do, D. D. and Bailey, J. E. (1986). Immobilization of enzymes in porous solids under restricted diffusion conditions. AIChE Journal 32 (7): 1088-1098.

Kirk, O. and Christensen, M. W. (2002). Lipases from *Candida antarctica*: unique biocatalysts from a unique origin. Organic Process Research & Development 6: 446-451.

Lowry, O. H., Rosenbrough, N. J., Farr, L. and Randal, R. (1951). Protein measurement with Folin phenol reagent. Journal of Biological Chemistry 193: 265-275.

Mei, Y., Miller, L., Gao, W. and Gross, R. (2003). Imaging the distribution and secondary structure of immobilized enzymes using infrared microspectroscopy. Biomacromolecules 4 (1): 70-74.

Ranz, W. E. and Marshall, W. R. (1952). Evaporation from drops. Chemical Engineering Progress 48: 141-146, 173-178.

Salcedo, R. L. (1992). Solving nonconvex nonlinear programming and mixed-integer nonlinear programming problems with adaptive random search. Industrial & Engineering Chemistry Research 31 (1): 262-273.

Salcedo, R. L., Gonçalves, M. J. and Azevedo, S. F. d. (1990). Improved random-search algorithm for non-linear optimization. Computers and Chemical Engineering 14 (10): 1111-1126.

Straathof, A. J. J., Rakels, J. L. L. and Heijnen, J. J. (1992). Enzyme kinetics in monophasic and biphasic aqueous-organic systems, in J. Tramper, Vermue, M. H., Beeftink, H. H. and Stockar, U. v., Eds. Enzyme kinetics in monophasic and biphasic aqueous-organic systems. Biocatalysis in Non-Conventional Media. Amstedam, Elsevier.

Trubiano, G., Borio, D. and Errazu, A. (2007). Influence of the operating conditions and the external mass transfer limitations on the synthesis of fatty acid esters using a *Candida antarctica* lipase. Enzyme and Microbial Technology 40 (4): 716-722.

van Roon, J. L., Joerink, M., Rijkers, M. P. W. M., Tramper, J., Schroen, C. G. P. H. and Beeftink, H. H. (2003). Enzyme distribution derived from macroscopic particle behavior of an industrial immobilized penicillin-G acylase. Biotechnology Progress 19 (5): 1510-1518.

Yadav, G. D. and Devi, K. M. (2004). Immobilized lipase-catalysed esterification and transesterification reactions in non-aqueous media for the synthesis of tetrahydrofurfuryl butyrate: comparison and kinetic modeling. Chemical Engineering Science 59: 373-383.

Yadav, G. D. and Lathi, P. S. (2004). Synthesis of citronellol laurate in organic media catalyzed by immobilized lipases: kinetic studies. J. Mol. Catal. B: Enzym. 27 (2-3): 113-119.

Yadav, G. D. and Trivedi, A. H. (2003). Kinetic modeling of immobilized-lipase catalyzed transesterification of n-octanol with vinyl acetate in non-aqueous media. Enzyme Microb. Technol. 32 (7): 783-789.

Yahya, A. R. M., Anderson, W. A. and Moo-Young, M. (1998). Ester synthesis in lipase-catalyzed reactions. Enzyme and Microbial Technology 23: 438-450.

Zhang, J., Wu, J. and Yang, L. (2004). The kinetic study on lipase-catalyzed asymmetric alcoholysis of a-cyano-benzyl acetate in organic media. J. Mol. Catal. B: Enzym. 31: 67-72.

Zhang, T., Yang, L. and Zhu, Z. (2005). Determination of internal diffusion limitation and its macroscopic kinetics of the transesterification of CPB alcohol catalyzed by immobilized lipase in organic media. Enzyme and Microbial Technology 36 (2-3): 203-209.

3. PRODUCTION OF DECYL ACETATE IN A BATCH REACTOR: MODELING AND SIMULATION

In this section, a batch reactor model is developed, taking into account the effect of internal and external mass transfer resistances, the heterogeneous intraparticle distribution of the enzyme and the thermodynamic non-ideality of the reaction mixture. Several experiments are performed in a batch reactor with catalyst particles of different sizes, amount of catalyst in the reactor and different initial concentrations of both substrates to test the capability of the model to predict the obtained results, without fitting any parameter. A steady-state model based on the same assumptions is also developed to perform an analysis of the influence of each of the model's parameters and different intraparticle enzyme distributions.

3.1 EXPERIMENTAL METHODS

3.1.1 ENZYMES AND CHEMICALS

Vinyl acetate, decanol and decyl acetate were obtained from Sigma-Aldrich (>99%). Hexane was purchased from Merck (pro-analysis). Novozym 435 was gently provided by Novozymes.

3.1.2 GENERAL METHOD FOR EXPERIMENTS IN BATCH REACTOR

All reactions were performed in magnetically stirred jacketed reactors of 100 mL capacity, at 30 ºC, 40 mL reaction volume and with hexane as the solvent. When relevant to the analysis, the magnetic bars were padded with soft paper to ensure that the particle size was maintained constant throughout the reaction.

Novozym 435 particles were separated in classes of different sizes through sieving. When particle crushing was necessary, it was either performed with a pestle (for small quantities) or by means of a magnetic stirrer bar.

To assess if the reaction could proceed in the absence of the catalyst, blank runs were also performed for 24 hours, maintaining all conditions but without any catalyst and no conversion was detected.

The occurrence of side reactions was ruled out since no additional peaks were detected in the chromatographic analysis and the amount of decyl acetate formed was always consistent with the decrease in concentration of the limiting reactant.

3.1.3 ANALYTICAL METHODS

Several 200 μL samples were withdrawn throughout the reactions and analyzed by gas chromatography in a Varian CP-3800 GC equipped with a TCD detector and auto sampler. A 25 m x 0.53 mm WCOT column was used in the analysis and the calibration was made with synthetic mixtures of the pure components. The operating temperatures were 270 ºC for the injector, 165 ºC for the column oven and 340 ºC for the TCD filament and helium was used as the carrier gas. All data presented are the average of three measurements.

3.2 BATCH REACTOR MODEL DEVELOPMENT

3.2.1 KINETIC MECHANISM

In the previous section, it has been shown that the kinetics of the transesterification reaction of vinyl acetate with decanol could be satisfactorily described by a simplified form of the Ping-pong bi-bi mechanism with inhibition by the alcohol, over a wide range of concentrations, as long as an activity based kinetic equation was used:

$$R = \frac{V_{max}^{a}}{\frac{K_{MA}^{a}}{a_A}\left(1+\frac{a_B}{K_I^{a}}\right)+\frac{K_B^{a}}{a_B}+1} \tag{3.1}$$

Unless otherwise stated, the values of the intrinsic kinetic constants in Equation (3.1) that will be used in the subsequent simulations are the ones presented in the previous section (Table 2.6).

3.2.2 INTRAPARTICLE MATERIAL BALANCE

The backbone of the model definition is the simultaneous reaction-diffusion phenomena occurring inside the pores of the catalyst particles. In general, before reaching the external surface of the catalyst particles, the substrates must firstly diffuse from the bulk medium across a stagnant layer of fluid. In batch reactors, the influence of external diffusion can usually be eliminated by increasing agitation above a certain level, nevertheless external diffusion limitations will be included in the model to maintain a broader range of applicability.

The present model is, thus, based on the following assumptions:

i) The enzyme is immobilized inside particles of radius R_P;

ii) The substrate's diffusion inside the particles can be described by Fick's first law and the diffusivities are constant inside the support (i.e. are independent of the composition of the medium in the range of concentrations that are verified inside the support);

iii) The bulk phase is perfectly mixed and the batch reactor is isothermal;

iv) The enzyme's activity is constant throughout the process.

v) The kinetic mechanism of the reaction can be described by the Ping-pong bi-bi mechanism with competitive inhibition by the alcohol.

In Novozym 435 the enzyme is immobilized in spherical particles of a poly(methyl metacrylate) based resin. Given the symmetry of such geometry, the intraparticle material balance equations for each substrate only need to be solved in the radial dimension and assume the following form:

$$\varepsilon_p \frac{\partial c_i}{\partial t} = \varepsilon_p D_{pi} \frac{1}{r^2} \frac{\partial}{\partial r}\left(r^2 \frac{\partial c_i}{\partial r} \right) - RW_E(r)\,\rho_{app} \tag{3.2}$$

where c_i represents the concentration of substrate i, t the reaction time, r the radial position inside the particle, ε_P the particle porosity, D_{pi} the diffusion coefficient of species i inside the pores, $W_E(r)$ the enzyme distribution inside the support, ρ_{app} the apparent density of the particle and R the reaction rate.

$W_E(r)$ yields the mass of enzyme immobilized at the position r ($g_{Enzyme}/g_{particle}$) and depends on the intraparticle enzyme distribution. For the most common catalyst distributions, $W_E(r)$ can generally be expressed as:

$$W_E(r) = W_E \cdot E(r) \tag{3.3}$$

where W_E represents the specific enzyme loading; the form of the function $E(r)$ will be discussed later for several intraparticle distributions.

As the reaction is generally started by feeding the catalyst to the reactor, there are initially no substrate molecules inside the particle. The spherical geometry requires symmetry with respect to the particle center and given the external diffusion limitations the following initial, (3.4), and boundary, (3.5), conditions can be used to solve Equation (3.2):

$$t = 0 \qquad 0 < r < R_P \qquad c_i = 0 \tag{3.4}$$

$$\begin{aligned} t > 0 \qquad r = 0 \qquad & \left.\frac{\partial c_i}{\partial r}\right|_{r=0} = 0 \\ r = R_P \qquad & \varepsilon_P D_P \frac{\partial c_i}{\partial r} = k_f (C_i - c_i) \end{aligned} \tag{3.5}$$

where R_P is the radius of the particle, C_i the concentration of species i outside the particle, in the bulk phase and k_f the mass transfer coefficient between the liquid and the catalyst surface.

3.2.3 BULK PHASE MASS BALANCE

Since the enzyme is immobilized inside the catalyst particles, no reaction takes place in the bulk phase. The bulk phase acts as a reservoir for the substrate molecules to gradually enter the pores of the particles. Considering external diffusion limitations in a stagnant layer of fluid surrounding the particles, the material balance for substrate i in the bulk phase yields:

$$V_L \frac{\partial C_i}{\partial t} = -k_{fi} \frac{3}{R_P} V_S \left(C_i - c_i\big|_{r=R_P} \right) \tag{3.6}$$

where V_L and V_S represent the volume occupied by the liquid and solid phases (catalyst particles), respectively. Note that $\frac{3}{R_P} V_S$ represents the [Number of particles] x [Specific surface of one particle].

As the initial concentration, C_{i0}, in the bulk phase is defined at each run, Equation (3.6) is subject to the following initial condition:

$$t = 0, \quad c_i = 0, \quad C_i = C_{i0} \tag{3.7}$$

3.2.4 COMPLETE MODEL

Equations (3.2)-(3.7) can be more conveniently expressed by introducing the dimensionless variables and parameters presented in Table 3.1, which gives rise to the final form of the model's equations:

$$\varepsilon_p \frac{\tau_{di}}{\tau_{d1}} \frac{\partial f_i}{\partial \theta} = \frac{\partial^2 f_i}{\partial x^2} + \frac{2}{x} \frac{\partial f_i}{\partial x} - \phi_i^2 E(x) \frac{R}{v_{max}} K_{M0i} \quad , i = 1, 2 \tag{3.8}$$

$$\frac{\tau_{di}}{\tau_{d1}} \frac{\partial F_i}{\partial \theta} = -3 \frac{V_S}{V_L} Bi_{mi} \left(F_i - f_i\big|_{x=1} \right) i = 1, 2 \tag{3.9}$$

Subject to the initial, (3.10), and boundary, (3.11)-(3.12), conditions:

$$\theta = 0, \quad f_1 = f_2 = 0, \forall x \quad F_1 = F_{10}, \quad F_2 = F_{20} \tag{3.10}$$

$$\left. \frac{\partial f_1}{\partial x} \right|_{x=0} = \left. \frac{\partial f_2}{\partial x} \right|_{x=0} = 0 \tag{3.11}$$

$$\left.\frac{\partial f_1}{\partial x}\right|_{x=1} = Bi_{mi}\left(F_i - f_i\big|_{x=1}\right) \tag{3.12}$$

Table 3.1. Dimensionless parameters and variables of the model.

Parameter	Designation
$f_i = \frac{ci}{C_{i0}}$	Dimensionless intraparticle concentration
$F_i = \frac{C_i}{C_{i0}}$	Dimensionless bulk concentration
$x = \frac{r}{R_P}$	Dimensionless intraparticle radial position
$\theta = \frac{t}{\tau_{d1}}$	Dimensionless time
$\tau_{di} = \frac{R_P^2}{\varepsilon_p D_{pi}}$	Internal diffusion time constant
$Bim_i = \frac{k_{fi} R_p}{\varepsilon_P D_{Pi}}$	Biot Number for mass transfer
$\phi_i = R_P\sqrt{\frac{v_{max}\rho_{app} W_E}{K_{Mi}\varepsilon_p D_{pi}}}$	Thiele Modulus
$K_{M0i} = \frac{K_{Mi}}{C_{i0}}$	Dimensionless Michaelis Constant
$K_{I0} = \frac{K_I}{C_{20}}$	Dimensionless competitive inhibition constant

$\frac{R}{v_{max}}$ can also be expressed as a function of dimensionless variables. So far, the model can be applied to any enzymatic mechanism by substituting *R* by the appropriate rate equation. In this case only the Ping-pong bi-bi with competitive inhibition by the alcohol will be considered, as it was proven to describe the experimental system. Hence, for the Ping-pong bi-bi mechanism with competitive inhibition by the second substrate, based on activities, the rate equation assumes the following form:

$$\frac{R}{v_{max}} = \frac{1}{\frac{K_{MA0}}{\gamma_1 f_1}\left(1+\frac{\gamma_2 f_2}{K_{I0}}\right)+\frac{K_{MB0}}{\gamma_2 f_2}+1} \tag{3.13}$$

Where γ_i represents the activity coefficient of species i. Note that, the thermodynamic activity is defined as:

$$a_i = \gamma_i c_i \tag{3.14}$$

As in the previous section, the activity coefficients will be calculated using the Modified UNIFAC Model (Dortmund) (Gmehling et al. 1993), a group-contribution method.

In the case the kinetics of the reaction can be described by Equation (3.13), this model presents 9 parameters (an additional parameter will be introduced later to account for heterogeneous distributions). One B_{im} is defined for each substrate to account for the competition between film diffusion and intraparticle diffusion; two Thiele moduli (ϕ_1 and ϕ_2), to account for the competition between the reaction phenomenon and the intraparticle diffusion of both substrates. The ratio of diffusion time constants $\frac{\tau_{d1}}{\tau_{d2}}$ accounts for possibly different diffusion rates of both substrates; the dimensionless kinetic constants (K_{M0A}, K_{M0B} and K_{I0}/K_{M0A}) and the volume ratio between the catalyst and the liquid phase (V_S/V_L) complete the model definition. Although K_{I0} alone is dimensionless, as it always appears coupled with K_{M0A}, the ratio K_{I0}/K_{M0A} was chosen as a parameter instead since it is this ratio that completely describes the competition between vinyl acetate and decanol for binding to a free active site of the enzyme in its native state.

The Thiele modulus could have been defined in several ways, depending on the choice for the characteristic reaction time constant. Bischoff (Bischoff 1965) defined a generalized form of the Thiele modulus that could be applied to any rate equation, while maintaining the dependency of the effectiveness factor with this dimensional parameter. For slab geometry, for instance, the generalized Thiele modulus is defined as:

$$\phi = \frac{V}{S}\frac{R(C^S)\rho_{app}}{\sqrt{2}}\left[\int_{C^{r=0}}^{C^S} \varepsilon_P D_P R \rho_{app} dC'\right]^{1/2} \tag{3.15}$$

where C^S represents the concentration at the surface of the slab and S, the surface area.

To avoid the numerical solution of Equation (3.15), simplified reaction time constants can be used in the Thiele modulus definition. In enzyme catalysis, for monosubstrate reactions following Michaelis-Menten kinetics, the Thiele modulus is usually defined as (Shiraishi et al. 1996; Xiu et al. 2000; Ladero et al. 2001; Al-Muftah and Abu-Reesh 2005; Al-Muftah and Abu-Reesh 2005):

$$\phi = R_P \sqrt{\frac{v_{max} \rho_{app} W_E}{K_M \varepsilon_p D_p}} \tag{3.16}$$

The curves obtained for the effectiveness factor as a function of the Thiele modulus using Equations (3.15) and (3.16) are similar, but display different ranges of influence of the Thiele modulus. In this case, as the reaction rate is overestimated in Equation (3.16), the range of influence of the Thiele modulus is displaced to higher values. The existence of inhibition steps will further accentuate these differences, as the reaction proceeds more slowly and this deceleration is not taken into account in Equation (3.16).

For multi-substrate reactions, one Thiele modulus can be defined for each substrate. According to Morbidelli et al. (Morbidelli et al. 2001), for a general reaction with j reactants, the Thiele modulus for reactant i would be defined as:

$$\phi_i = R_P \sqrt{\frac{R(C_1, C_2 ... C_j)}{C_i \varepsilon_p D_{pi}}} \tag{3.17}$$

The simplified definition that was introduced in the current model, aimed at making the Thiele modulus of transesterification reactions easily relatable to the previous definition for Michaelis-Menten reactions. A different characteristic reaction rate was chosen for each substrate ($\frac{v_{max}}{K_{Mi}} \rho_{app} W_E$) for ease of definition and mathematical convenience; alternative approaches are possible and would simply lead to different dimensionless parameters or small readjustments in Equations (3.8)-(3.9).

3.2.5 INTRAPARTICLE DISTRIBUTION AND DEFINITION OF E(r)

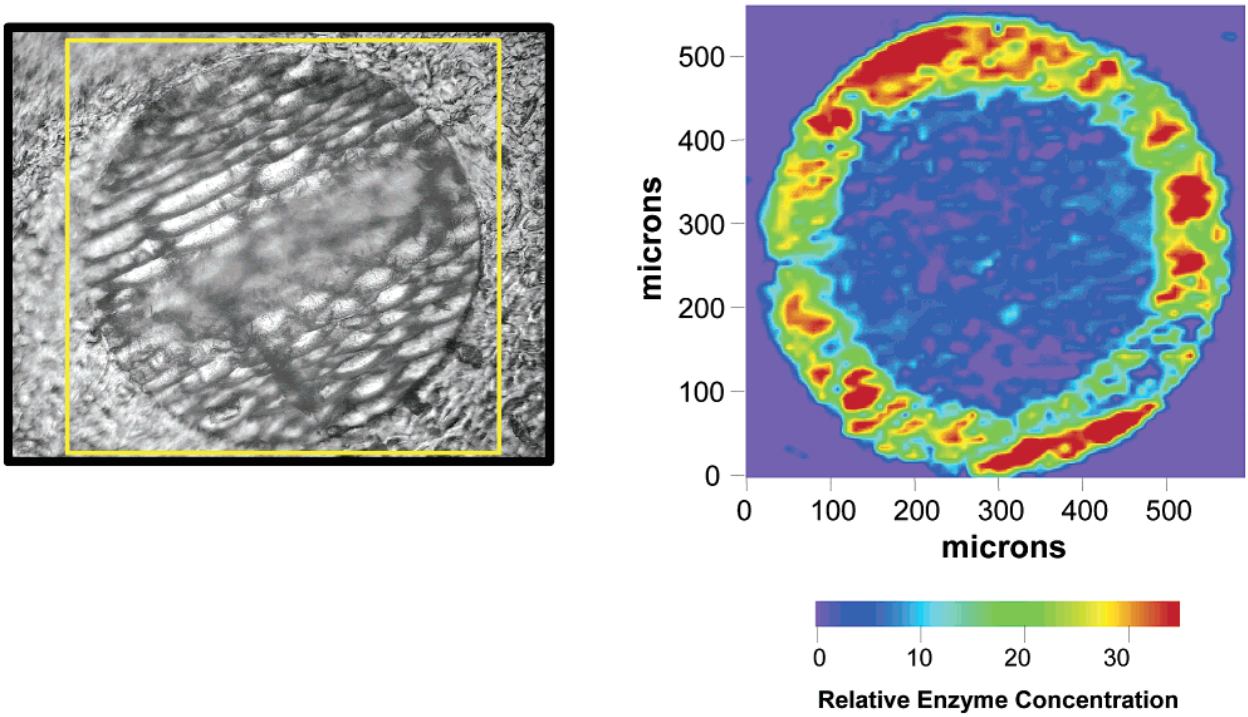


Figure 3.1. Visible light image (left) of the Novozym 435 bead embedded in paraffin and cross-sectioned. The right panel shows the enzyme distribution throughout the center section of the Novozym 435 bead (Mei et al. 2003).

In the previous chapter, evidences were shown that indicated that the intraparticle enzyme distribution in Novozym 435 was not homogeneous, which is in line with findings presented by other authors (Mei, et al. 2003).

Mei et al. demonstrated, by studying the internal composition of Novozym 435 particles using synchrotron infrared microspectroscopy that in this catalyst the enzyme is immobilized only in an external section of the particles. For a particle size around 600μm (which is approximately the average diameter of the Novozym 435 particles) the enzyme was shown to be located in a section of around 80-100μm in the external part of the particle. Across that section the local amount of immobilized enzyme showed some variations but, for modeling purposes, can reasonably be assumed constant.

This type of distribution, where the catalyst is not homogeneously distributed but only immobilized in a portion of the particle is a common feature in catalyst design and can

usually be tailored to optimize its performance (Park et al. 1981; Juang and Weng 1984; Morbidelli et al. 2001). When the catalyst is immobilized in an outer portion of the support, the distribution is designated as an egg-shell. In the opposite end there is the egg-yolk distribution, where the catalyst is immobilized in the inner section. Accordingly, the intermediate case where the catalyst is immobilized in the middle section is referred to as egg-white distribution. The egg-shell distribution will lead to a reduction of diffusion limitations, when they exist, as the reactants only need to diffuse across the catalyst outer layer to be in contact with the entire amount of available catalyst. The egg-yolk distribution, on the other hand, is usually the most protective against catalyst deactivation. The egg-white distribution offers a compromise between the latter two. Conceptually, the choice of distribution, when designing the catalyst will be made by weighing the importance of the previously mentioned phenomena and by the kinetics of the reaction that will be catalyzed (Juang and Weng 1984; Morbidelli et al. 2001). In general, when internal diffusion limitations are present an egg-shell distribution is more appropriate for positive order reactions, while negative order reactions are enhanced by placing the catalyst in the inner part of the support (Morbidelli et al. 2001).

In the particular case of enzyme reactions, the extent over which the intraparticle distribution would affect biocatalysis was theoretically investigated, early in the eighties, for reactions following Michaelis-Menten kinetics with and without product and substrate inhibition. Park et al. (Park et al. 1981) analyzed the distributions mentioned above and Juang and Weng (Juang and Weng 1984) extended the analysis to convex and concave distributions that could result from incomplete adsorption during the immobilization stage or backwashing with the appropriate solvent, respectively. Borchert and Buchholz (Borchert and Buchholz 1984) experimentally obtained this kind of distributions for Trypsin immobilized on controlled pore glass; more recently, van Roon et al. (van Roon et al. 2005) reported a convex distribution for Assemblase, a commercial immobilized penicillin-G acylase.

To account for different intraparticle distributions in the model the function *E(r)* was defined. For distributions where the mass of enzyme per mass of catalyst particle is constant throughout a section of the particle (e.g. homogeneous, egg-shell, egg-white or egg-yolk), *E(r)* can be defined as the ratio between the volume of one particle and the volume of the section that contains immobilized enzyme, in the following manner:

$$\begin{cases} E(r) = \dfrac{R_P^3}{R_e^3 - R_i^3}, & R_i \le r \le R_e \\ E(r) = 0, & R_i > r > R_e \end{cases} \tag{3.18}$$

where R_e represents the radial position of the outer limit of the section containing immobilized enzyme (which equals the particle radius, for the egg-shell and homogeneous distributions) and R_i the radial position of the inner limit of the same section (which reduces to 0 for the egg-yolk and homogeneous distributions). For radial positions located outside the section that contains enzyme, $E(r)$ assumes the value of zero, eliminating the reaction term in the intraparticle material balance Equation (3.2).

Thus, assuming that the enzyme is uniformly distributed across the entire section that contains immobilized catalyst, $W_E.E(r)$ yields the local amount of enzyme in $g_{enzyme}/g_{particle}$. The particular form of $E(r)$ for each of the mentioned enzyme distributions is as follows:

Homogeneous: $$E(r)=1 \tag{3.19}$$

Egg-shell: $$\begin{cases} E(r) = \dfrac{R_P^3}{R_P^3 - R_i^3}, & r \ge R_i \\ E(r) = 0, & r < R_i \end{cases} \tag{3.20}$$

Egg-white: $$\begin{cases} E(r) = \dfrac{R_P^3}{R_e^3 - R_i^3}, & R_i \le r \le R_e \\ E(r) = 0, & R_i > r > R_e \end{cases} \tag{3.21}$$

Egg-yolk: $$\begin{cases} E(r) = \left(\dfrac{R_P}{R_e}\right)^3, & r \le R_e \\ E(r) = 0, & r > R_e \end{cases} \tag{3.22}$$

Or, in terms of the dimensionless radial position, x:

Homogeneous: $$E(x)=1 \tag{3.23}$$

Egg-shell: $$\begin{cases} E(x) = \dfrac{1}{1 - x_i^3}, & x \ge x_i \\ E(x) = 0, & x < x_i \end{cases} \tag{3.24}$$

Egg-white:
$$\begin{cases} E(x) = \dfrac{1}{x_e^3 - x_i^3}, & x_i \le x \le x_e \\ E(x) = 0, & x_i > x > x_e \end{cases} \tag{3.25}$$

Egg-yolk:
$$\begin{cases} E(x) = \dfrac{1}{x_e^3}, & x \le x_e \\ E(x) = 0, & x > x_e \end{cases} \tag{3.26}$$

The experimental validation of the model will be performed for an egg-shell distribution. The other distributions will be used for a theoretical comparison of the performances of different biocatalyst designs.

3.3 EFFECTIVENESS FACTOR AND STEADY STATE MODEL DEVELOPMENT

When analyzing simultaneous reaction-diffusion phenomena, it is useful to scale down the reaction system to one particle immerse in a reaction medium (bulk) of constant composition and study its behavior in steady state. An effectiveness factor, η, constitutes a valuable tool to evaluate the effect of the different parameters and phenomena by comparing the observable reaction rate, R_{Obs}, with the reaction rate that would be obtained in the absence of diffusion limitations, R_{Bulk}, i.e., if the concentration of the several species in the reaction medium along the entire particle were the same as the concentrations in the bulk:

$$\eta = \frac{R_{Obs}}{R_{Bulk}} \tag{3.27}$$

3.3.1 STEADY STATE MODEL DEVELOPMENT

The steady state model for one particle can be derived from the model presented above for the batch reactor, by introducing the condition that the system is in steady state:

$$\frac{\partial f_i}{\partial \theta} = \frac{\partial F_i}{\partial \theta} = 0 \tag{3.28}$$

The bulk phase material balance is no longer necessary since the concentration of the bulk medium is assumed constant. Accordingly, Equations (3.8)-(3.12) reduce to:

$$\frac{d^2 f_i}{dx^2} + \frac{2}{x}\frac{df_i}{dx} - \phi_i^2 E(x)\frac{R}{v_{max}} K_{M0i} = 0 \quad , i = 1, 2 \tag{3.29}$$

Subject to the initial, (3.30), and boundary, (3.31)-(3.32), conditions:

$$\theta = 0, \quad f_1 = f_2 = 0, \forall x \quad F_1 = F_{10}, \quad F_2 = F_{20} \tag{3.30}$$

$$\left.\frac{df_1}{dx}\right|_{x=0} = \left.\frac{df_2}{dx}\right|_{x=0} = 0 \tag{3.31}$$

$$\left.\frac{df_i}{dx}\right|_{x=1} = Bim_i \left(F_i - f_i|_{x=1}\right) \quad , i = 1, 2 \tag{3.32}$$

As an alternative approach, the general model Equations (3.8)-(3.12) can be used by replacing the bulk phase material balance, Equation (3.9), with:

$$\frac{\partial F_i}{\partial \theta} = 0, \; i = 1, 2 \tag{3.33}$$

The model can then be solved for $\theta \rightarrow \infty$ to obtain the steady-state solution.

3.3.2 EFFECTIVENESS FACTOR CALCULATION

The effectiveness factor can be calculated using its definition, Equation (3.27). However, from the steady state condition, the observable reaction rate must equal the rate of diffusion at the surface of the particle. For component 1 of the reaction medium:

$$R_{Obs} = \frac{3}{\phi_1^2} v_{max} \left.\frac{df_1}{dx}\right|_{x=1} \tag{3.34}$$

Introducing Equation (3.34) in Equation (3.27) gives rise to an alternative method for evaluating the effectiveness factor:

$$\eta = \frac{3}{\phi_1^2} \frac{v_{max}}{R_{Bulk}} \left. \frac{df_1}{dx} \right|_{x=1} \tag{3.35}$$

Once the model's equations are solved in order to obtain the intraparticle concentration profiles, the effectiveness factor can easily be obtained from Equation (3.35).

3.4 MODEL NUMERICAL SOLUTION

The Batch reactor model's Equations (3.8)-(3.12) were numerically solved using PDECOL (Madsen and Sincovec 1979), a Fortran routine package for solving coupled non-linear partial differential equations.

The steady state profiles and effectiveness factors were obtained using the same model and the same routine package, by substituting Equation (3.9) with Equation (3.33) and solving for $\theta \rightarrow \infty$, i.e. the time after which there are no further changes in the intraparticle concentration gradients that are formed.

3.5 RESULTS AND DISCUSSION

3.5.1 PARAMETERS USED FOR THE SIMULATION OF THE EXPERIMENTAL DATA - PHYSICAL CHARACTERIZATION OF THE CATALYST PARTICLES AND DIFFUSION COEFFICIENTS

Table 3.2 presents the values of all parameters required for the model's simulation of the experimental results.

Several physical properties of the catalyst appear in the model parameters, namely the particle porosity, the apparent density, and the specific enzyme loading. The specific enzyme loading was already presented in the previous chapter (Table 2.2) for several particle sizes and the other properties were determined by mercury porosimetry in a *Poremaster 60* from *Quantachrome Instruments* and by helium picnometry in an *Accupyc 1330*.

Also necessary for the simulations was the thickness of the outer shell where the enzyme is immobilized for the different particle sizes that were used to perform the reactions. It was shown in the previous chapter that, assuming that the thickness of the shell is independent of the particle size, a shell of around 80μm was consistent with the specific enzyme loadings. Mei et al. (Mei et al. 2003) reported an outer shell of around 80-100μm for a Novozym 435 particle with a diameter of ~600μm which is consistent with this calculation. Thus, a shell thickness of 80μm will be used for simulating the experimental data.

The molecular diffusion coefficients were estimated by the Wilke-Chang method (Reid et al. 1977) (Appendix B).

The molecular diffusivities relate to the effective diffusivities in the following manner:

$$D_e = \frac{\varepsilon_P D}{\tau^*} = \varepsilon_P D_P \tag{3.36}$$

where D_e represents the effective diffusivity, D the molecular diffusivity and τ^* the tortuosity factor.

Table 3.2. Parameters used in the simulations.

Parameters used in the simulations		
Catalyst Particle Characterization	ε_P (cm^3_{pores}/ $cm^3_{particle}$)	0.42
	ρ_{app} (g/cm^3)	720
	Shell Thickness (μm)	80
	$W_E^{d_P=460\mu m}$ ($g_{enzyme}/g_{particle}$)	0.092
	$W_E^{d_P=360\mu m}$ ($g_{enzyme}/g_{particle}$)	0.108
	$W_E^{d_P=240\mu m}$ ($g_{enzyme}/g_{particle}$)	0.125
Mass transfer properties	D_{P1} (cm^2/s)	2.30×10^{-5}
	D_{P2} (cm^2/s)	1.35×10^{-5}
Activity Based Kinetic Parameters	V_{max} ($mol/g_{Enz}.min$)	0.542
	K_{MA} (M)	0.0862
	K_{MB} (M)	0.0788
	K_I (M)	0.125

Given the lack of available data for the tortuosity factor of Novozym 435, the typical value of 2 was used. The molecular diffusivities obtained by the Wilke-Chang method were then divided by 2 to obtain the pore diffusivities that are presented in Table 3.2.

The activity based kinetic parameters were already determined in the previous chapter.

3.5.2 MODEL VALIDATION

To validate the model with experimental data the transesterification reaction of vinyl acetate and decanol was performed with catalyst particles of different sizes and several initial concentrations of each substrate. The model's equations were solved for each case using the parameters presented in Table 3.2 in order to obtain the bulk concentration profiles that were then compared with the experimental data.

In the previous chapter, experimental data obtained with different particle sizes was presented with the purpose of illustrating the effect of internal diffusion limitations (Figure 2.2 and Figure 2.5). Figure 3.2 and Figure 3.3 present the results of the simulations obtained for these two sets of experiments.

When testing for the existence of internal mass transfer resistances, by varying the particle size while maintaining the amount of enzyme unchanged, overlapping curves were obtained for 360 μm 460 μm particles, despite the presence of mass transfer limitations. There was a significant enhancement of the reaction rate below a certain particle size, which was notorious when crushed particles were used. This is not a typical behavior, as the curves obtained as the particle size is reduced tend to approach due to the reduction in the diffusion path, until they overlap, indicating that the diffusion rate is fast enough for the process to be controlled by the chemical reaction.

The model was able to satisfactorily predict the experimental results for different particle sizes.

The enhancement in the reaction rate is well predicted for crushed particles. This was already expected since, without mass transfer resistances, the model should lead to the same results presented in the previous chapter where no mass transfer resistances were considered.

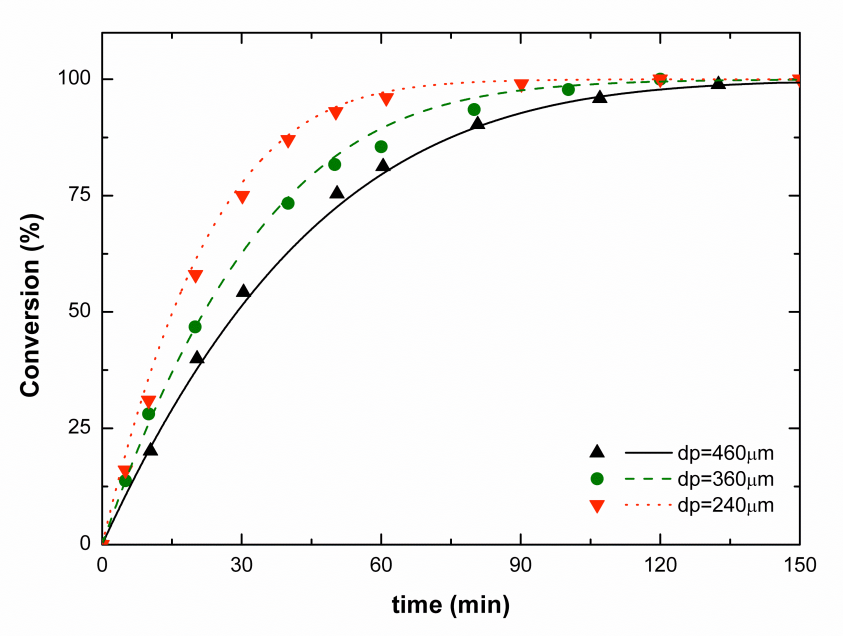


Figure 3.2. Experimental data (▲, ●, ▼) and model predictions (—, ---, ···) for different particle sizes. Reaction conditions: [A]=[B]=0.1 M, W_S=0.56 mg/mL and T=30 ºC for all assays.

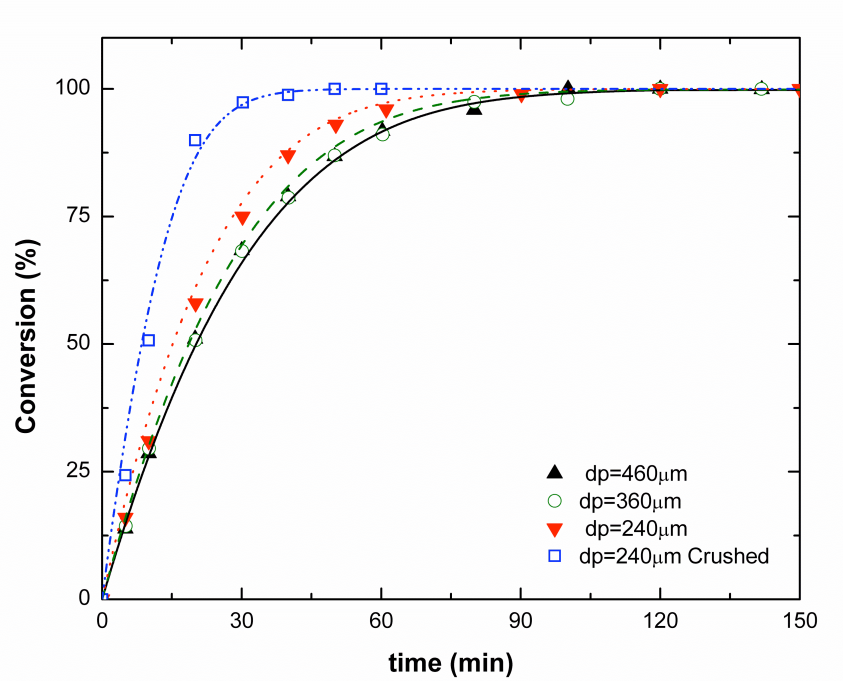


Figure 3.3. Experimental data (▲, ○, ▼, □) and model predictions (—, ---, ···, -·-) for different particle sizes. [A]=[B]=0.1 M, W_{Enzyme}=0.069 mg_{Enzyme}/mL and T=30 ºC for all assays.

The conversion curves obtained with 360 μm 460 μm particles using the same amount of enzyme are very close and in good agreement with the experimental data. The fact that the curves obtained by simulation are close but do not exactly overlap is probably due to small errors in the determination of the specific enzyme loading. For example, a variation of less than 4% in the enzyme loading of the 360 μm particles (from 0.108 to 0.104 $g_{Enzyme}/ g_{Particle}$) is enough for the conversion curves to overlap.

Another possibility worth considering is that the thickness of the enzyme shell might depend on the particle size, which would be the case if this type of distribution was in part the result of diffusion limitations during the enzyme immobilization procedure. In the previous chapter calculations were made to estimate the thickness of the enzyme shell based on the following assumptions:

- The amount of immobilized enzyme is constant throughout the shell;
- Locally, the amount of enzyme per volume of support is the same, regardless of the particle size;
- The thickness of the shell is independent of the particle size.

An alternative approach would be, based on the experimental evidences that the enzyme distribution in the 240μm particles can be considered homogeneous:

- The amount of immobilized enzyme is constant throughout the shell;
- Locally, the amount of enzyme per volume of support is the same, regardless of the particle size;
- The enzyme intraparticle distribution in the 240 μm particles is homogeneous;
- The thickness of the shell depends of the particle size.

Table 3.3 presents the values obtained for the thickness of the enzyme shell based on the new assumptions.

Figure 3.4 presents the model predictions for the cases mentioned above and additionally, the curves that would be obtained with a homogeneous distribution.

Table 3.3. Thickness of the enzyme shell for Novozym 435 particles of different sizes, assuming that the thickness of the shell is dependent of the particle size and the 240 µm particles are homogeneous.

Average Particle Size (µm)	Thickness of the enzyme shell (µm)
460	83.6
360	89.0
240	Homogeneous

Considering a different shell thickness for each particle size, the curves obtained for 460µm and 360µm particles are slightly closer than in the previous case; nevertheless, for the complete overlapping a difference of 10% would be required in the specific enzyme loading.

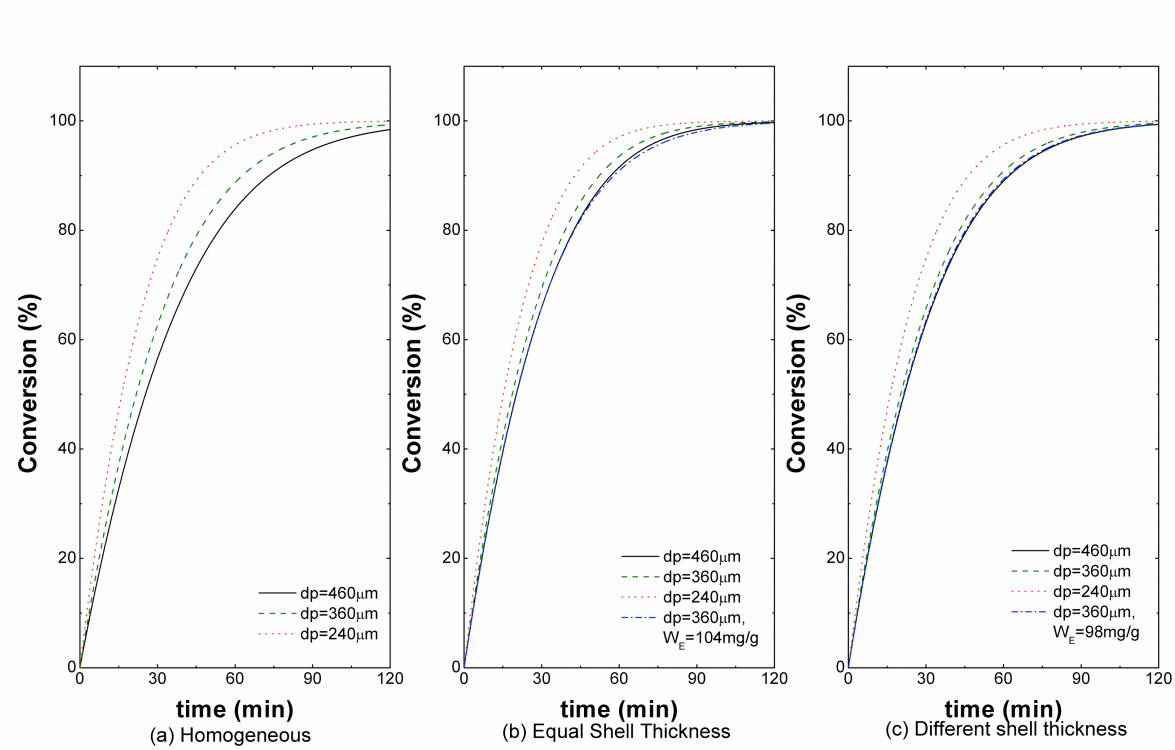


Figure 3.4. Model predictions for different particle sizes, [A]=[B]=0.1M, W_{Enzyme}=0.069 mg_{Enzyme}/mL and T=30 ºC, assuming: (a) Homogeneous enzyme distribution (b) Egg-shell distribution with shell thickness independent of the particle size (c) Shell thickness dependent of particle size, considering 240µm particles present a homogeneous distribution.

Considering a homogeneous distribution, this behavior is not predicted by the model and a more typical dependence of the conversion curves with the particle size is obtained.

The curves obtained for 240 µm particles are practically the same for any of the considered distributions. As it was mentioned previously, an enzyme shell of around 80 µm represents more than 95% of the volume of the particle, which is enough for the distribution to be considered homogeneous. For the remaining particle sizes, the reaction rate increases as the thickness of the enzyme shell decreases. The thinner the enzyme shell is, the closer to the surface of the particles the enzyme will be, thus reducing the diffusion path of the substrate molecules in order to contact with the entire amount of available catalyst; additionally, as the enzyme loading is the same in both cases, locally, a thinner shell leads to a higher mass of enzyme per volume of particle. Whenever diffusion limitations are relevant, for positive ordered reaction mechanisms, thinner shells will lead to higher reaction rates. This subject will be discussed in more detail in the next section.

In order to further evaluate the predictive capacity of the model, additional experiments were performed, varying the particle size, the amount of catalyst and the initial concentrations of each reagent. Both the experimental results and the simulations obtained with the model are presented in Figure 3.5, Figure 3.6 and Figure 3.7.

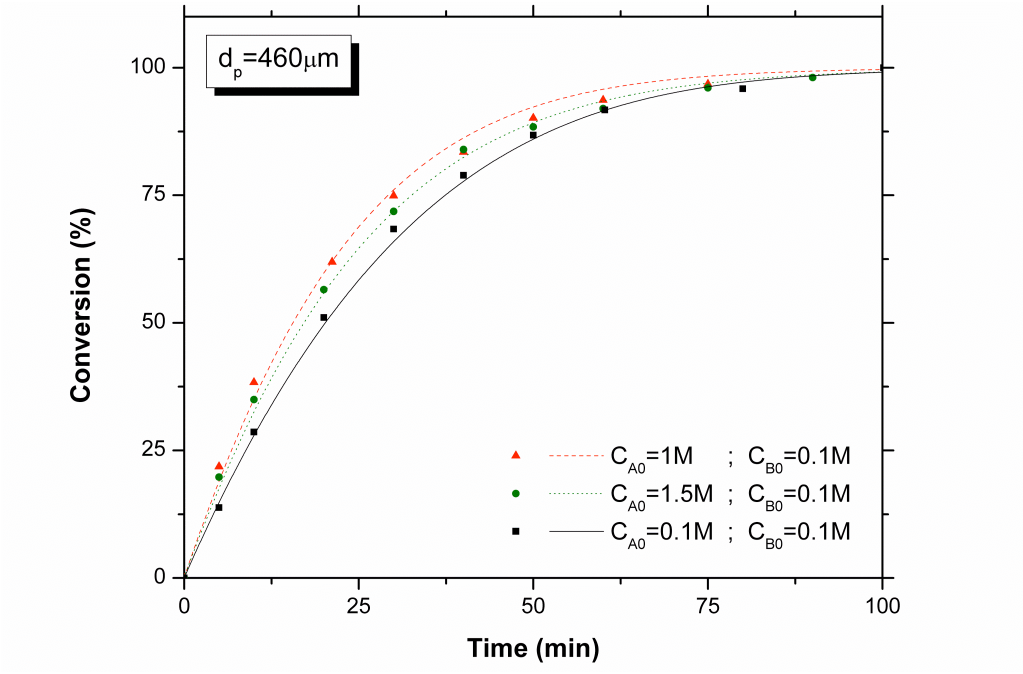


Figure 3.5. Experimental results (symbols) and model predictions (lines) for different initial concentrations of vinyl acetate. d_P=460 µm, W_S=0.76 mg/mL and T=30 ºC.

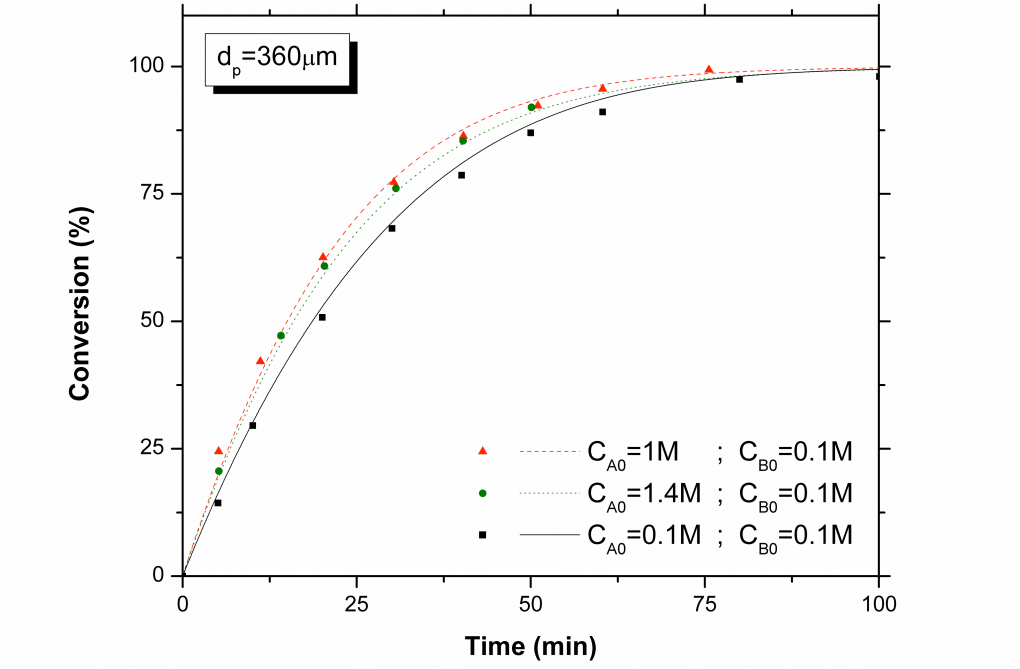


Figure 3.6. Experimental results (symbols) and model predictions (lines) for different initial concentrations of vinyl acetate. d_P=360 μm, W_S=0.64 mg/mL and T=30 ºC.

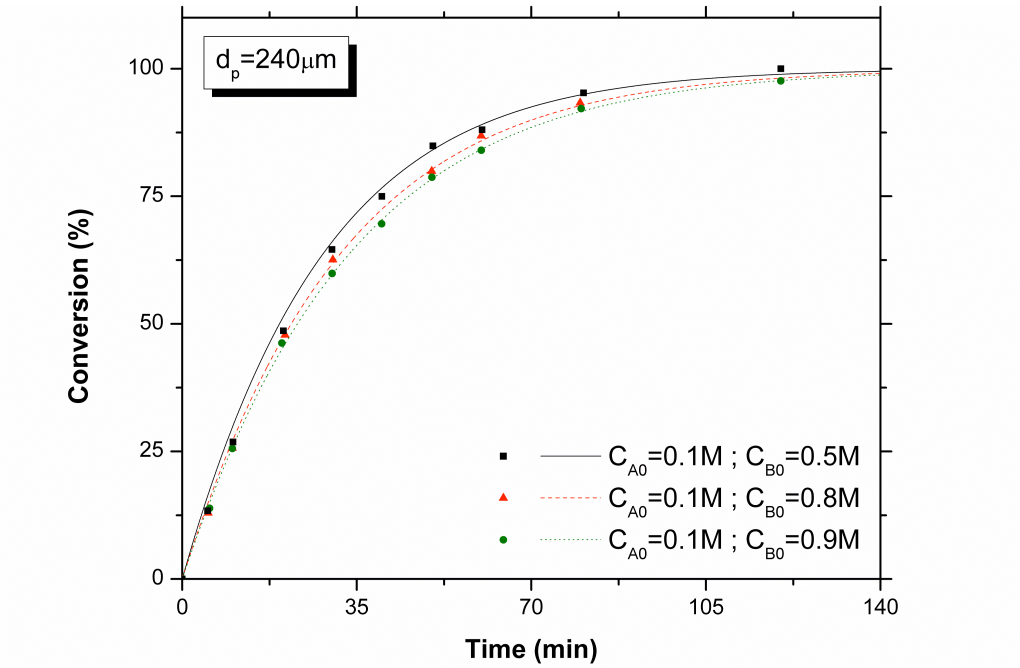


Figure 3.7. Experimental results (symbols) and model predictions (lines) for different initial concentrations of decanol. d_P=240 μm, W_S=0.64 mg/mL and T=30 ºC.

The model is able to satisfactorily predict the experimental results. As in the previous chapter, when there is an excess of vinyl acetate, the model predicts a slightly lower reaction rate for higher concentrations of this reagent, a tendency that the experimental results seem to confirm.

In the previous chapter it was shown that padding the magnetic stirring bars was important to ensure that the particle size was not reduced during the experiments. Figure 3.8 presents the model's predictions for the experimental results presented in Figure 2.3 where the padding accidentally detached from one magnetic bar at a reaction time of approximately 40 min. To simulate this case, the model was solved considering the original particle size until t=40min and a very small particle size (40 μm) from that point on.

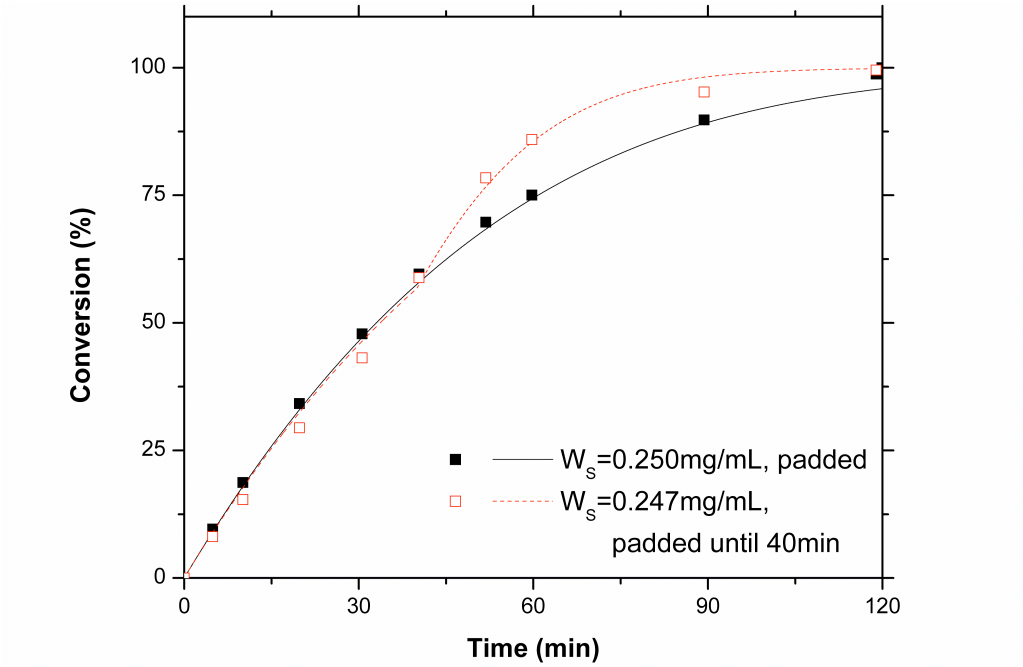


Figure 3.8. Experimental results (symbols) and model predictions (lines) for different initial concentrations of decanol. d_P=240 μm, W_S=0.64 mg/mL and T=30 ºC.

3.5.3 EFFECT OF THE PARAMETERS OF THE MODEL

The effect of the model parameters will be analyzed mainly by focusing on one particle in steady-state. Thus, the influence of each parameter will be measured by the effectiveness factor, as defined by Equations (3.27) and (3.35).

To facilitate the discussion, the analysis will initially be centered in the intraparticle diffusion and reaction phenomena, which is accomplished by considering a very large Biot number. Afterwards, the influence of external diffusion will be introduced and analyzed. In batch reactors, the influence of external diffusion can usually be eliminated by increasing the agitation speed, but in other types of reactors, such as the packed bed continuous reactor, external mass transfer resistances can influence the outcome of processes more frequently.

3.5.3.1 EFFECT OF THE KINETIC PARAMETERS AND THIELE MODULUS

The kinetic parameters of the reaction are present in the parameters K_{M0i}, K_{I0}, and the Thiele moduli. To facilitate the discussion and the graphical representation of the effectiveness factor curves, the Thiele modulus will be assumed equal for both substrates.

Analyzing the definition of the Thiele modulus, it can easily be shown that:

$$\phi_1 = \phi_2 \frac{\tau_{D1}}{\tau_{D2}} \frac{K_{M0B}}{K_{M0A}} \frac{C_{B0}}{C_{A0}} \tag{3.37}$$

For the reaction of Vinyl acetate and Decanol in n-hexane, the values of the Michaelis constant for each substrate are of the same order of magnitude. The same applies to the diffusivities; hence, if both substrates are initially present in the same concentration, ϕ_1 and ϕ_2 will present similar values.

For these simulations, a value of 0.08 M was considered for K_{MA} and K_{MB} and equal initial concentrations and diffusivities. The K_M and diffusivities were then varied to obtain different K_{M0i} and Thiele modulus, respectively. Particles with a diameter of 460 μm presenting an egg-shell distribution were considered (80 μm shell) and all other parameters used in the simulations are the same as in the previous sections. K_{I0} was also varied to illustrate the effect of the competitive inhibition by the second substrate (decanol) in the effectiveness factor. The results of the simulations are presented in Figure 3.9.

The Thiele modulus compares the reaction and intraparticle diffusion rates. Small values of the Thiele modulus represent the cases in which the reaction is much slower than the diffusion phenomenon, eventually making the latter irrelevant for the outcome of the overall process. In that case, the process is controlled by the reaction and the observable reaction rate

is similar to the intrinsic reaction rate (η→1). On the other hand, high values of the Thiele modulus indicate severe diffusion limitations. As the reaction is much faster than the diffusion of the substrates, they are entirely consumed before they reach the centre of the particle; ultimately, for very high Thiele modulus, the reactants are consumed as soon as they enter the pores of the particle, very close to the surface, and the process is exclusively controlled by diffusion (η→0). Between these two limiting cases, the reaction and diffusion rates are of the same order of magnitude; none of the phenomena is entirely dominant and both influence the outcome of the catalytic process. It is in this case, for intermediate values of the Thiele modulus, that the effectiveness factor is more sensitive to this parameter.

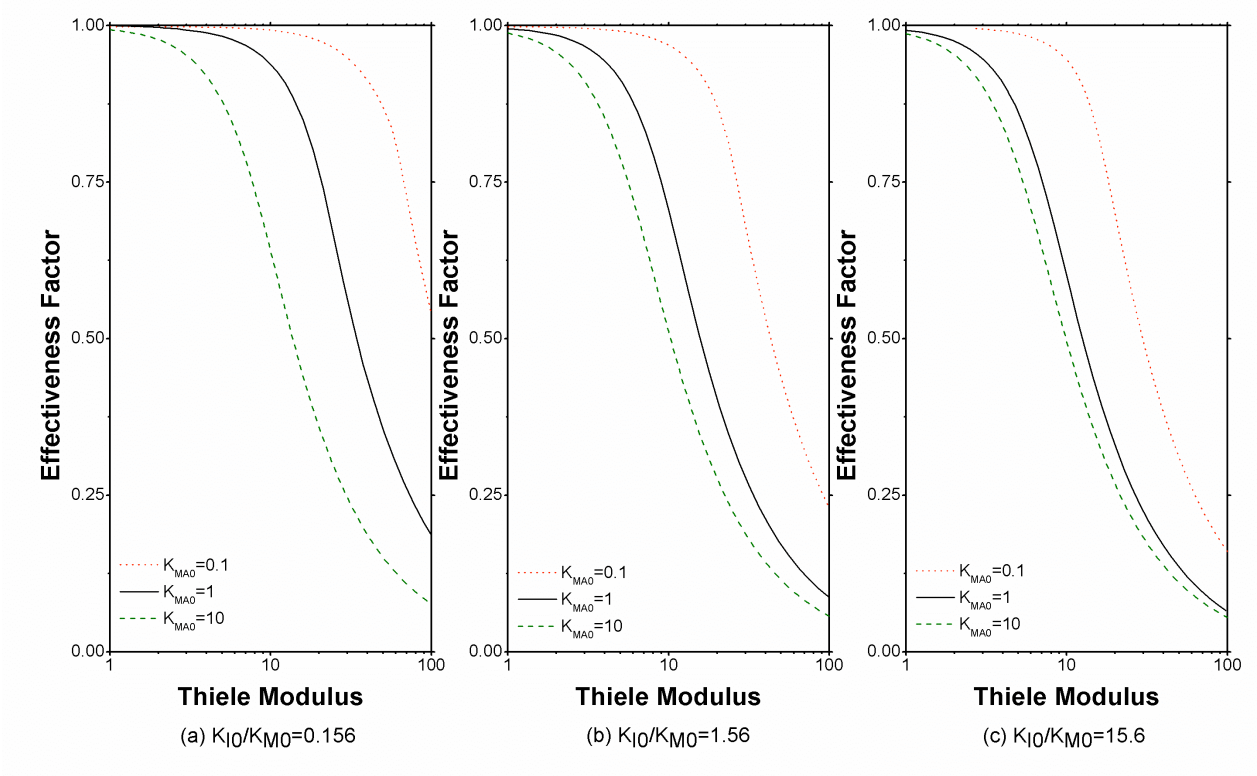


Figure 3.9. Effect of the kinetic parameters and Thiele modulus on the effectiveness factor (a) K_{I0}/K_{M0}=0.156 (b) K_{I0}/K_{M0}=1.56 (c) K_{I0}/K_{M0}=15.6

Typically, the range over which the Thiele modulus influences the process is between 0.3 and 3 (ϕ^2 between approximately 0.1 and 10; diffusion 10 times faster or slower than the reaction, respectively) (Froment and Bischoff 1990). In the current definition of the Thiele modulus a simplification of the characteristic reaction time is used, which overestimates the

actual reaction rate, thus displacing the range of influence of the Thiele modulus to higher values (~1-100, depending on K_{M0i} and K_{I0}/K_{MA0}). This discrepancy between the actual reaction rate and the one considered in the Thiele modulus will be larger for lower values of K_{I0}/K_{MA0}.

High values of K_{I0}/K_{MA0} indicate that the competitive inhibition by the alcohol is less significant (i.e. the enzyme in its native state has a stronger affinity for the ester). On the other hand, when K_{I0}/K_{MA0} is small there is a strong inhibitory effect by the alcohol, slowing down the reaction. Since the inhibitory effect is not contemplated in the definition of the Thiele modulus, its presence leads, for the same Thiele modulus, to higher effectiveness factors and displaces the range of influence of the Thiele modulus to higher values. On the other hand, when K_{I0}/K_{MA0} is large enough, the inhibition step becomes negligible and the effectiveness factor curves become independent of this parameter.

Increasing K_{MA0} decreases the reaction rate which, similarly to what is observed in the previous example, should lead to a higher effectiveness factor. Figure 3.9, however, shows that for the same value of the Thiele modulus, the effectiveness factor is higher for low K_{MA0}. Figure 3.9 was obtained by varying K_M and D_P; when increasing K_{M0} 10 times by increasing K_M, the same value of the Thiele modulus is achieved by reducing D_P 10 times. The diffusion rate, proportional to D_P, will hence decrease 10 times, but the reaction rate will decrease less; overall, the ratio between reaction rate and diffusion rate will increase, leading to a lower effectiveness factor for a higher K_{M0}, despite the fact that the reaction rate is lower. To isolate the effect of a higher K_{M0}, different Thiele modulus must be considered. As can be seen in Table 3.4, increasing only K_M, will lead to higher K_{M0} but lower Thiele modulus and, correspondingly, higher effectiveness factors.

Table 3.4. Effectiveness factor for different K_{M0} while keeping all other parameters constant

K_{M0}	Thiele Modulus	Effectiveness factor
0.1	32	0.65
1	10	0.70
10	3.2	0.90

3.5.3.2 EFFECT OF DIFFERENT THIELE MODULUS FOR EACH SUBSTRATE

In general, in the case the reaction rate is inhibited by any of the reactants (negative order reaction), diffusion limitations can give rise to effectiveness factors larger than 1 (Park et al. 1981; Juang and Weng 1984; Morbidelli et al. 2001), provided that both the diffusion limitations and the inhibition are strong enough.

In the Ping-pong bi-bi kinetic model, mathematically expressed by Equation (3.1), competitive inhibition is considered by means of the term $\frac{K_{MA0}}{K_{I0}}\frac{a_2}{a_1}$; inhibition is thus stronger:

- the smaller the value of K_{I0}/K_{MA0};
- the larger the activity coefficient ratio $\frac{a_2}{a_1}$

The effectiveness factor is then most likely to be enhanced to values larger than 1, whenever the ratio $\frac{a_2}{a_1}$ is smaller inside the particles than in the bulk phase, i.e., when the alcohol diffuses through the particle more slowly than the ester. This is the case when the diffusivity of the alcohol is smaller than the diffusivity of the ester and, hence $\frac{\tau_{d2}}{\tau_{d1}} < 1$. This enhancement should also be more pronounced if the enzyme in its native state has a strong affinity for the alcohol, mathematically translated by a small value of K_{I0}/KM_{A0}.

To analyze the effect of these two cases, the effectiveness factor was calculated for several values of ϕ_2 (by varying $\frac{\tau_{d2}}{\tau_{d1}}$), while maintaining ϕ_1 constant, for different K_{I0}/KM_{A0}. In accordance with the previous sections, all other parameters used in the simulations are the same as above. Figure 3.10 presents the results of these simulations.

Similarly to what was presented above, K_{I0}/K_{MA0} has a significant influence on the effectiveness factor in some regions. For the same value of ϕ_1, smaller K_{I0}/K_{MA0} lead to higher effectiveness factors, as the reaction rate is slowed down by the inhibitory effect of the alcohol, and this is not accounted for in the definition of the Thiele modulus. There are, however, some interesting regions and limiting cases worth analyzing.

For $\phi_1 = 1$, all effectiveness factor curves tend to overlap at low ϕ_2. When both Thiele moduli are close to 1, there are no significant diffusion limitations and no intraparticle concentration gradients are formed; the process is controlled by the reaction, leading to an effectiveness factor of 1, regardless of K_{I0}/K_{MA0}. For $\phi_1 = 10$ the curves no longer tend to an effectiveness factor of 1 and do not overlap for low ϕ_2. In this case, a Thiele modulus of 10 means there are still diffusion limitations for the ester ($\lim_{\phi_2 \to 0} \eta < 1$) and that they become less significant as the reaction rate is lower, i.e. as the inhibition becomes stronger ($\eta^{K_{I0}/K_{MA0}=0.156} > \eta^{K_{I0}/K_{MA0}=1.56} > \eta^{K_{I0}/K_{MA0}=15.6}$).

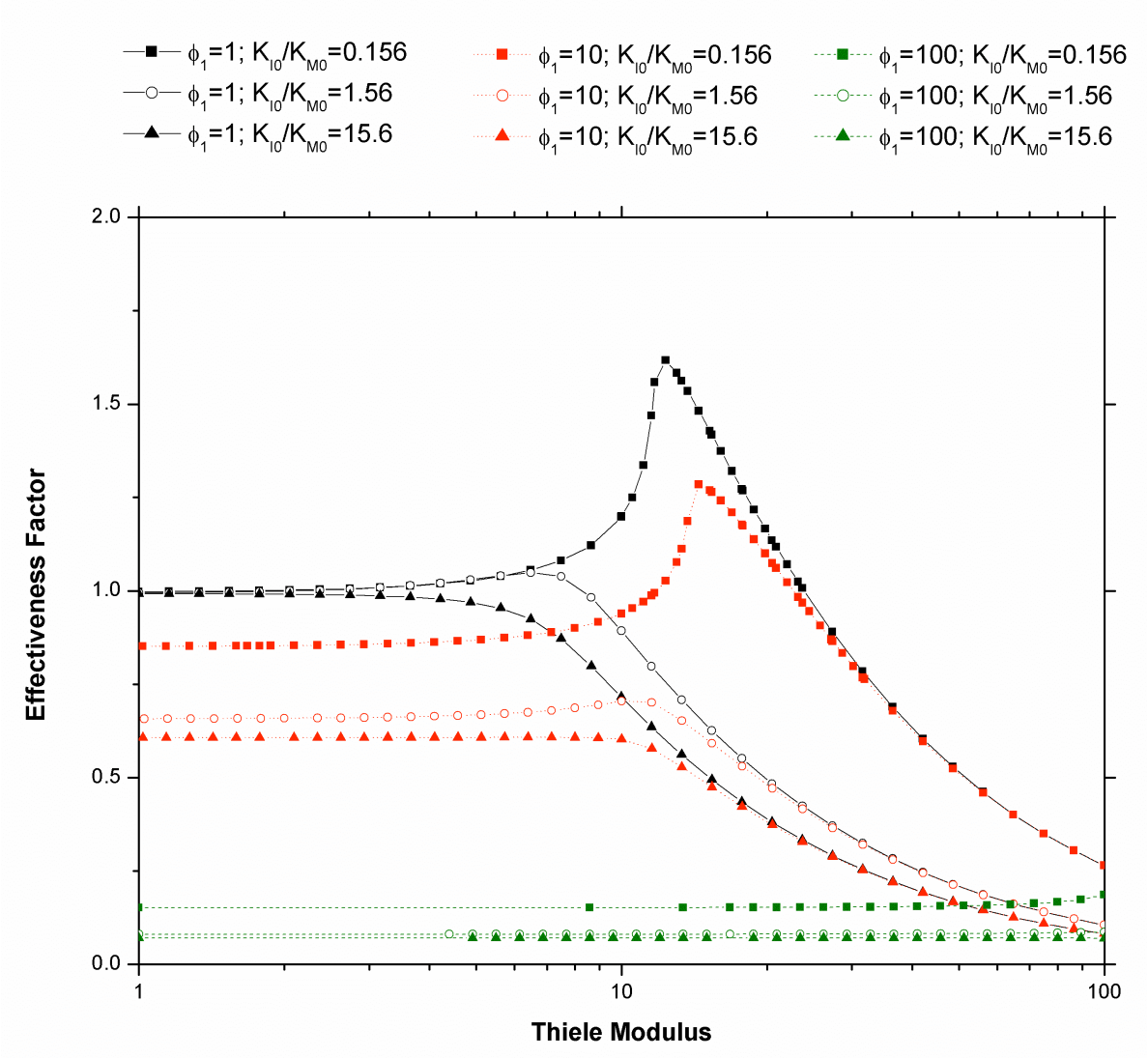


Figure 3.10. Simulations obtained with different values of ϕ_1 and ϕ_2. — ϕ_1=1; ··· ϕ_1=10; --- ϕ_1=100. ■ K_{I0}/K_{MA0}=0.156; ○ K_{I0}/K_{MA0}=1.56; ▲ K_{I0}/K_{MA0}=15.6.

For $\phi_1 = 100$, the effectiveness factor is very low, regardless of the value of ϕ_2. In this case, the diffusion of the first substrate is much slower than the reaction and the process is limited and controlled by the former. Eventually, when the inhibition by the alcohol is significant the effectiveness factor is a little higher, and starts peeking when the rate of diffusion of the alcohol is equally slow ($\phi_2 \cong \phi_1 \cong 100$), since it generally lowers $\frac{a_2}{a_1}$.

For the same value of K_{I0}/K_{MA0} (equal symbols in Figure 3.10), the curves obtained for the effectiveness factor overlap for high values of ϕ_2. This represents the case when the diffusion of the ester is sufficiently faster than the diffusion of the alcohol (ϕ_1 sufficiently lower than ϕ_2) to ensure that diffusion limitations are negligible for the ester and its concentration is constant throughout the particle. Here, only the much slower diffusion of the alcohol is significant for the overall process, and defines the effectiveness factor.

Effectiveness factors larger than one appear under specific conditions. The inhibitory effect of the alcohol must be significant and the diffusion of the alcohol must be slower than the diffusion of the ester, but not so much that not enough molecules are available to bind to the enzyme-acyl complex in the second step of the kinetic mechanism. With the kinetic parameters and the physical properties of the catalyst that were used in the simulations, and represent the experimental system, for $\phi_1 = 10$ (Dp~10^{-4}) and strong inhibition (K_{I0}/K_{MA0}=0.156) Thiele modulus larger than one would appear if the second substrate had a diffusivity between $2x10^{-5}$ and $7x10^{-5}$, i.e. 1.4 to 5 times lower. If the limitations to the diffusion of the ester are negligible (e.g. $\phi_1 = 1$), the region over which the effectiveness factor rises above one is broader.

For a value of K_{I0}/K_{MA0} of 1.56 (which corresponds to the experimental system) and a Thiele modulus of 10, the effectiveness factor does not rise above 1 regardless of the difference in diffusivities between both subtracts. In this case, due to the intraparticle concentration gradient that is formed for the ester, the reaction rate is always slower than under bulk conditions. Effectiveness factors slightly above 1 would only occur in the case of stronger inhibition (e.g. K_{I0}/K_{MA0}=0.156), provided that the increase in the reaction rate caused by the lower concentration of the alcohol inside the particle (↓inhibition) would be larger than the decrease caused by the lower concentration of the ester.

3.5.3.3 EFFECT OF ENZYME DISTRIBUTION

To illustrate the influence of how the enzyme is distributed inside the support particles, a series of simulations were performed using the same specific enzyme amount distributed according to four common distributions: egg-yolk, egg-shell, egg-white, and homogeneous. The results are presented in Figure 3.11 and were obtained for $\phi_1 = \phi_2$, K_{I0}/K_{MA0}=1.56, K_{MA0}=K_{MB0}=1 and in the absence of external diffusion limitations.

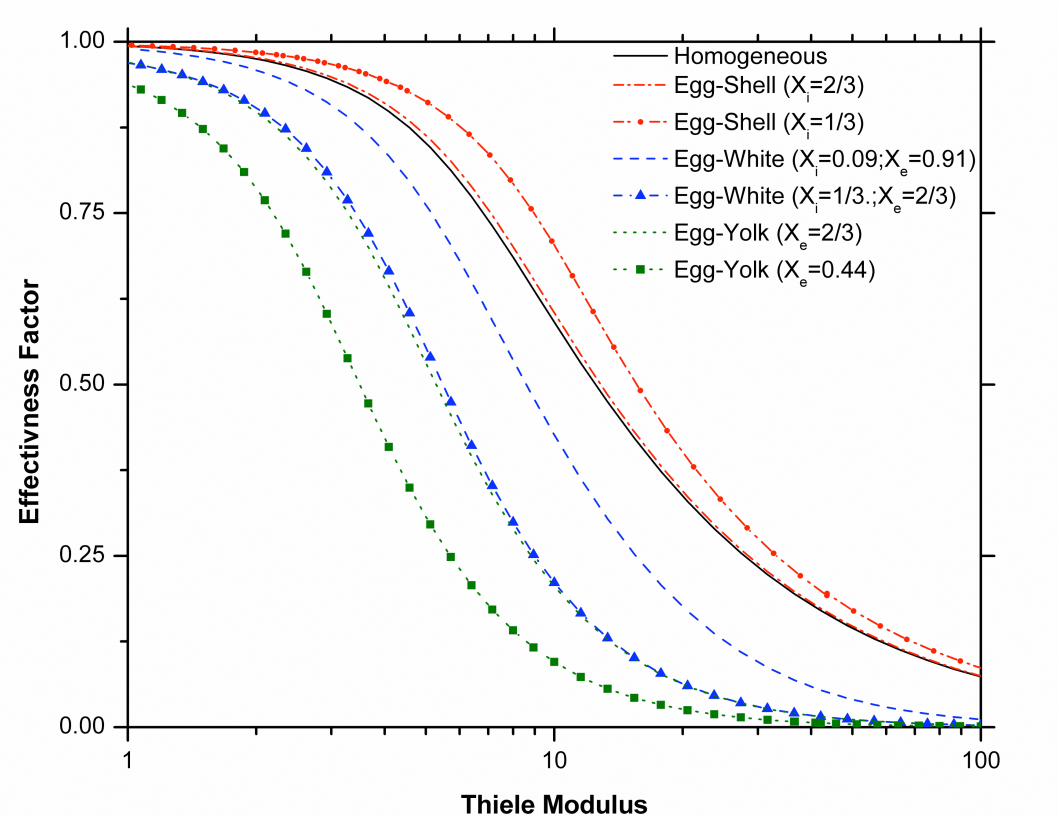


Figure 3.11. Effectiveness factor vs. Thiele modulus for different intraparticle enzyme distributions (K_{I0}/K_{MA0}=1.56, K_{MA0}=K_{MB0}=1).

If intraparticle diffusion resistances are negligible ($\phi \rightarrow 0$), the enzyme distribution is irrelevant as the concentration of the substrates across the particle will equal the bulk concentration at any position and the entire amount of enzyme present will be used in the catalytic process ($\eta \rightarrow 1$). However, when intraparticle diffusion resistances are relevant, the distribution of the enzyme inside the support can have a dramatic impact in the effectiveness

factor. In general, for the ping-pong bi-bi kinetic mechanism with competitive inhibition by the alcohol and with the parameters used for the simulation, the closer the enzyme is to the surface of the particle, the higher the effectiveness factor will be. This is the typical behavior for a reaction system described by a positive order reaction rate equation. Whenever internal diffusion limitations are relevant, the substrate molecules diffusing towards the center of the particle will be entirely consumed before reaching it. If there is enzyme located in a region the substrates will not reach (C_A=C_B=0 M), it will not be used for catalyzing the reaction, and as a result, the overall reaction process will be slower (R_{obs}↓).

To compare the different distributions it was chosen to divide the particle radius in 3 parts, and the obtained radial positions were used as boundaries (x_i, x_e) for the several distributions.

Comparing the simulation obtained with egg shell (red curves) and homogeneous distributions (black curve), it is clear that the egg-shell distribution leads to a more effective use of the immobilized enzyme and that the effectiveness factor will be higher the closer the enzyme is to the surface, i.e. the thinner the enzyme shell is (x_i→1). There is practically no difference between the effectiveness factor curves obtained for the homogeneous distribution and the egg-shell distribution with x_i=1/3. This is due to the fact that the inner portion of the particle defined by 1/3 of its radius represents less than 5% of the total volume of the particle. As the thickness of the egg-shell becomes larger the effectiveness factors will be lower and the effectiveness factor curves will tend to the one obtained for homogeneous distribution.

For the egg-white distribution (blue curves), using the case of x_i=1/3, x_e=2/3, two cases can be analyzed:

i) x_i remains constant while x_e is varied;
ii) x_i is varied while x_e remains constant;

In the first case, if x_e is larger the enzyme will be closer to the surface, which will lead to a higher effectiveness factor. The results obtained with an egg-white distribution as x_e gets larger will approach the ones of an egg-shell distribution of same x_i; both distributions will be the same when x_e=1. When comparing the effectiveness factor curve in Figure 3.11 obtained for x_i=1/3, x_e=2/3 and the egg-shell distribution with x_i=1/3 it can be seen that the latter leads to higher effectiveness factors.

In the second case, if x_i is smaller, the enzyme is more widespread towards the centre of the particle. At the limit, as x_i→0, the distribution is equivalent to an egg-yolk distribution

(green curves). When comparing the effectiveness factor curve in Figure 3.11 obtained for x_i=1/3, x_e=2/3 and the egg-Yolk distribution with x_e=2/3 it can be seen that both distributions lead to practically the same results. Again, this is a consequence of the inner portion of the particle defined by 1/3 of its radius representing less than 5% of the total volume of the particle; nevertheless, it can be seen that higher effectiveness factors are obtained for larger x_i.

The curve presented for an egg-white distribution with x_i=0.09, x_e=0.91 represents the case when the local enzyme concentration (mass of enzyme/volume of particle) is the same as in the egg-shell distribution with x_i=1/3. Again it can be seen that the egg-shell distribution will lead to higher effectiveness factors.

For the egg-yolk distribution, Figure 3.11 clearly shows that the closer the enzyme is to the surface ($x_e \rightarrow 1$) the larger the effectiveness factor will be. In the limit, when x_e=1, the distribution becomes homogeneous.

To complete the analysis, Figure 3.12 presents the steady state intraparticle concentration profiles for some of the cases presented above in Figure 3.11, for ϕ=5.

For the homogeneous distribution, the reaction and diffusion phenomena are present throughout the entire particle, leading to the typical parabolic concentration profile.

For the egg-shell distribution, the reaction is limited to an outer region of the particle (x>1/3). In this case, in the inner region of the particle that contains no enzyme (0<x<1/3) the substrates can only diffuse; in this region, initially without any substrate molecules, the concentration of the substrates will rise until it is the same for every radial position. The same behavior can be found with the egg-white distribution.

With the egg-white distribution there are two regions over which no reaction takes place (x<1/3 and x>2/3). This can be clearly identified in Figure 3.12 by the flat concentration line in the inner region (similar to the egg-shell distribution) and the slight inflection in the curve near x=2/3; this inflection is a result of the accentuation in the concentration gradient caused by the consumption of the substrates by the reaction.

The egg-yolk distribution leads to an intraparticle profile that resembles both the egg-white and the homogeneous distributions. In this case, the inflection in the concentration curve occurs in the outer region of the particle but, since the reaction takes place until the centre of the particle, the profile follows a parabolic shape until x=0.

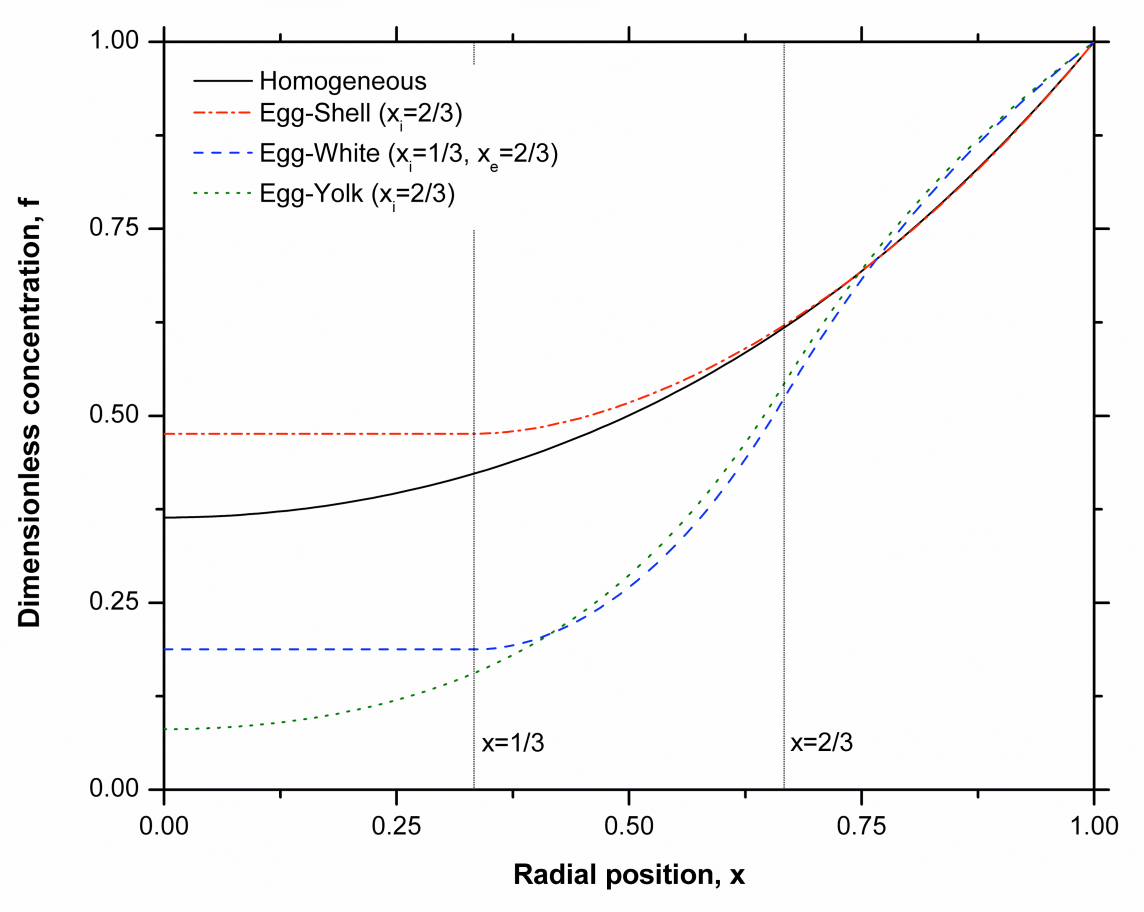


Figure 3.12. Intraparticle dimensionless concentration profiles for different enzyme distributions (ϕ=5, K_{I0}/K_{MA0}=1.56, $K_{MA0}=K_{MB0}$=1).

3.5.3.4 EFFECT OF EXTERNAL MASS TRANFER LIMITATIONS (BI_M)

In general, in order to reach the catalyst particle, molecules must firstly diffuse from the bulk across a stagnant layer of fluid that surrounds the particle. Comparatively to the internal diffusion and/or reaction rate, when the external diffusion rate is of the same order of magnitude or lower, this phenomenon will have an influence in the outcome of the process and must be considered. In the present model, external diffusion is accounted for in Bi_m, the Biot mass transfer number, which compares the characteristic times of internal and external diffusions. Considering only these two phenomena, for large Bi_m, external diffusion is much faster than internal diffusion, and the latter becomes the limiting step; in this case, the concentration on the surface of the particle will be the same as in the bulk. For small values of

the Biot number, external diffusion is much slower than internal diffusion, and a concentration gradient will form across the stagnant layer of fluid, eventually leading to a lower concentration at the surface of the particle than in the bulk.

The remaining parameters of the model will complete the description of the system by introducing the reaction phenomenon. Figure 3.13 presents simulations for several Bi_m, ϕ and K_{I0}/K_{M0}. The same Thiele modulus and Biot number was used for both substrates and a K_{M0} of 1 was used.

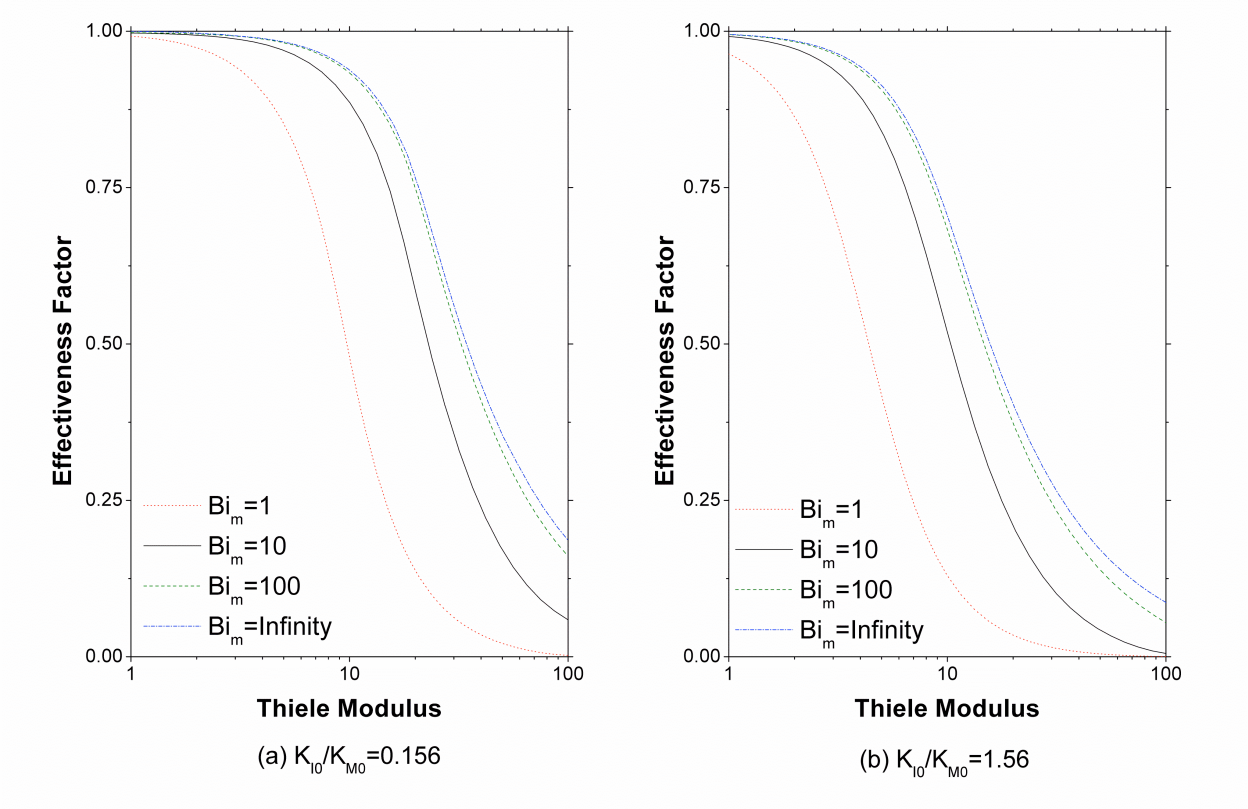


Figure 3.13. Effect of Bim on effectiveness factor (K_{M0}=1) (a) K_{I0}/K_{M0}=0.156 (b) K_{I0}/K_{M0}=1.56.

For the same Thiele modulus, the presence of external diffusion limitations ($Bi_m \rightarrow 0$) reduces the global effectiveness factor. External diffusion limitations reduce the concentration of the reactants at the surface of the particles which, for the present kinetic mechanism and parameters used in the simulations, leads to lower reaction rates.

Increasing the Biot number will increase the effectiveness factor until the limiting case in which the external diffusion rate is much faster than the internal diffusion or reaction rates

(Bi→∞); this case corresponds to the absence of external diffusion limitations and the effectiveness factor vs. Thiele modulus curves overlap.

For very low Thiele modulus, the effectiveness factor curves for different Bi_m will tend to 1. In this case, the reaction becomes the rate limiting step and both the external and internal mass transfer resistances become irrelevant.

As in the cases presented above, the presence of inhibition by the alcohol ($K_{I0}/K_{M0}\rightarrow 0$) will reduce the reaction rate in a way that is not considered in the Thiele modulus. Thus, keeping all other parameters constant, reducing K_{I0}/K_{M0} leads to a higher effectiveness factor. This is depicted in Figure 3.13, by displacement of the effectiveness factor curves to the right when inhibition is stronger, as the range of influence of the Thiele modulus is shifted to higher values.

It is worth noting that, similarly to the case presented above for different Thiele modulus, if inhibition is strong enough and the diffusion of the alcohol across the stagnant film is slower than the diffusion of the ester, effectiveness factors higher than one can possibly rise from external diffusion limitations as well.

3.6 CONCLUSIONS

A model for a batch reactor performing the transesterification of vinyl acetate with decanol in n-hexane, catalyzed by Novozym 435 (*Candida antarctica* lipase B) was developed. The model included the effect of internal and external mass transfer resistances, the heterogeneous intraparticle distribution of the enzyme and the thermodynamic non-ideality of the reaction mixture, by using an activity coefficient based kinetic equation.

For any general kinetic mechanism, the model presents at least 6 dimensionless parameters (an additional parameter will be introduced later to account for heterogeneous distributions):

- 2 B_{im}, accounting for the competition between the film and intraparticle diffusion of each substrate;
- 2 Thiele modulus to account for the competition between the reaction phenomenon and the intraparticle diffusion of both reagents;

- The ratio of diffusion time constants $\frac{\tau_{d1}}{\tau_{d2}}$ accounting for possibly different diffusion rates of both substrates;
- The volume ratio between the catalyst and the liquid phase (V_S/V_L)

3 additional parameters must be included for the Ping-pong bi-bi kinetic mechanism with competitive inhibition by the alcohol, the dimensionless kinetic constants $K_{M0A,}$ K_{M0B} and K_{I0}/K_{M0A}.

If a heterogeneous intraparticle enzyme distribution is used, additional parameters should be included and depend on the distribution itself. For an egg-shell distribution, the parameter x_i, the dimensionless radial position of the inner boundary of the egg-shell is enough to describe the distribution.

The model was able to predict several sets of experimental data obtained with catalyst particles of several sizes and different initial concentrations of each reagent. All parameters used in the simulations were either estimated or experimentally measured:

- The kinetic parameters were determined in the previous chapter with independent data obtained in the absence of diffusion limitations;
- Internal diffusion was assumed to follow Fick's first law and the diffusion coefficients were estimated by the Wilke-Chang method.
- The thickness of the enzyme shell was estimated from the specific enzyme loading for particles of different sizes, assuming that the amount of enzyme/volume of support is independent of the particle size;
- The particle porosity and apparent density were determined by mercury porosimetry and helium picnometry.
- The influence of external diffusion limitations was eliminated and hence, there was no need to estimate the mass transfer coefficients for film diffusion.

When the particle diameter is very small (crushed particles) the model predictions are consistent with the prediction of the batch reactor model developed in the previous chapter, that considers no mass transfer resistances.

A steady state model based on the same assumptions of the previous one was developed in order to analyze the influence of the model parameters in the effectiveness factor as well as the effect of different intraparticle distributions.

In general, the typical dependency of the effectiveness factor with the Thiele modulus was found, but the range of values of the Thiele modulus that influence the outcome of the process is higher than usual and depends on the dimensionless kinetic parameters. This is due to the fact that in the definition of the Thiele modulus a simplified characteristic reaction rate is used that overestimates the actual reaction rate. Accordingly, all changes in the dimensionless kinetic parameters that change the reaction rate in a way that is not accounted for in the Thiele modulus definition change the range of influence of this parameter. For example, a lower K_{I0}/K_{M0A} reduces the reaction rate leading, for the same value of the Thiele modulus to a higher effectiveness factor, thus displacing the range of influence of this parameter to higher values.

Effectiveness factors higher than one may arise in some conditions provided that inhibition is strong enough, translated by a low K_{I0}/K_{M0A}; and that the diffusion of the inhibiting substrate, the alcohol, is slower than the diffusion of the ester. In the case of the reaction system under study such effectiveness factors are unlikely to occur due to the mild inhibition.

Regarding the enzyme distribution, it was shown that for the transesterification of vinyl acetate and decanol, the observable reaction rate is favored by distributions that place the enzyme closer to the surface. This is the general case of a positive order reaction mechanism. The model is able to predict the intraparticle concentration gradients which are notoriously different depending on the enzyme distribution.

In the case of the experimental reaction system, the presence of internal mass transfer resistances will generally lower the effectiveness factor.

3.7 NOMENCLATURE

a_i	Activity of component i
a_{nm}	UNIFAC group interaction parameter between groups n and m
Bim	Biot number for mass transfer
c_i	Intraparticle concentration of component i (M)
C_i	Concentration of component i in the bulk phase (M)
C^S	Concentration of component i in the surface of the particles (M)
D	Molecular diffusivity (cm^2/s)
De	Effective diffusivity (cm^2/s)
D_P	Pore diffusivity (cm^2/s)
d_p	Particle diameter (μm)

f_i	Dimensionless intraparticle concentration of component i
F_i	Dimensionless concentration of component i in the bulk phase
k_f	Mass transfer coefficient between the liquid and the catalyst surface (cm/s)
K_I	Competitive inhibition constant (M)
K_{I0}	Dimensionless competitive inhibition constant
K_{Mi}	Michaelis constant for substrate i (M)
K_{Mi0}	Dimensionless Michaelis constant for substrate i
N_{Points}	Number of experimental points used in the optimization
R	Radial intraparticle position (μm)
R	Reaction rate (mol/g_{enzyme}.min)
R_{Obs}	Observable reaction rate (mol/g_{enzyme}.min)
R_{Bulk}	Reaction rate at Bulk conditions (mol/g_{enzyme}.min)
R_E	Radial position of the external boundary of the section of the particle that contains enzyme (μm)
R_I	Radial position of the internal boundary of the section of the particle that contains enzyme (μm)
R_p	Particle radius (μm)
S	Surface Area (μm)
T	Temperature (ºC)
T	Time (min)
V_L	Volume of the liquid phase in the reactor
V_S	Volume of the solid phase (catalyst) in the reactor
V_{max}	Maximum forward reaction rate (mol/g_{Enzyme}.min)
W_E	Specific enzyme loading ($g_{Enzyme}/g_{catalyst\ particles}$)
$W_E(r)$	Enzyme intraparticle distribution function ($g_{Enzyme}/g_{catalyst\ particles}$)
W_S	Amount of catalyst particles within the reactor (mg/mL)
X_i	Conversion of component i (%)
X	Dimensionless radial position

Greek Symbols

γ_i	Activity coefficient of the component i
ε_P	Particle porosity ($cm^3_{pores}/cm^3_{particle}$)
η	Effectiveness factor
θ	Dimensionless time
ρ_{app}	Apparent density ($g/cm^3_{particle}$)
τ_D	Internal diffusion time constant (s)
ϕ	Thiele modulus

Subscripts

1	Vinyl Acetate
2	Decanol
A	Vinyl Acetate
B	Decanol

Superscripts

0	Initial
a	Activity based

3.8 BIBLIOGRAPHY

Al-Muftah, A. E. and Abu-Reesh, I. M. (2005). Effects of internal mass transfer and product inhibition on a simulated immobilized enzyme-catalyzed reactor for lactose hydrolysis. Biochemical Engineering Journal 23 (2): 139-153.

Al-Muftah, A. E. and Abu-Reesh, I. M. (2005). Effects of simultaneous internal and external mass transfer and product inhibition on immobilized enzyme-catalyzed reactor. Biochemical Engineering Journal 27 (2): 167-178.

Bischoff, K. B. (1965). Effectiveness factors for general reaction rate forms. AIChE Journal 11 (2): 351-355.

Borchert, A. and Buchholz, K. (1984). Improved biocatalyst effectiveness by controlled immobilization of enzymes. Biotechnology and Bioengineering 26 (7): 727-736.

Froment, G. F. and Bischoff, K. B. (1990). Chemical reactor analysis and design (Second Edition). New York, John Wiley and Sons.

Gmehling, J., Li, J. and Schiller, M. (1993). Modified UNIFAC model. 2. Present parameter matrix and results for different thermodynamic properties. Industrial & Engineering Chemistry Research 32 (1): 178-193.

Juang, H.-D. and Weng, H.-S. (1984). Performance of biocatalysts with nonuniformly distributed immobilized enzyme. Biotechnology and Bioengineering 26 (6): 623-626.

Ladero, M., Santos, A. and García-Ochoa, F. (2001). Diffusion and chemical reaction rates with nonuniform enzyme distribution: an experimental approach. Biotechnology and Bioengineering 72 (4): 458-467.

Madsen, N. K. and Sincovec, R. F. (1979). Algorithm 540: PDECOL, general collocation software for partial differential equations. ACM Trans. Math. Soft. 5: 326-351.

Mei, Y., Miller, L., Gao, W. and Gross, R. (2003). Imaging the distribution and secondary structure of immobilized enzymes using infrared microspectroscopy. Biomacromolecules 4 (1): 70-74.

Morbidelli, M., Gavriilidis, A. and Varma, A. (2001). Catalyst design: optimal distribution of catalyst in pellets, reactors and membranes Cambridge, Cambridge University Press.

Park, S. H., Lee, S. B. and Ryu, D. D. Y. (1981). Design of a nonuniformly distributed biocatalyst. Biotechnology and Bioengineering 23 (11): 2591-2600.

Reid, R. C., Prausnitz, J. M. and Sherwood, T. K. (1977). The Properties of Gases and Liquids (Third Edition). New York, McGraw-Hill.

Shiraishi, F., Hasegawa, T., Kasai, S., Makishita, N. and Miyakawa, H. (1996). Characteristics of Apparent Kinetic Parameters in a Packedbed Immobilized Enzyme Reactor. Chem. Eng. Sci. 51: 2847-2852.

van Roon, J. L., Groenendijk, E., Kieft, H., Schroen, C. G. P. H., Tramper, J. and Beeftink, H. H. (2005). Novel approach to quantify immobilized-enzyme distributions. Biotechnology and Bioengineering 89 (6): 660-669.

Xiu, G.-H., Jiang, L. and Li, P. (2000). Mass-transfer limitations for immobilized enzyme-catalyzed kinetic resolution of racemate in a batch reactor. Ind. Eng. Chem. Res. 39: 4054-4062.

4. PRODUCTION OF DECYL ACETATE IN A PACKED BED REACTOR: MODELING AND SIMULATION

In this section the transesterification of vinyl acetate and decanol is performed in a packed bed reactor and a reactor model is developed and tested for this system. The stability of the enzyme is also tested in continuous operation mode. Additionally the solvent free production of decyl acetate is tested in a batch reactor, the main differences in comparison to its production in hexane are analyzed and the capacity of the model presented in Section 3 to describe the solvent free system is tested

4.1 EXPERIMENTAL METHODS

4.1.1 ENZYMES AND CHEMICALS

Vinyl acetate, decanol and decyl acetate were obtained from Sigma-Aldrich (>99%). Hexane was purchased from Merck (pro-analysis). Novozym 435 was gently provided by Novozymes.

4.1.2 EXPERIMENTAL SETUP

The continuous tubular packed bed reactor consisted in a glass column of variable length from *Omnifit*, used for low and mid pressure liquid chromatography, with 6.6 mm internal diameter and achievable bed height of 40-120 mm.

The column was packed with Novozym 435 particles of 460 μm to a bed height of 55 mm. For the packing, the catalyst particles were placed in a beaker with hexane; the empty

column was then filled with hexane and the catalyst particles were placed inside in small amounts. This procedure ensures the absence of air pockets inside the reactor, which would interfere with the hydrodynamics and lead to an ineffective use of the catalyst.

The experimental apparatus constructed from the structure of a supercritical fluid chromatograph *(SFC 200A* from *Suprex*) in which the chromatography column was replaced by the packed bed reactor, inside chromatograph's oven, which was used for temperature control. The detector was bypassed and the outlet stream was collected in a closed flask.

For the reaction mixture a solution of vinyl acetate and decanol in n-hexane was prepared and the chromatograph's syringe pump was used to feed the packed bed reactor.

In each experiment, both the flow rate and the temperature were confirmed by measuring both parameters in the outlet stream. Flow rate was measured with a chronometer and a graduated cylinder and the temperature, with a thermometer.

Samples were taken directly to glass vials, and analyzed by GC.

4.1.3 ANALYTICAL METHODS

Several 500μL samples were withdrawn and analyzed by gas chromatography in a Varian CP-3800 GC equipped with a TCD detector and auto sampler. A 25m x 0.53 mm WCOT column was used in the analysis and the calibration was made with synthetic mixtures of the pure components. The operating temperatures were 270 ºC for the injector, 165 ºC for the column oven and 340 ºC for the TCD filament and helium was used as the carrier gas. All data presented are the average of three measurements.

4.2 DIMENSIONAL ANALYSIS OF THE REACTOR

In a continuous packed bed tubular reactor, several mass transfer and fluid flow phenomena can occur and might influence the performance of the reactor.

In an empty tube, a pressure drop is usually established between both ends, as a result of the friction between the flowing fluid and the tube's walls. In a packed bed, the presence of the catalyst particles provides additional resistance to the flow, further contributing to a decrease in pressure.

Regarding the flow profile, additionally to the basic convective transport, dispersion can occur in the axial and radial directions.

All these phenomena are strongly dependent of the flow regime, as defined by the Reynolds number (Bird et al. 2001). For flow in a packed bed of spherical particles:

$$Re_P = \frac{\rho_f u_S d_P}{\mu_f (1-\varepsilon_b)} \tag{4.1}$$

$Re_P<10$	Laminar flow
$Re_P>2000$	Turbulent flow

where ρ_f, represents the fluid density, u_S the fluid's superficial velocity, d_p the diameter of the catalyst particles, μ_f the fluid viscosity and ε_b the porosity of the bulk.

For industrial reactors turbulent flow is commonly achieved, at lab scale however, due to the reduced flow rates and particle sizes used, this is often not the case.

Figure 4.1 presents the Reynolds number, based on the dimensions of the catalyst particles used to perform all experiments and the physical properties of hexane at 30ºC, as a function of the flow rate, for several bulk porosities.

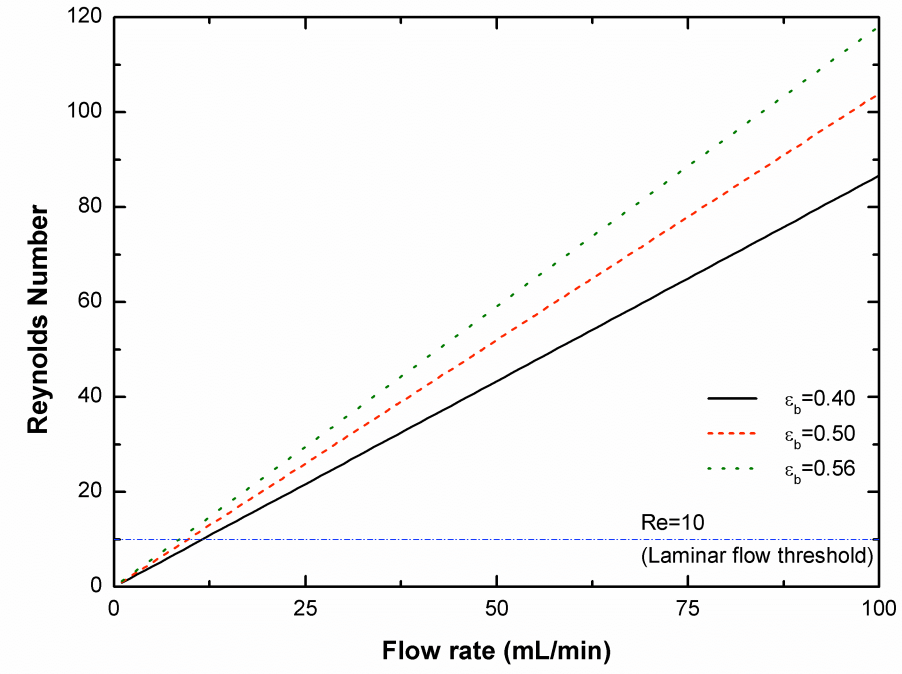


Figure 4.1. Reynolds number as a function of the flow rate, for different bulk porosities. d_p=460µm, T=30 ºC.

It is clear from Figure 4.1 that for the flow rates expected for a reactor of such dimensions, turbulent flow is ruled out. The flow regime will be either laminar or transient; the corresponding impact will now be analyzed in more detail.

4.2.1 ESTIMATION OF PREASSURE DROP

The Ergun Equation is widely used to estimate the pressure drop across packed tubes (Froment and Bischoff 1990):

$$\frac{(-\Delta p)}{L}\frac{d_P}{\rho_f u_S^2}\frac{\varepsilon_b^3}{1-\varepsilon_b} = \frac{150}{Re_P} + 1.75 \qquad (4.2)$$

where Δp represents the pressure drop, and L the length of the tube. From Ergun's equation, the pressure drop increases with the flow rate and tube length and decreases with the porosity and particle size.

Figure 4.2 presents the pressure drop across the reactor, based on the dimensions of the tubular reactor, the catalyst particles used to perform all experiments and the physical properties of hexane at 30ºC, as a function of the flow rate, for several bulk porosities.

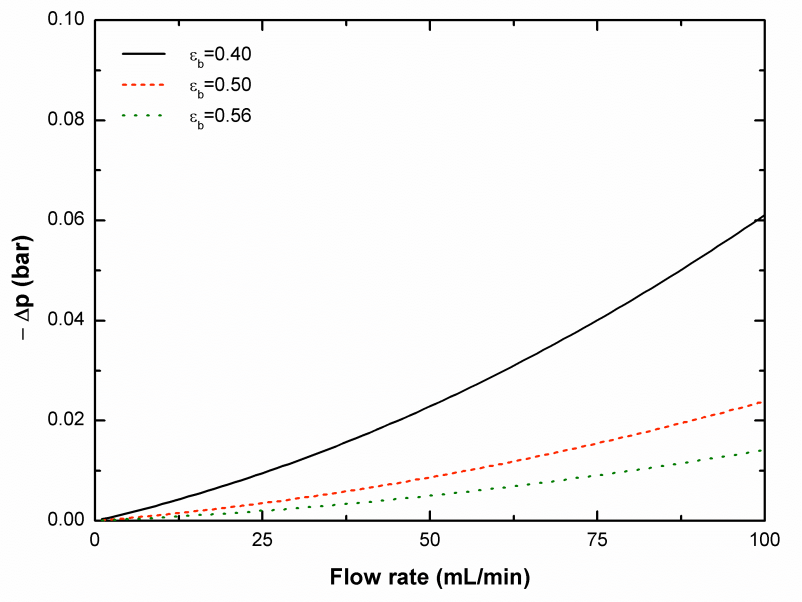


Figure 4.2. Pressure drop across the packed bed reactor as a function of the flow rate, for different bulk porosities. d_p=460 µm, d_T=6.6 mm, L=55 mm, T=30ºC.

From Ergun's equation, the pressure drop is not expected to be high. Considering that experimental flow rates below 30mL/min are expected, the pressure drop will be lower than 0.01bar. For bulk porosities above 0.5 it will even be lower than 0.05bar. The pressure will thus be considered constant throughout the reactor.

4.2.2 INFLUENCE OF AXIAL DISPERSION

Mixing in the axial direction (back mixing) on a packed bed tubular reactor can be induced by both turbulence and the presence of the packing (Froment and Bischoff 1990). When plug flow is used to describe the flow across the reactor, axial dispersion is commonly superimposed to account for deviations to this ideal mechanism.

For isothermal reactions performed in packed columns, it has been shown that axial dispersion can be neglected if the L/d_p, the ratio between the tube length and the diameter of the packing, is greater than 50 (Carberry 1976). For non-isothermal reactions the threshold increases to 150. For the reactor and catalyst used in all experiments, $L/d_p=120$. Since for the concentrations used the reaction can be considered isothermal, axial mixing is, in principle, not necessary to describe the reactor.

It can be derived from the definition of the time constant of diffusive processes that the packed bed reactor may be approximated as a series of n CSTRs, n defined as (Carberry 1976):

$$n = \frac{L}{2d_p} Pe_{ax} \tag{4.3}$$

Actual data for axial dispersion in packed tubes compiled by Wilhelm (Wilhelm 1962), show that for the range of Reynolds numbers corresponding to the experimental conditions used, the axial-dispersion Peclet number is approximately 0.4. Hence, the packed bed could be treated as a series of c.a. 24 CSTRs. On the other hand, a series of more than 20 CSTRs behaves like plug-flow reactor; further supporting that axial dispersion should be negligible.

4.2.3 RADIAL CONCENTRATION PROFILES

Radial dispersion in a packed bed is often reviewed as a result of stream splitting coming from the flow around the catalyst particles (Carberry 1976). This can be visualized by imagining that when a stream hits a particle it will be divided around it. This process will occur repeatedly leading to radial dispersion/mixing. Radial dispersion is often desired, as it lumps radial concentration profiles, in the cross section of the tube.

Flow in an empty tube is commonly expressed as:

$$u = 2\bar{u}\left[1 - \left(\frac{r_T}{R_T}\right)^n\right] \tag{4.4}$$

where $\bar{u}$ represents the average velocity, r, the radial position in the reactor and R, the radius of the tube.

For laminar flow n=2, leading to a parabolic velocity profile in the radial direction. In the opposite end, for $n \rightarrow \infty$, the velocity is the same in any radial position apart from the wall, and plug flow is obtained, a behavior which is closer to turbulent flow. Particularly for laminar and transient regimes, radial dispersion can contribute to lump this radial profile by inducing radial mixing, contributing to an approach to plug flow. The smaller the aspect ratio of the tube, L/d_t, however, the less likely it is that the radial mixing is effective enough for the flow to be successfully described as plug flow.

For non-isothermal reactions, radial concentration profiles can also result from temperature profiles. For an exothermic reaction, since heat is usually being removed at the reactor's wall, the temperature will be higher in the axis of the tube, leading to faster reaction rates in this position, and consequently to a faster consumption of the reactants in the axis of the tube. Furthermore, the temperature profile can also lead to mass transfer towards the reactor's wall, generated by natural convective heat transfer.

As stated above, for the experimental packed-bed, the influence of thermal effects should be negligible and hence, concentration profiles induced by temperature differences can be ruled out. Given the typically low flow rates used in laboratory scale, a flow induced radial profile (parabolic) is likely to occur. On the other hand, radial mixing (radial dispersion) is expected to exist due to the presence of the packing which contributes to lump this profiles. The exact extent of the radial mixing and the importance of the radial concentration profile in

the system are hard to estimate. The reactor modeling approach will be to firstly test the capacity to describe the reactor considering plug flow and subsequently introduce radial dispersion or other flow patterns if necessary.

4.2.4 INFLUENCE OF EXTERNAL DIFFUSION

Unlike the batch reactor, where external diffusion limitations are simple to overcome with agitation devices, in a packed bed reactor, external diffusion can be reduced by increasing the flow rate. On a laboratory scale, where low flow rates are commonly used, external diffusion is likely to exist.

To estimate the mass transfer coefficients between the liquid and the catalyst surface, the Ranz-Marshall correlation is commonly used (Ranz and Marshall 1952):

$$Sh=2+0.6Re_{p*}^{1/2}Sc^{1/3} \tag{4.5}$$

where *Sh* represents the Sherwood number, Re_{p*}, the Reynolds number and *Sc*, the Schmidt number, as defined in Table 4.1.

Table 4.1. Dimensionless numbers present in the Ranz-Marshall correlation.

Designation	Parameter	Physical interpretation
Reynolds number (based on particle diameter)	$Re_{p*} = \frac{\rho u_S d_p}{\mu_f}$	Ratio of inertial and viscous forces
Schmidt number	$Sc = \frac{\mu_f}{\rho_f D_m}$	Ratio of momentum and mass diffusivity
Sherwood number	$Sh = \frac{Lk_f}{D_m}$	Ratio of convective and diffusive mass transport

After estimating the film diffusion mass transfer coefficients, the Biot number can be calculated to analyze the influence of external diffusion limitations. Figure 4.3 presents the Biot number as a function of the flow rate. As expected, the Biot number increases with the flow rate, indicating that film diffusion becomes less relevant at higher flow rates, nonethe-

less, for Biot numbers below 100, external mass transfer limitations are still expected exist and will thus be included in the reactor model.

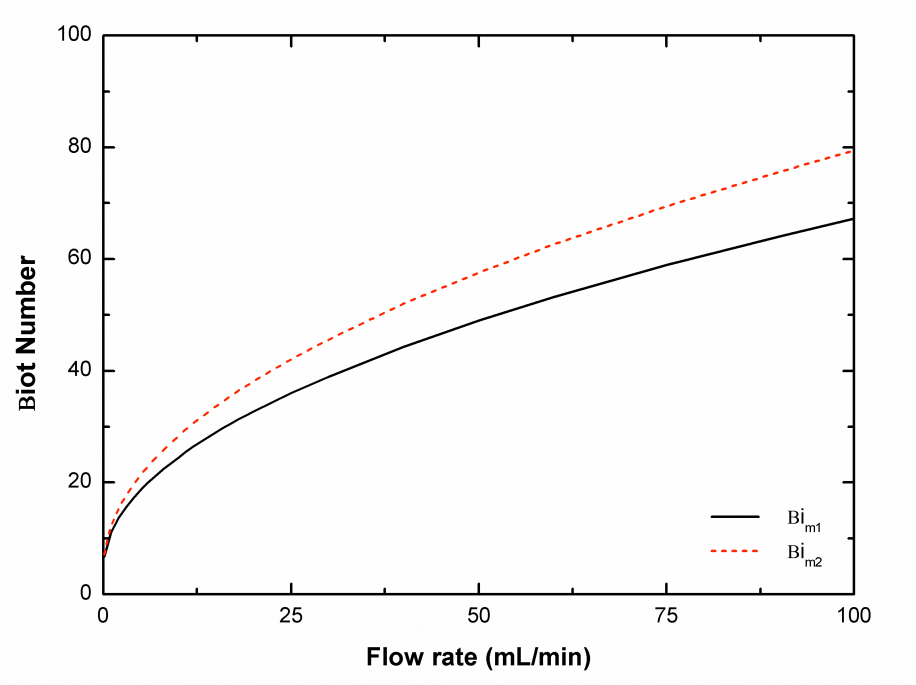


Figure 4.3. Biot number as a function of the flow rate. d_p=460 μm, T=30 ºC.

4.3 PACKED BED REACTOR MODEL DEVELOPMENT

4.3.1 INTRAPARTICLE MATERIAL BALANCE

The intraparticle material balance describes the material flows inside each catalyst particle and, hence, does not depend on the type of reactor. Based on the same assumptions presented in the previous chapter, the intraparticle material balance yields the same equations. Thus, for component *i*:

$$\varepsilon_p \frac{\partial c_i}{\partial t} = \varepsilon_p D_{pi} \frac{1}{r^2} \frac{\partial}{\partial r}\left(r^2 \frac{\partial c_i}{\partial r} \right) - RW_E(r)\,\rho_{app} \tag{4.6}$$

$$t = 0 \qquad 0 < r < R_P \qquad c_i = 0 \tag{4.7}$$

$$
\begin{aligned}
&t > 0 \qquad r = 0 \qquad \left.\frac{\partial c_i}{\partial r}\right|_{r=0} = 0 \\
&\qquad\quad r = R_P \qquad \varepsilon_P D_P \frac{\partial c_i}{\partial r} = k_f \left(C_i - c_i\right)
\end{aligned}
\tag{4.8}
$$

where c_i represents the concentration of substrate i; t, the time, r, the radial position inside the particle; ε_P, the particle porosity; D_{pi}, the diffusion coefficient of species i inside the pores; $W_E(r)$, the enzyme distribution function, as defined in the previous chapter; ρ_{app}, the apparent density of the catalyst particle; and R, the reaction rate; R_P is the radius of the particle; C_i, the concentration of species i outside the particle, in the bulk phase; and k_f, the mass transfer coefficient between the liquid and the catalyst surface.

4.3.2 BULK PHASE MATERIAL BALANCE

As in the batch reactor model presented in the previous chapter, no chemical reactions occur in the bulk phase, therefore the bulk phase material balance only needs to account for transport phenomena between the bulk phase and the surface of the catalyst particles and for the flow and dispersion mechanisms. As stated above, axial dispersion is expected to be negligible and radial dispersion will at first not be accounted for. Regarding the flow mechanism, plug flow will be assumed. Considering external diffusion limitations across a stagnant fluid film around the particles, the material balance for the component *i* in packed bed rector yields:

$$
-\varepsilon_B \frac{\partial C_i}{\partial t} = \frac{\partial \left(u_S C_i\right)}{\partial l} + k_{fi} \frac{3}{R_P} \frac{\rho_B}{\rho_{app}} \left(C_i - c_i\big|_{r=R_P}\right) \tag{4.9}
$$

$$
t = 0 \qquad C_i = 0 \tag{4.10}
$$

$$
z = 0 \qquad C_i = C_{i0} \tag{4.11}
$$

where u_S represents the superficial velocity of the fluid phase; C_i the concentration of component *i*; k_f, the mass transfer coefficient between the liquid and the catalyst surface; R_P, the radius of the catalyst particles; ρ_B, the bulk density, c_i, the intraparticle concentration of

component *i*; ε_B, the bulk density; *l*, the longitudinal position in the packed bed reactor and C_{i0} the concentration of component *i* in the feed stream.

4.3.3 COMPLETE MODEL

By introducing the dimensionless variables and parameters presented in Table 4.2, Equations (4.6)-(4.11) can be more conveniently expressed, leading to the final form of the model's equations:

$$\varepsilon_p \frac{\tau_{di}}{\tau_{d1}} \frac{\partial f_i}{\partial \theta} = \frac{\partial^2 f_i}{\partial x^2} + \frac{2}{x} \frac{\partial f_i}{\partial x} - \phi_i^2 E(x) \frac{R}{v_{max}} K_{M0i} \quad , i = 1, 2 \tag{4.12}$$

$$\varepsilon_B \frac{\partial F_i}{\partial \theta} = \frac{\tau_{D1}}{\tau} \frac{\partial F_i}{\partial z} - 3Bi_{mi} \frac{\tau_{Di}}{\tau_{D1}} \frac{\rho_B}{\rho_{app}} \left(F_i - f_i \big|_{x=1} \right) \tag{4.13}$$

Subject to the initial and boundary conditions:

$$\theta = 0, \quad f_i = 0, \quad \forall x \tag{4.14}$$

$$z = 0, \quad F_i = F_{i0} \tag{4.15}$$

$$\left. \frac{\partial f_i}{\partial x} \right|_{x=0} = 0 \tag{4.16}$$

$$\left. \frac{\partial f_1}{\partial x} \right|_{x=1} = Bi_{mi} \left(F_i - f_i \big|_{x=1} \right) \tag{4.17}$$

Knowing the composition of the packed bed reactor feed stream, the model's equations can then be integrated across the reactor length (from z=0 to z=L), in order to calculate the concentration of all species in the packed bed reactor at any position and any given time.

Table 4.2. Dimensionless parameters and variables of the packed bed reactor model.

Parameter	Designation
$f_i = \frac{ci}{C_{i0}}$	Dimensionless intraparticle concentration
$F_i = \frac{C_i}{C_{i0}}$	Dimensionless bulk concentration
$x = \frac{r}{R_P}$	Dimensionless intraparticle radial position
$z = \frac{l}{L}$	Dimensionless reactor longitudinal position
$\theta = \frac{t}{\tau_{d1}}$	Dimensionless time
$\tau = \frac{L}{u_S}$	Space time
$\tau_{di} = \frac{R_P^2}{\varepsilon_p D_{pi}}$	Internal diffusion time constant
$Bi_{mi} = \frac{k_{fi} R_p}{\varepsilon_P D_{Pi}}$	Biot Number for mass transfer
$\phi_i = R_P \sqrt{\frac{v_{max} \rho_{app} W_E}{K_{Mi} \varepsilon_p D_{pi}}}$	Thiele Modulus
$K_{M0i} = \frac{K_{Mi}}{C_{i0}}$	Dimensionless Michaelis Constant
$K_{I0} = \frac{K_I}{C_{B0}}$	Dimensionless competitive inhibition constant

The packed bed reactor model has several parameters in common with the batch reactor model presented in the previous section. Changing the reactor type does not affect the phenomena occurring at an intraparticle level hence, the parameters related with the reaction, intraparticle mass transfer and mass transfer in the solid-fluid interface remain unaltered, namely; the Thiele modulus, ϕ_i; the Biot number, Bi_{mi}; and the dimensionless kinetic parameters, K_{M0i} and K_{I0}. The space time, τ, arises from the fact that, contrary to the batch reactor,

the packed bed reactor is an open system; τ provides an indication of the time the solution is in contact with the catalyst before leaving the reactor.

4.4 Results and Discussion

Analysing the model's parameters, after defining the reaction and the reactor (bed size, packing, type of catalyst and dimensions), the outlet concentration will be defined by the space time and the composition of the feed stream.

A solution of vinyl acetate and decanol in n-hexane (0.1 M of each reactant) was fed to a packed bed reactor (L=55 mm, d=6.6 mm, ε_B=0.56) with Novozym 435 catalyst particles of 460 μm, at different flow rates (thus, varying space time). Figure 4.4, presents the results obtained experimentally and the model predictions. The parameters used in the simulations are presented in Table 4.3.

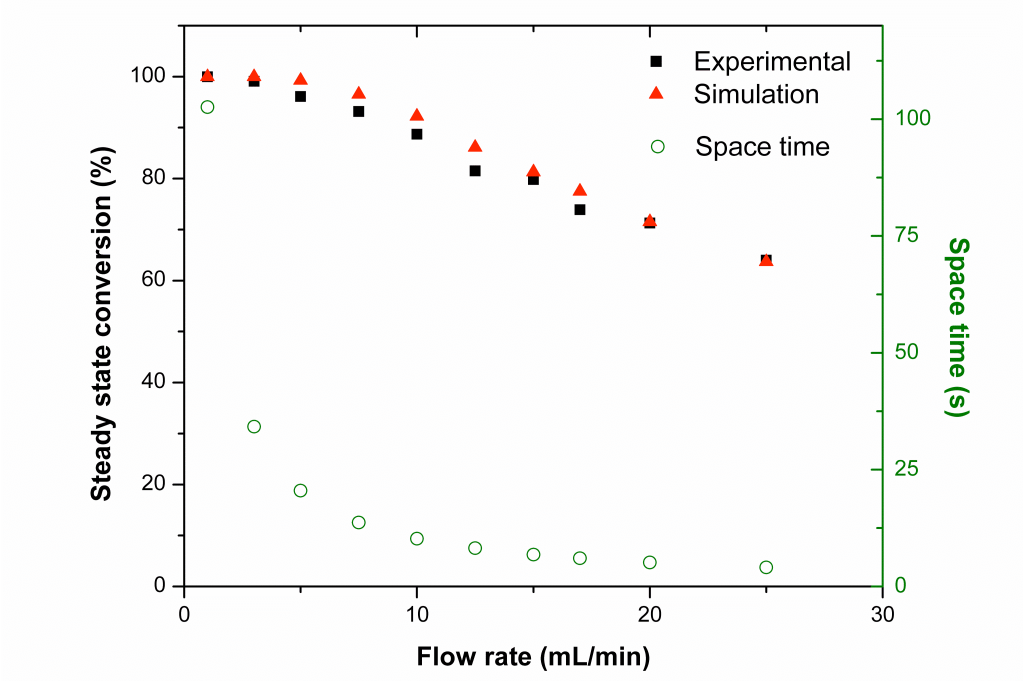


Figure 4.4. Effect of flow rate on the steady state conversion and space time. Feed composition: [A]=[B]=0.1 M; Reactor: L=55 mm, d=6.6 mm, ε_B=0.56; catalyst: d_p=460 μm. T=30 ºC for all essays.

The steady state conversion varies considerably with the flow rate. Increasing the flow rate decreases the space time and, hence, the average time that the fluid stream will stay inside the reactor, in contact with the catalyst. Thus, increasing the flow rate decreases the steady state conversion, unless the catalyst bed is over dimensioned, i.e., if complete conversion is achieved before reaching the reactor outlet; this occurs for flow rates below 3mL/min.

The model predictions for the steady state conversion are in accordance with the experimental data. As in the batch reactor model, all parameters used in the simulations were either experimentally measured or estimated. The obtained bulk porosity, 0.56, is high when compared to typical bulk porosities obtained in packed beds of spherical particles (~0.40-0.50). Usually, better packing can be achieved through vibration methods but in this case, their application is limited by the risk of damaging the glass reactor.

Table 4.3. Parameters used in the simulations

Parameters used in the simulations		
Catalyst Particle Characterization	ε_P (cm^3_{pores}/ $cm^3_{particle}$)	0.42
	ρ_{app} (g/cm^3)	720
	R_P (μm)	460
	Shell Thickness (μm)	80
	W_E($g_{enzyme}/g_{particle}$)	0.092
Mass transfer properties	D_{P1} (cm^2/s)	2.30×10^{-5}
	D_{P2} (cm^2/s)	1.35×10^{-5}
	$K_{fl,2}$	Flow rate dependent. Estimated with the Ranz-Marshall correlation[1]
Activity Based Kinetic Parameters	V_{max} ($mol/g_{Enz}.min$)	0.542
	K_{MA} (M)	0.0862
	K_{MB} (M)	0.0788
	K_I (M)	0.125
Reactor parameters	L (mm)	55
	d_T (mm)	6.6
	ε_B (cm^3_{void}/ $cm^3_{reactor}$)	0.56

[1](Ranz and Marshall 1952)

To study the stability of the catalyst, the reactor operated continuously for 26 hours at a flow rate of 3 mL/min. The flow rate was chosen to provide complete conversion at the reactor outlet; in order to ensure that a decrease in the catalyst activity would have a measurable impact on the conversion, while spending the minimum amount of reagents as possible. Additionally, after 25 h of operation, the flow rate was increased in order to amplify the effect of a possible deactivation of the catalyst. The obtained experimental results and the corresponding model predictions are presented in Figure 4.5.

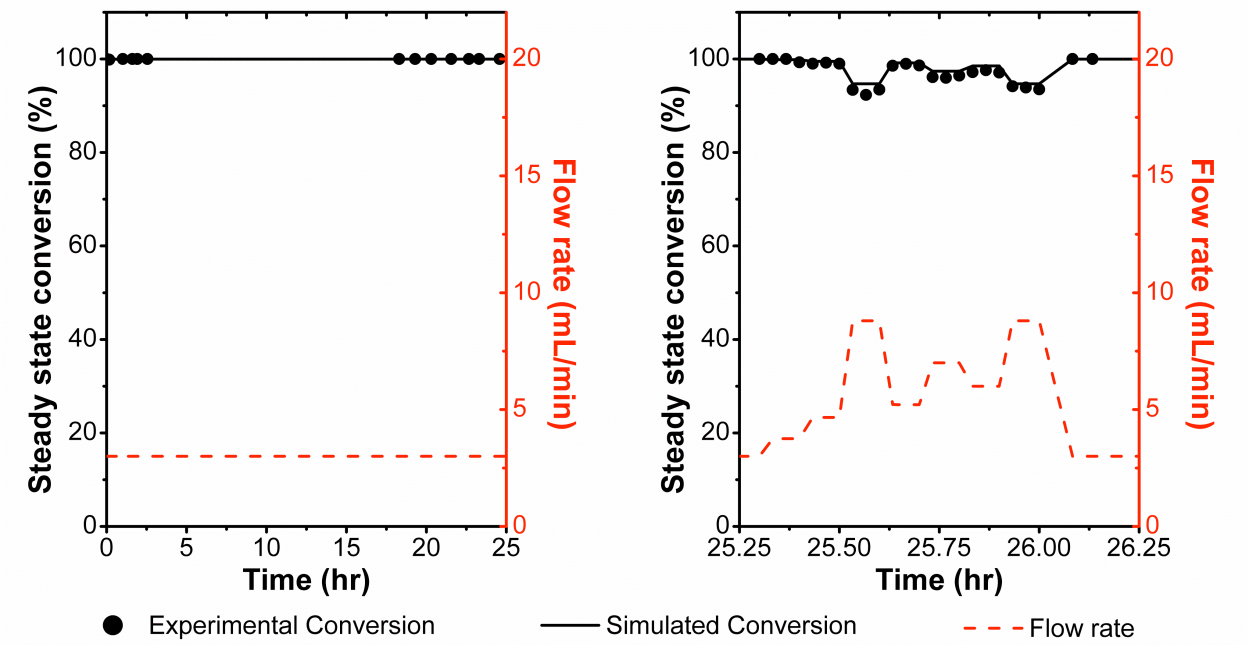


Figure 4.5. Steady state conversion as function of time. Feed composition: [A]=[B]=0.08 M; Reactor: L=55 mm, d=6.6 mm, ε_B=0.56; catalyst: d_p=460 μm. T=30 ºC.

Enzyme deactivation has been shown to depend on both temperature and composition of the medium the enzyme is exposed to (Klibanov 2001). In this case, no measurable decrease in catalyst activity was verified after 26 hours of continuous operation; which is in line with the findings of other authors (Yadav and Trivedi 2003; Ghamgui et al. 2004), supporting that Novozym 435 is a very stable biocatalyst; consequently, the present reactor model is able to satisfactorily predict the conversion for the several flow rates tested after 25 h without accounting for any catalyst deactivation.

The volumetric productivity, *VP*, is a measure of the productivity of a reactor and can be defined as:

$$VP = \frac{C_{exit}^{Product} \times Q}{V_{Reactor}} \tag{4.18}$$

Where $C_{exit}^{Product}$ represents the concentration of the product in the outlet stream and $V_{reactor}$, the reactor volume. Figure 4.6 presents the volumetric productivity of the experimental packed bed reactor as a function of the flow rate.

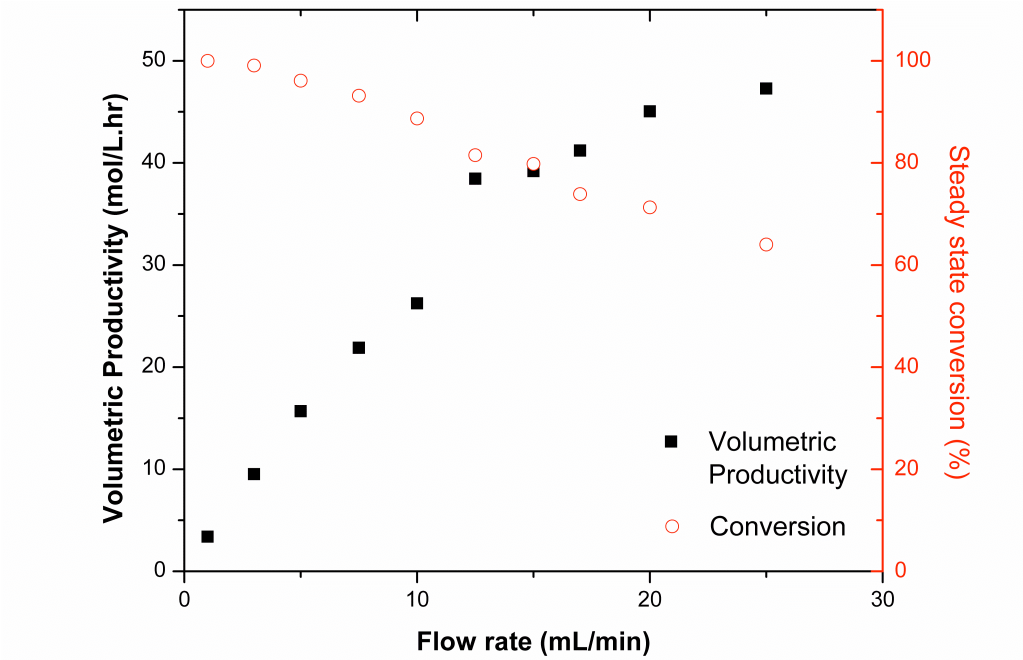


Figure 4.6. Volumetric productivity and steady state conversion as a function of the flow rate. Feed composition: [A]=[B]=0.1 M; Reactor: L=55 mm, d=6.6 mm, ε_B=0.56; catalyst: d_p=460 µm. T=30 ºC for all essays.

To achieve complete conversion with the reactor used in these experiments, a flow rate of less than 3mL/min is required. Increasing the flow rate will then decrease the steady state conversion; however, for example, duplicating the flow rate will not decrease the conversion by half. Correspondingly, the volumetric productivity of the reactor increases with the flow rate but the concentration of decyl acetate in the outlet stream will be lower and unreacted vinyl acetate and decanol will still remain in solution which requires additional or more

complex downstream separation processes in order to obtain high purity decyl acetate, which is undesirable in commercial applications.

Sraathof et al. compiled data on currently established biocatalytic industrial processes (Straathof et al. 2002). On average, these industrial processes present a yield of 78% and a final product concentration of 108 g/L. For the production of acids or alcohols, in which lipases can be used to perform the reverse hydrolytic reaction of the one performed in this work, product concentrations up to 800 g/L are reported with an average yield up to 90%.

Complete conversion can be achieved in the transesterification reaction of vinyl acetate and decanol, however, a concentration of 0.1M of each reactant in hexane, as used in the experiments presented above in a packed bed reactor correspond to 20g/L of decyl acetate after complete conversion, significantly below the average of the industrially established processes presented by Sraathof et al. Such dilute solutions seldom constitute attractive commercial applications since they lead to low productivities and usually, to high costs for solvent separation and recycling (Straathof et al. 1992; van Tol et al. 1995; Sandoval et al. 2001). The maximum concentration of decyl acetate that can be obtained in the outlet stream corresponds to solvent free operation. In this case, hexane would no longer be used as a solvent and an equimolar mixture of vinyl acetate and decanol would be fed to the reactor. In principle, with a correct dimensioning of the reactor and a choice of flow rate that would lead to complete conversion, a stream of pure decyl acetate (with the corresponding concentration of 707 g/L) would be obtained, eliminating the necessity of additional downstream separation steps, and leading to a significant increase in productivity. Thus, the possibility of solvent free operation is worth analyzing.

Considering solely the reaction rate equation, a solvent free system would lead to a higher reaction rate. Compared with a 0.1 M reaction mixture of vinyl acetate and decanol in hexane, the initial reaction rate in the absence of diffusion limitations should be 2.5 times higher for a solvent free system. A concentration increase of this magnitude can, however, significantly affect the behaviour of the reaction system. The wide concentration difference between the beginning and end of the reaction can, for example, lead to variations in the diffusion coefficients of the reactants, their activity coefficients and the polarity/hidrophobicity of the mixture. In fact, the selection of a solvent can, in many cases, be motivated by improvements in the enzyme activity, stability or selectivity (Klibanov 2001; Hazarika et al. 2002); although part of these effects can be explained by changes in the activities of the several species in solution, possible interactions between the solvent/reaction medium and the enzyme are not accounted for. It is hence not guaranteed that the use of an

activity based kinetic equation can completely describe the impact of changing or eliminating solvents in the reaction rate (van Tol et al. 1995; Sandoval et al. 2001; Straathof et al. 2002). Additionally, as a result of the reaction's exothermic nature, thermal effects will also be enhanced with the increase in concentration of the reactants. Thus, it is not granted that the behaviour of a solvent free system will be the same as when a solvent is used and it is of interest to analyse if the developed models, tested with hexane as a solvent, are able to describe solvent free operation.

Before introducing experimental results obtained without solvent, it is worth to analyse the impact of eliminating hexane in the several phenomena accounted for in the present models.

Figure 4.7 illustrates the variation of the activity coefficients of all species throughout a solvent free reaction, together with several other sets of initial conditions tested experimentally, presented before in Figure 2.12.

The activity coefficient of vinyl acetate in the liquid phase does not vary with the course of the reaction. On the other hand, as in the other equimolar reaction conditions in hexane the activity coefficient of decanol presents a significant variation. Overall, the activity coefficients of both reactants are lower than the ones obtained for the other sets of conditions in hexane. This fact once again partially illustrates why concentration based kinetic equations are unsuitable to describe the reaction rates obtained in different solvents or in the absence of a solvent. The effect of the change in the medium in the reactants activity is hence accounted for, in the present model, but its possible effect on the enzyme itself is not. The applicability of the kinetic parameters obtained in hexane will then depend of possible differences in solvent-enzyme interactions.

Regarding intraparticle diffusion, the elimination of hexane from the mixture and the increase in the reactants concentrations are expected to impact the intraparticle diffusion coefficients and, hence, the diffusion rates. Prior to the beginning of the reaction, the reaction medium consists of a binary mixture of vinyl acetate and decanol; as the reaction proceeds and decyl acetate is formed, a ternary mixture is obtained. Closer to the end of the reaction, the diffusion coefficients of both reactants should approximate the ones obtained in infinite dilution in decyl acetate.

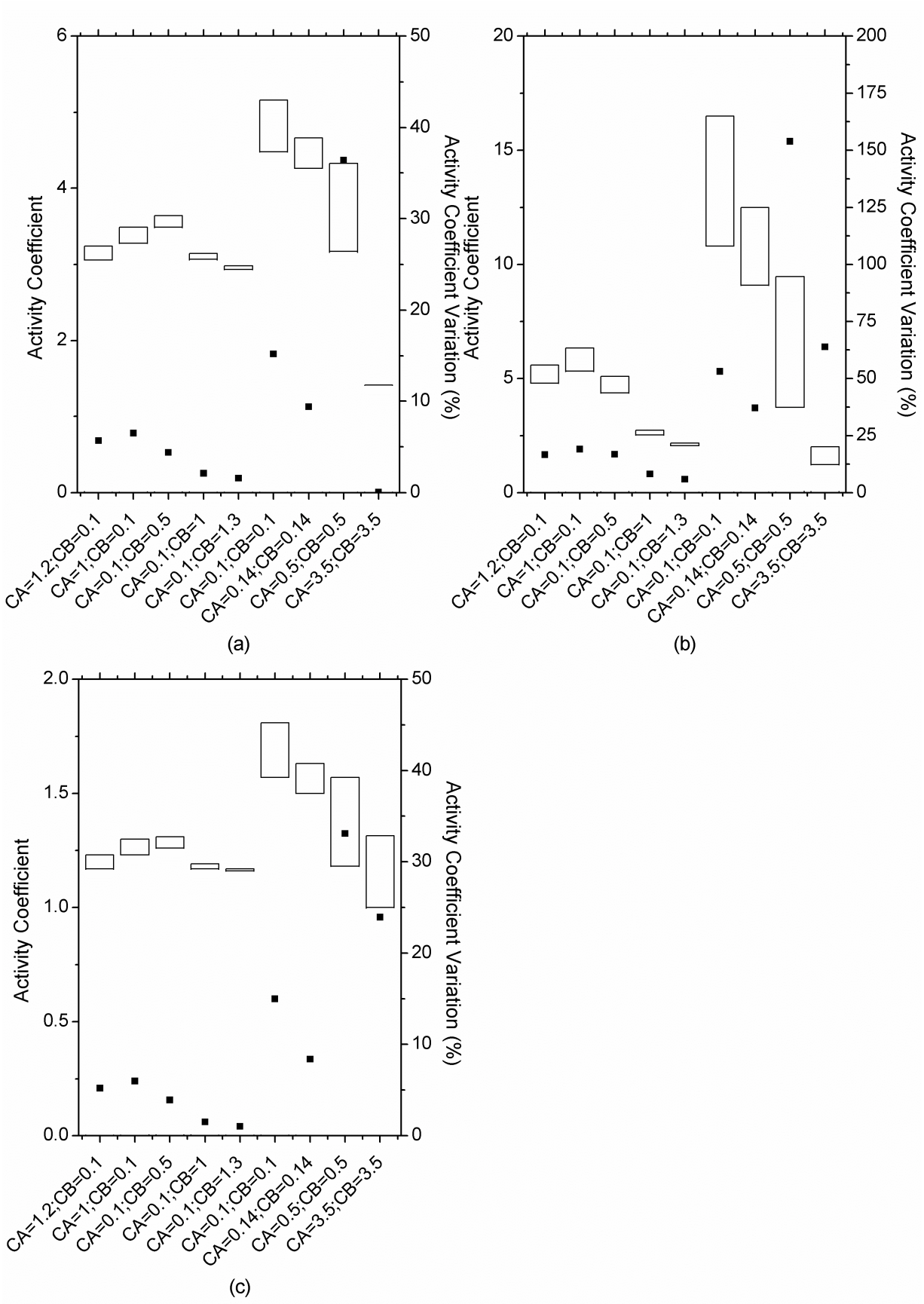


Figure 4.7. Initial and final activity coefficient (bars) and percentage variation (■) throughout the reaction for several sets of initial conditions **(a)** vinyl acetate **(b)** decanol **(c)** decyl acetate.

The Wilke-Chang method, described in Appendix C, was used to calculate the binary diffusion coefficients of vinyl acetate in decanol in infinite dilution and vice-versa, and the binary diffusion coefficients of each reactant in decyl acetate. The correction proposed by Vignes was then used to estimate the binary diffusion coefficients for an equimolar mixture of vinyl acetate and decanol, corresponding to the beginning of the reaction. As in the previous chapter, a tortuosity factor of 2 is assumed. Table 4.4 presents the obtained pore diffusion coefficients. Since temperature effects are likely to occur, the diffusion coefficients were estimated for a higher temperature as well.

Table 4.4. Diffusion coefficients of the reactants in solvent free operation and in decyl acetate

Pore diffusion coefficients	T=30ºC	T=40ºC	
Vinyl Acetate			
$D_P^{0.5}{}_{\text{vinyl acetate/decanol}}$	3.11×10^{-6}	4.02×10^{-6}	Beginning of reaction
$D_P^{0}{}_{\text{vinyl acetate/decyl acetate}}$	4.49×10^{-6}	5.58×10^{-6}	End of reaction
Decanol			
$D_P^{0.5}{}_{\text{decanol/vinyl acetate}}$	3.11×10^{-6}	4.02×10^{-6}	Beginning of reaction
$D_P^{0}{}_{\text{decanol/decyl acetate}}$	2.65×10^{-6}	3.30×10^{-6}	End of reaction

The obtained intraparticle diffusion coefficients are one order of magnitude below the ones obtained in hexane, indicating that diffusion should be slower than in the previously addressed case. The diffusion coefficients in the beginning and end of the reaction present similar values; given the high concentration differences throughout the course of the reaction their precise variation with the composition of the medium should be determined by a more complex method, such as the Maxwell-Stefan model (Cussler 1997). Since the values obtained for the initial and final stages of the reaction are of the same order of magnitude, for simulation purposes, the intraparticle diffusion coefficients will be considered independent of the composition of the medium and the average value between the beginning and the end of the reaction will be used. Regarding the effect of temperature, a 10 ºC temperature rise slightly increases the intraparticle diffusion coefficients but does not change their order of magnitude, hence, the intraparticle diffusion coefficients will be considered constant in this temperature range. Since the intrinsic reaction rate is expected to be higher and the diffusion

coefficients lower, internal diffusion limitations are expected to be present in the solvent free system as well.

In order to experimentally test the possibility of a solvent free operation and to analyse the behaviour of the system in these conditions, additional experiments were performed in a batch reactor. An equimolar mixture of vinyl acetate and decanol should lead to a concentration of 3.5 M. The experiments were performed with an initial concentration of 3.4 M because n-decane was used as an internal standard for the chromatographic analysis. Since at such high concentration, the samples would saturate the chromatograph detector, each sample was priorly diluted with n-hexane and an internal standard was added to the reaction mixture to account for experimental variations in the preparation of the sample.

These experiments were performed with catalyst particles from a different production batch, accordingly, the procedure used to describe the catalyst used in terms of particle size and enzyme load was repeated for the new batch. The enzyme particles were divided in groups according to particle size, and the specific enzyme load was determined by a modified Lowry method (described in Appendix A). Table 4.5 presents the different particle size groups and the obtained enzyme load.

Table 4.5. Specific enzyme content for Novozym 435 particles of different sizes.

Average Particle Size (μm)	**Enzyme Load ($g_{enzyme}/g_{particle}$)**
589	0.054
463	0.062
324	0.084
274	0.089

As for the previously used catalyst particles, Equation (2.13) was then used to estimate the thickness of the enzyme shell for the new production batch and a value of c.a. 60μm was obtained, indicating that the enzyme is located in a thinner shell when compared to the Novozym 435 particles used so far. The value of 60 μm will be used in all subsequent simulations.

As the reaction conditions were changed significantly from the previous experiments performed in a batch reactor it is necessary to re-evaluate the influence of diffusion limitations. Hence, firstly, several experiments were performed with different agitation speed. The obtained results are presented in Figure 4.8, together with results obtained by simulation.

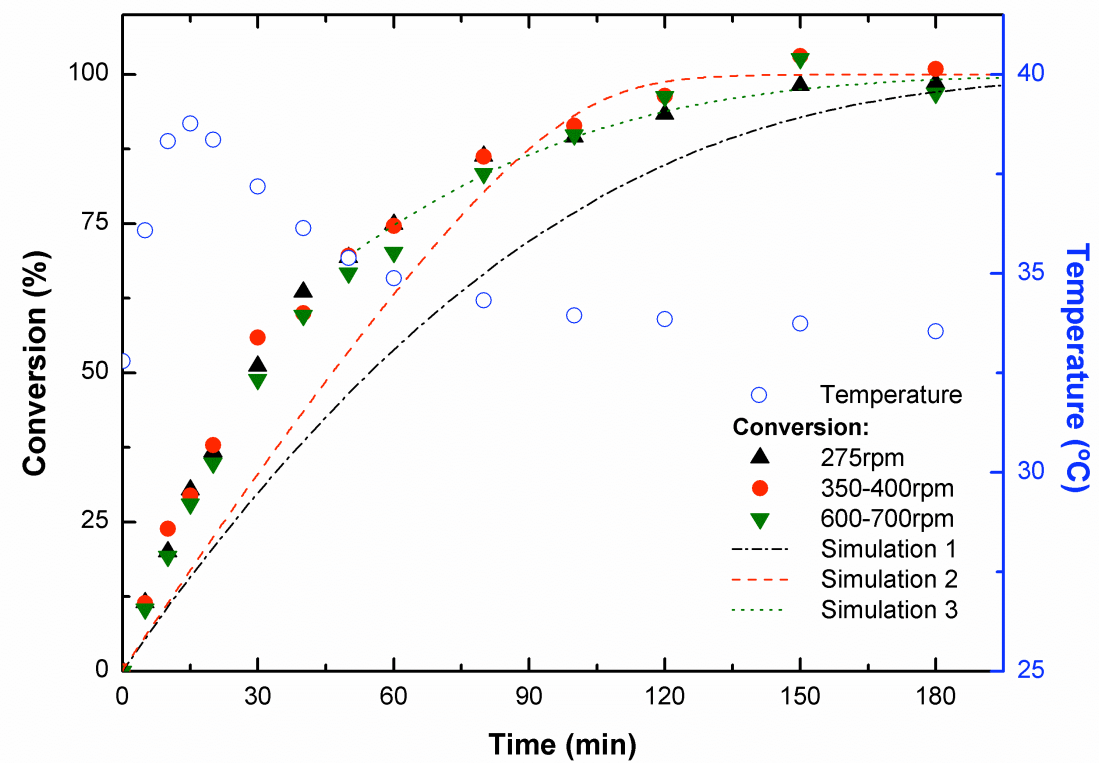


Figure 4.8. Conversion and temperature as a function of time. [A]=[B]=3.4 M, W_{Enzyme}=0.15 mg_{Enzyme}/mL and d_p=463 μm for all essays. Simulation 1: simulation with internal diffusion limitations; Simulation 2: simulation without internal diffusion limitations; Simulation 3: partial simulation starting at 69.5% conversion.

The enzyme is still active in the solvent free system. Compared to the results obtained in n-hexane, for a concentration of 0.1 M of vinyl acetate and decanol the increase in the initial reaction rate is higher than the prediction based only in the reaction rate equation and consequently, by the batch reactor model presented in the previous chapter (simulation 1).

A sharp temperature rise was verified in the initial stage of the reaction, reaching a value of approximately 40 ºC, followed by a slower decrease until it returned to its initial value. It is well established that CAL B presents good thermal stability, particularly in an immobilized form (Hari Krishna and Karanth 2001; Kirk and Christensen 2002; Yadav and Devi 2004; Yadav and Lathi 2004). Novozym 435 was reported to be stable up to 60 ºC, with an increase of the observable reaction rate with temperature (Hari Krishna and Karanth 2001; Kirk and Christensen 2002; Yadav and Devi 2004; Yadav and Lathi 2004). The measured temperature

increase is thus expected to lead to higher reaction rates, contributing to the observed differences.

As the mass transfer coefficients were estimated, a simulation without internal diffusion limitations was performed to test if higher diffusion coefficients could lead to the reaction rate obtained experimentally (simulation 2). As can be seen in Figure 4.8, the initial reaction rate obtained experimentally is still higher than the reaction rate predicted by the model in the absence of diffusion limitations, ruling out mass transfer, as the main cause of this difference.

If the observed differences between the experimental data and the simulations are caused by a temperature induced enhancement of the reaction rate, the model should be able to describe the system at later stages of the reaction, provided that the temperature is close enough to 30 ºC to allow the applicability of the kinetic parameters obtained in hexane. Thus, an additional simulation was performed starting from the composition obtained at a reaction time of 50 min, when the temperature is already decreasing to its initial value (simulation 3). The results obtained in this way are in agreement with the experimental data, supporting that the differences between the experimental results and the simulations are caused by the increase in temperature in the initial stages of the reactions and that, provided that the temperature is the same for which the kinetic parameters were obtained. To accurately account for these temperature effects, further studies would be necessary to determine the dependence of the rate constants with temperature and an energy balance should be included to determine the variation of temperature with time.

In addition to the temperate effects, it is possible that enzyme-reaction medium interactions may also contribute to the differences between the simulations and the experimentally obtained data. For this to be the case, given the good agreement between simulation 3 and the experimental data, enzyme-reaction medium interactions should vary significantly with the composition of the medium. Analyzing the variation of the activity coefficients of all species in solution with the course of the reaction, presented in Figure 4.3, it seems unlikely that the behavior of the species in solution change significantly in a way that could justify such differences reaction rate. Temperature is thus expected to be the main factor contributing to the enhancement of reaction rate.

Following the evaluation of external mass transfer limitations, additional experiments were performed with particles of different sizes, to evaluate the influence of internal diffusion limitations. The obtained results are presented in Figure 4.9.

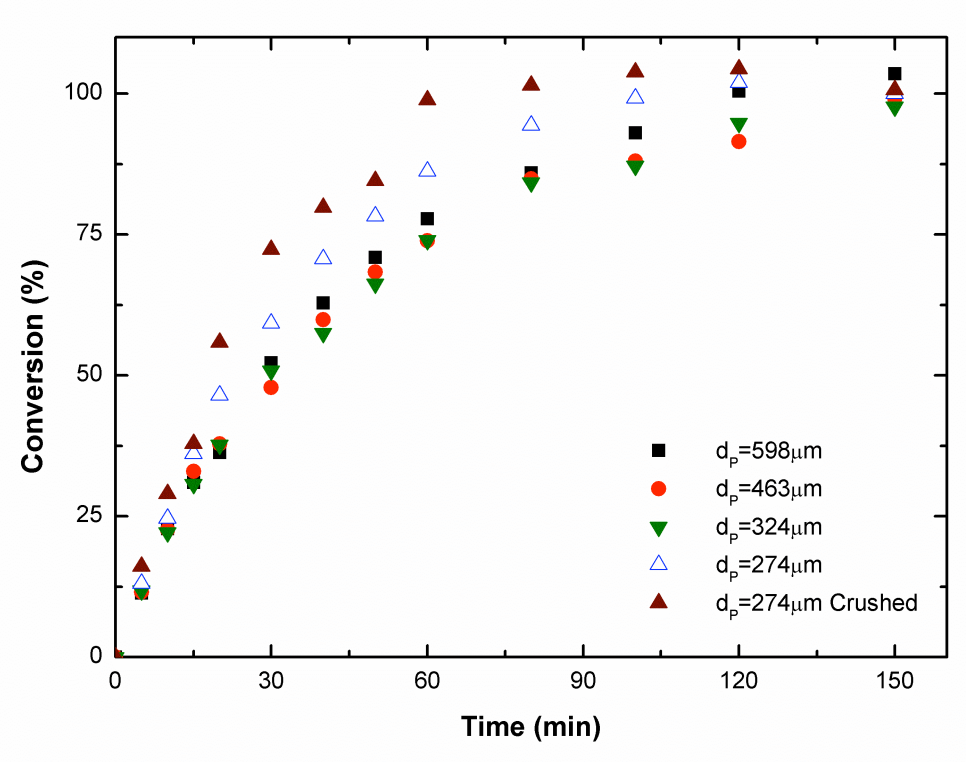


Figure 4.9. Effect of particle diameter on the reactants conversion as a function of time. Reaction conditions: [A]=[B]=3.4 M, W_{Enzyme}=0.15 mg_{Enzyme}/mL and $T_{initial}$=30 ºC for all assays.

The dependence of the reaction rate with the particle size is in accordance with the results obtained in hexane and presented in section 2 (Figure 2.5). Again, the presence of internal diffusion limitations is not noticeable for larger particle sizes, but is clear for sufficiently small particle diameters, particularly for crushed particles. This effect is further clarified in Figure 4.10 by means of the initial reaction rate.

The results presented above indicate that solvent free operation is possible without noticeable negative impact in enzyme activity and reaction rate. Nevertheless, further studies should be conducted to evaluate the impact of eliminating hexane as a solvent on catalyst stability, since it is known that the reaction medium can have an impact on the enzyme stability (Klibanov 2001).

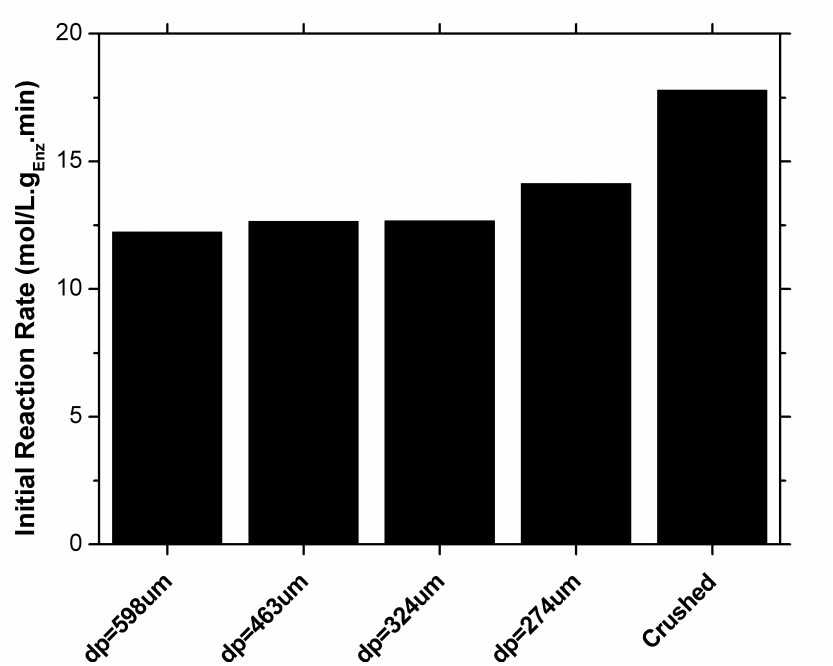


Figure 4.10. Effect of particle diameter on the initial reaction rate. Reaction conditions: [A]=[B]=3.4 M, W_{Enzyme}=0.15 mg_{Enzyme}/mL and $T_{initial}$=30 ºC for all assays.

4.5 CONCLUSIONS

A model for a packed bed reactor performing the transesterification of vinyl acetate with decanol in n-hexane, catalyzed by Novozym 435 (*Candida antarctica* lipase B) was developed. The model was based on the batch reactor model presented in the previous section and includes the effect of internal and external mass transfer resistances, the heterogeneous intraparticle distribution of the enzyme and the thermodynamic non-ideality of the reaction mixture, by using an activity based kinetic equation. The model does not account for axial and radial dispersion, and pressure drop along the reactor and the plug flow mechanism is assumed.

Considering the ping-pong bi-bi kinetic mechanism and an egg-shell intraparticle enzyme distribution, the model presents 10 dimensionless parameters:

- 2 B_{im}, accounting for the competition between the film and intraparticle diffusion of each substrate;

- 2 Thiele modulus to account for the competition between the reaction phenomenon and the intraparticle diffusion of both reagents;
- The ratio of diffusion time constants $\frac{\tau_{d1}}{\tau_{d2}}$ accounting for possibly different diffusion rates of both substrates;
- The space time τ;
- the dimensional radial position of the inner boundary of the egg-shell, x_i;
- The dimensionless kinetic constants $K_{M0A,}$ K_{M0B} and K_{I0}/K_{M0A}

Several experiments were performed in a packed reactor. The steady state conversion was measured for different flow rates and was in good agreement with the model's predictions. Contrary to the case of the batch reactor, where agitation is simple to induce, external diffusion limitations were present in the packed bed reactor due to the low flow rates used. The film diffusion coefficients to account for this phenomenon were estimated through the Ranz-Marshall correlation.

The reactor operated for 26 consecutive hours without any measurable loss in enzyme activity. These results are in accordance with previous findings of other authors and indicate that Novozym 435 is a stable biocatalyst under the reaction conditions used (30 ºC, 0.1 M of each reactant in hexane).

From a commercial point of view, operating without solvent constitutes a very interesting alternative, since it eliminates the necessity of downstream separation processes. Thus, additional experiments were performed in a batch reactor with an equimolar mixture of vinyl acetate and decanol, without any solvent. There were no evidences of a reduction in enzyme activity in the absence of hexane. A temperature increase of 10 ºC was obtained in the initial stage of the reaction, caused by its exothermic nature. Internal diffusion limitations were shown to exist in solvent free as well, and the same behavior presented in section 2 was verified; the results obtained with catalyst particles of different sizes once again show that the presence of internal mass transfer limitations is not detected with larger particle sizes, but become evident if the particle size is sufficiently reduced.

In terms or reactor modeling, due to the increased concentration of the reactants in solvent free operation, the applicability of the developed model was in this case limited by the temperature increase verified due to the exothermic nature of the reaction. The model was nevertheless able to describe the reaction course once the temperature of the reaction medium

returned to values close to 30 ºC, indicating that the activity based kinetic equation used is applicable even in the absence of hexane. This indicates that enzyme-reaction medium interactions are similar in both systems. Since the activity coefficients of vinyl acetate and decanol and lower than the ones obtained in the experiments performed in hexane, a concentration based kinetic equation with kinetic parameters determined in hexane would fail to describe the solvent free system, further confirming the potential of this approach.

Thus, in order for the developed model to be fully applicable to the solvent free system further studies to determine the dependence of the rate constants with temperature are required and an energy balance equation must be included to predict the temperature profiles.

4.6 NOMENCLATURE

[i]	Concentration of component i (M)
A	Vinyl acetate
B	Decanol
Bi_m	Biot number for mass transfer
$C_{exit}^{Product}$	Concentration of decyl acetate in the outlet of the reactor (M)
C_i	Concentration of component i in the bulk phase (M)
c_i	Intraparticle concentration of component i (M)
De	Effective diffusivity (cm^2/s)
Dm	Molecular diffusivity (cm^2/s)
d_p	Particle diameter (μm)
D_P	Pore diffusivity (cm^2/s)
$D_P{}^0{}_{AB}$	Pore diffusivity of component A in component B at infinite dilution (cm^2/s)
$D_P{}^{0.5}{}_{AB}$	Pore diffusivity of component A in component B at a mole fraction of 0.5 (cm^2/s)
dT	Packed bed reactor diameter (mm)
F_i	Dimensionless concentration of component i in the bulk phase
f_i	Dimensionless intraparticle concentration of component i
k_f	Mass transfer coefficient between the liquid and the catalyst surface (cm/s)
K_I	Competitive inhibition constant (M)
K_{I0}	Dimensionless competitive inhibition constant
K_{Mi}	Michaelis constant for substrate i (M)

K_{Mi0}	Dimensionless Michaelis constant for substrate i
L	length of the packed bed reactor (mm)
L	longitudinal position in the reactor (mm)
P	preassure (bar)
Peax	Peclet number for axial dispersion
Q	Flow rate (mL/min)
R	Radial intraparticle position (μm)
R	Reaction rate (mol/g_{enzyme}.min)
Re_P	Reynolds number for packed beds based on particle diameter
Re_{P*}	Reynolds number based on particle diameter
R_p	Particle radius (μm)
R_T	Packed bed reactor radius (mm)
Sc	Schmidt number
Sh	Sherwood number
T	Temperature (ºC)
t	Time (min)
u	velocity (m/min)
$\bar{u}$	average velocity (m/min)
u_S	Superficial velocity (m/min)
V_{max}	Maximum forward reaction rate (mol/g_{Enzyme}.min)
VP	Volumetric productivity (mol/Lreactor.hr)
$V_{Reactor}$	Reactor volume (L)
W_E	Specific enzyme loading ($g_{Enzyme}/g_{catalyst\ particles}$)
$W_E(r)$	Enzyme intraparticle distribution function ($g_{Enzyme}/g_{catalyst\ particles}$)
x	Dimensionless radial position
X_i	Conversion of component i (%)

Greek Symbols

γ_i	Activity coefficient of the component i
ε_B	Bulk porosity ($cm^3_{pores}/cm^3_{Reactor}$)
ε_P	Particle porosity ($cm^3_{pores}/cm^3_{particle}$)
θ	Dimensionless time
μ_f	Fluid viscosity (Pa.s)
ρ_B	Bulk density ($g/cm^3_{Reactor}$)

ρ_f	Fluid density (g/cm^3)
ρ_{app}	Apparent density (g/cm$^3_{particle}$)
τ	Space time (min)
τ_D	Internal diffusion time constant (s)
ϕ	Thiele modulus

Subscripts

1	Vinyl Acetate
2	Decanol
A	Vinyl Acetate
B	Decanol

Superscripts

0	Initial

4.7 BIBLIOGRAPHY

Bird, R. B., Stewart, W. E. and Lightfoot, E., N. (2001). Transport phenomena (Second Edition). John Wiley & Sons.

Carberry, J. J. (1976). Chemical and catalytic reaction engineering, McGraw-Hill.

Cussler, E. L. (1997). Diffusion: mass transfer in fluid systems (Second edition). Cambridge University Press.

Froment, G. F. and Bischoff, K. B. (1990). Chemical reactor analysis and design (Second Edition). New York, John Wiley and Sons.

Ghamgui, H., Karra-Chaabouni, M. and Gargouri, Y. (2004). 1-Butyl oleate synthesis by immobilized lipase from *Rhizopus oryzae:* a comparative study between n-hexane and solvent-free system. Enzyme Microb. Technol. 35: 355-363.

Hari Krishna, S. and Karanth, N. G. (2001). Lipase-catalyzed synthesis of isoamyl butyrate - A kinetic study. Biochim. Biophys. Acta (BBA)/Protein Structure and Molecular Enzymology 1477 (2): 262-267.

Hazarika, S., Goswami, P., Dutta, N. N. and Hazarika, A. K. (2002). Ethyl oleate synthesis by Porcine pancreatic lipase in organic solvents. Chemical Engineering Journal 1 (15): 61-68.

Kirk, O. and Christensen, M. W. (2002). Lipases from *Candida antarctica*: unique biocatalysts from a unique origin. Organic Process Research & Development 6: 446-451.

Klibanov, A. M. (2001). Improving enzymes by using them in organic solvents. Nature 409: 241-246.

Ranz, W. E. and Marshall, W. R. (1952). Evaporation from drops. Chemical Engineering Progress 48: 141-146, 173-178.

Sandoval, G. C., Marty, A. and Condoret, J.-S. (2001). Thermodynamic activity-based enzyme kinetics: Efficient tool for nonaqueous enzymology. AIChE Journal 47 (3): 718-726.

Straathof, A. J. J., Panke, S. and Schmid, A. (2002). The production of fine chemicals by biotransformations. Current Opinion in Biotechnology 13 (6): 548-556.

Straathof, A. J. J., Rakels, J. L. L. and Heijnen, J. J. (1992). Enzyme kinetics in monophasic and biphasic aqueous-organic systems, in J. Tramper, Vermue, M. H., Beeftink, H. H. and Stockar, U. v., Eds. Enzyme kinetics in monophasic and biphasic aqueous-organic systems. Biocatalysis in Non-Conventional Media. Amstedam, Elsevier.

van Tol, J. B. A., Jongejan, J. A., Duine, J. A., Kierkels, H. G. T., Gelade, E. F. T., Mosterd, F., van der Tweel, J. J. and Kamphuis, J. (1995). Thermodynamic and kinetic parameters of lipase-catalyzed eater hydrolysis in biphasic systems with varying organic solvents. Biotechnology and Bioengineering 48 (3): 179-189.

Wilhelm, R. H. (1962). Progress towards the a priori design of chemical reactors. Pure and Applied Chemistry 5 (3-4): 403-422.

Yadav, G. D. and Devi, K. M. (2004). Immobilized lipase-catalysed esterification and transesterification reactions in non-aqueous media for the synthesis of tetrahydrofurfuryl butyrate: comparison and kinetic modeling. Chemical Engineering Science 59: 373-383.

Yadav, G. D. and Lathi, P. S. (2004). Synthesis of citronellol laurate in organic media catalyzed by immobilized lipases: kinetic studies. J. Mol. Catal. B: Enzym. 27 (2-3): 113-119.

Yadav, G. D. and Trivedi, A. H. (2003). Kinetic modeling of immobilized-lipase catalyzed transesterification of n-octanol with vinyl acetate in non-aqueous media. Enzyme Microb. Technol. 32 (7): 783-789.

5. CONCLUSIONS AND FUTURE WORK

The transesterification of vinyl acetate and decanol in hexane catalyzed by Novozym 435 was shown to follow a Ping-pong bi-bi kinetic mechanism with competitive inhibition by decanol.

The determination of the enzyme content Novozym 435 particles of different sizes revealed that smaller particles have higher specific enzyme content ($g_{Enzyme}/g_{Particle}$), which should be taken into account when analyzing data obtained with particles of different sizes. Furthermore, the specific enzyme loading of the different particle sizes are consistent with an egg-shell distribution, with an enzyme outer layer of c.a. 80 μm for one production lot and 60 μm for a different one.

Experiments performed in a batch reactor with catalyst particles of different sizes showed that internal diffusion limitations exist, while the influence of external limitations was eliminated through stirring. The egg-shell distribution of the enzyme inside the particles seems to influence the results obtained with different particle sizes but the influence of internal diffusion limitations is particularly visible the particle size approaches that of the enzyme layer or the particles are crushed.

The intrinsic kinetic parameters of the reaction were calculated, according to a Ping-pong bi-bi kinetic model with competitive inhibition by the alcohol. The determination was based on experiments performed with crushed particles to eliminate the influence of internal diffusion limitations. Since Vinyl acetate was used as a reactant, and the corresponding product, vinyl alcohol, tautomerizes to acetaldehyde, the rate equation typically used for initial reaction rates was able to describe the entire course of the reaction. An activity based kinetic equation had to be used to describe the whole range of concentrations tested (0.1-1.25 M of each reactant), as the activity coefficients of both substrates vary significantly over this range of compositions. The activity coefficients were calculated by the Modified UNIFAC Model of Dortmund.

A model for a batch reactor performing the transesterification of vinyl acetate with decanol in n-hexane, catalyzed by Novozym 435 (*Candida antarctica* lipase B) was developed. The model included the effect of internal and external mass transfer resistances, the heterogeneous intraparticle distribution of the enzyme and the thermodynamic non-ideality of the reaction mixture, by using an activity based kinetic equation. The model was able to success-

fully predict the results obtained with Novozym 435 particles of different sizes and different initial concentrations of both substrates without fitting any parameter.

A steady state model based on the same assumptions of the previous one was developed in order to analyze the influence of the model parameters in the effectiveness factor as well as the effect of different intraparticle distributions. In general, the typical dependency of the effectiveness factor with the Thiele modulus was found, but the range of values of the Thiele modulus that influence the outcome of the process is higher than usual and depends on the dimensionless kinetic parameters. In the Thiele modulus, a simplified characteristic reaction rate is used that overestimates the actual reaction rate. Accordingly, all changes in the dimensionless kinetic parameters that change the reaction rate in a way that is not accounted for in the Thiele modulus definition change the range of influence of this parameter. Effectiveness factors higher than one may arise if very specific conditions are met. The competitive inhibition by the alcohol must be strong enough, translated by a low K_{I0}/K_{M0A}; and its diffusion must be slower than the diffusion of the ester.

Regarding the enzyme distribution, it was shown that for the transesterification of vinyl acetate and decanol, the observable reaction rate is favored by distributions that place the enzyme closer to the surface.

A model for a packed bed reactor performing the transesterification of vinyl acetate with decanol in n-hexane, catalyzed by Novozym 435 (*Candida antarctica* lipase B) was developed. The model accounts for internal and external mass transfer resistances, the heterogeneous intraparticle distribution of the enzyme and the thermodynamic non-ideality of the reaction mixture. The model does not account for axial and radial dispersion, and pressure drop along the reactor and the plug flow mechanism is assumed.

Several experiments were performed in a packed reactor which was operated continuously for 26 consecutive hours without any measurable loss in enzyme activity. The steady state conversion was measured for different flow rates and was in good agreement with the model's predictions. Contrary to the case of the batch reactor, where agitation is simple to induce, external diffusion limitations were present in the packed bed reactor due to the low flow rates used. The film diffusion coefficients to account for this phenomenon were estimated through the Ranz-Marshall correlation.

Additional experiments were performed without solvent in a batch reactor with an equimolar mixture of vinyl acetate and decanol. No evidences of a reduction in enzyme activity were found when compared to the results obtained in hexane but a temperature increase of 10 ºC was obtained in the initial stage of the reaction. As in hexane, intraparticle diffusion

limitations were found to exist and similar results were obtained when using particles of different sizes.

The applicability of the developed batch reactor model was in this case limited by the temperature increase obtained in the initial stage of the reaction. The model was nevertheless able to describe the reaction course once the temperature of the reaction medium returned to values close to 30 ºC, indicating that the activity based kinetic equation used should be applicable even in the absence of hexane. This indicates that enzyme-reaction medium interactions are similar in both systems. Since the activity coefficients of vinyl acetate and decanol are lower than the ones obtained in the experiments performed in hexane, a concentration based kinetic equation with kinetic parameters determined in hexane would fail to describe the solvent free system, further confirming the potential of this approach.

In terms of future work, the suggestions can be divided in 3 major areas:

- Influence of reaction medium
- Target product
- Reactor modeling

In terms of reaction medium, further studies should be conducted in a solvent free system, which is of major commercial importance. Since the concept was shown to work, particular focus should be given to the enzyme stability in such system.

For further know-how development and to evaluate the boundaries of the thermodynamic activity based kinetic equations, different solvents (with different polarities) should be tested as well.

After studying and modelling the production of long chain esters, it is suggested that attention should be paid to enantioselective esterification processes, for example to produce drugs or drug precursors for the pharmaceutical industry, given the high market value of such products.

In terms reactor modelling, for the present system, the dependency of the kinetic parameters with temperature should be determined, to attempt to fully describe the solvent free system.

The study and modelling of enzyme deactivation mechanisms, is also an interesting field, as the deactivation is shown to be dependent on temperature and on the reaction medium, but the availability of models to describe the latter is limited.

The inclusion of the influence of the water content of the reaction medium in the reactor model also constitutes an interesting field, as with a reactor model available it's influence in equilibrium (in esterification reaction, for example), reaction rate and enzyme activity can be accounted for separately.

APPENDIXES

A. MODIFIED LOWRY METHOD FOR THE DETERMINATION OF THE CONTENT OF ADSORBED PROTEINS

The original Lowry method is a standard method for quantifying proteins (Lowry et al., 1951). In this method, the Folin-Ciocalteau reagent is reduced by proteins in alkaline solutions, mostly by tyrosine and tryptophan residues, forming a blue copper-protein complex with an absorption peak at 745-750nm. The copper binds to the protein and enables the electron transfer to the Folin-Ciocalteau reagent, particularly in the surroundings of aromatic groups (such as tyrosine and tryptophan).

As the original Lowry method is not suitable for immobilized proteins, the modified Lowry method comprises a preliminary desorption step, as follows:

- 5mg of catalyst particles are placed in an Eppendorf with a punctured lid and 1mL of a 1M NaOH solution is added;
- The Eppendorf is then placed in a 100ºC water bath for 10min. The puncture in the lid prevents the pressure build up during this step;
- Afterwards, the eppendorf is placed on ice for 5min and vortexed;
- The eppendorf is then placed in a centrifuge at 5400rpm for 10min, and then 200µL of the obtained solution are taken into new a new eppendorf.

The enzyme that was previously immobilized is now in this solution. The solution is diluted 1:10 and the conventional Lowry method is then applied:

- 1mL of Lowry reagent is added to 200µL of the solution prepared in the previous step; the obtained solution is vortexed for 5min and left to react for 10min;
- 200 µL of Folin-Ciocalteau reagent is then added to the mixture; the obtained solution is vortexed for 5min and left to react for 30min.
- The absorvance at 750nm is then measured and correlated with the enzyme amount.

A blank essay was prepared in the same way but with 200µL of distilled water instead of the enzyme solution obtained in the desorption step. The calibration curve was obtained with

Bovine Serum Albumin (BSA) solutions of different concentrations (20, 50, 100, 150 e 200 μg/mL). All determinations were performed twice.

The following solutions are used in the method:

a) Solution 1: 3%(w/v) of Na_2CO_3 (Anhydrous) and 0.4%(w/v) of NaOH in water

b) Solution 2: 4% (w/v) aqueous solution of Sodium and Potassium Tartrate;

c) Solution 3: 2% (w/v) aqueous solution of $CuSO_4.5H_2O$;

d) Lowry reagent: in a 25mL volumetric balloon mix 0,25mL of Solution 2 with 0,25mL of Solution 3 and complete to 25mL with solution 1. Solution 2 must be the first one in the balloon to prevent precipitation of copper.

e) Folin-Ciocalteau reagent.

f) BSA aqueous solution (200 μg/mL).

BIBLIOGRAPHY

Lowry OH, Rosenbrough NJ, Farr L, Randal R. 1951. Protein measurement with Folin phenol reagent. Journal of Biological Chemistry 193:265-275.

B. MODIFIED UNIFAC MODEL OF DORTMUND

Activity coefficients can be estimated by several methods. The Modified UNIFAC Model of Dortmund (Gmehling et al., 1993) is a group contribution model that allows a reliable prediction of different thermodynamic properties in wide rages of temperature and composition. Relatively to the original UNIFAC method, this model significantly improves the description of phase equilibria at lower concentrations.

In the Modified UNIFAC, as in the original method, the activity coefficient is obtained from the sum of a combinatorial and a residual part; for a given component i:

$$\ln \gamma_i = \ln \gamma_i^C + \ln \gamma_i^R \tag{B.1}$$

In the modified UNIFAC method the combinatorial term was empirically changed with respect to the original method by the introduction of V_i':

$$\ln \gamma_i^C = 1 - V_i' + \ln V_i' - 5q_i\left(1 - \frac{V_i}{F_i} + \ln \frac{V_i}{F_i}\right) \tag{B.2}$$

with V_i' defined as:

$$V_i' = \frac{r_i^{3/4}}{\sum_j x_j r_j^{3/4}} \tag{B.3}$$

The expressions for V_i and F_i are the same as in the original UNIFAC:

$$V_i = \frac{r_i}{\sum_j x_j r_j} \tag{B.4}$$

$$\mathrm{F_i} = \frac{q_i}{\sum_j x_j q_j} \tag{B.5}$$

The parameters r_i and q_i calculated as follows:

$$\mathrm{r}_i = \sum_k \upsilon_k^{(i)} R_k \tag{B.6}$$

$$\mathrm{q}_i = \sum_k \upsilon_k^{(i)} Q_k \tag{B.7}$$

The residual part was also modified through the introduction of temperature dependent interaction parameters:

$$\Psi_{nm} = \exp\left(- \frac{a_{nm} + b_{nm} T(K) + c_{nm} T(K)^2}{T(k)} \right) \tag{B.8}$$

The residual part is hence defined as:

$$\ln\gamma_{\mathrm{i}}^{\mathrm{R}} = \sum_k \nu_k^{(i)} \left(\ln \Gamma_k - \ln \Gamma_k^{(i)} \right) \tag{B.9}$$

Where the parameters Γ_k, θ_m and X_m are defined as:

$$\ln \Gamma_k = Q_k \left[1 - \ln\left(\sum_m \theta_m \Psi_{mk} \right) - \sum_m \frac{\theta_m \Psi_{km}}{\sum_n \theta_n \Psi_{nm}} \right] \tag{B.10}$$

$$\theta_m = \frac{Q_m X_m}{\sum_n Q_n X_n} \tag{B.11}$$

$$X_m = \frac{\sum_j \nu_m^{(j)} x_j}{\sum_j \sum_n \nu_n^{(j)} x_j} \tag{B.12}$$

This method was then used to calculate the activity coefficients of all species in solution in the reaction media. Tables B.1 and B.2 present the group assignment for each molecule and the respective parameters used for the calculations.

Table B.1. Parameters Rk and Qk for all the groups that constitute the molecules present in the reaction media (Gmehling et al., 1993).

	Group*	**R_k**	**Q_k**
Vinyl Acetate	(1) CH_3COO	1.2700	1.6286
	(1) CH_2=CH	1.2832	1.6016
Decanol	(1) CH_3	0.6325	1.0608
	(9) CH_2	0.6325	0.7081
	(1) OH	1.2302	0.8927
Decyl Acetate	(1) CH_3COO	1.2700	1.6286
	(1) CH_3	0.6325	1.0608
	(9) CH_2	0.6325	0.7081
Hexane	(2) CH_3	0.6325	1.0608
	(4) CH_2	0.6325	0.7081

* (i) number between brackets indicates the number of groups k in the respective molecule

Table B.2. Group interaction parameters (a_{nm}, b_{nm}, c_{nm}) for all the groups that constitute the molecules present in the reaction media (Gmehling et al., 1993).

a_{nm} (K)	CH_3	CH_2	CH_2=CH	CH_3COO	OH
CH_3	0	0	189.66	98.656	277.0
CH_2	0	0	189.66	98.656	277.0
CH_2=CH	-95.418	-95.418	0	980.74	2649.0
CH_3COO	632.22	632.22	-582.82	0	31.40
OH	1606.0	1606.0	1566.0	973.80	0

b_{nm}	CH_3	CH_2	CH_2=CH	CH_3COO	OH
CH_3	0	0	-0.2723	1.9294	-4.674
CH_2	0	0	-0.2723	1.9294	-4.674
CH_2=CH	-0.06171	-0.06171	0	-2.4224	-6.5080
CH_3COO	-3.3912	-3.3912	1.6732	0	1.5380
OH	-4.7460	-4.7460	-5.8090	-5.6330	0

c_{nm} (K^{-1})	CH_3	CH_2	CH_2=CH	CH_3COO	OH
CH_3	0	0	0	-0.003133	0.001551
CH_2	0	0	0	-0.003133	0.001551
CH_2=CH	0	0	0	0	0.004822
CH_3COO	0.003928	0.003928	0	0	-0.004885
OH	0.0009181	0.0009181	0.004822	0.007690	0

NOMENCLATURE

a_i	Activity of component i
a_{nm}	UNIFAC group interaction parameter between groups n and m
b_{nm}	UNIFAC group interaction parameter between groups n and m
c_{nm}	UNIFAC group interaction parameter between groups n and m
F_i	auxiliary property for component i (surface fraction/mole fraction)
q_i	relative van der Waals surface area of molecule i
Q_k	relative van der Waals surface area of structural group k
r_i	relative van der Waals volume of molecule i
R_k	relative van der Waals volume of structural group k
V_i	auxiliary property for component i (volume fraction/mole fraction)
V_i'	empirically modified V_i-value
X_i	group mole fraction of group i
x_i	mole fraction of component i

Greek Symbols

Γ_k	group activity coefficient of group k in the mixture
$\Gamma_k^{(i)}$	group activity coefficient of group k in the pure substance i
γ_i	Activity coefficient of the component i
θ_m	surface fraction of group m
$\nu_k^{(i)}$	number of structural groups of type ***k*** in molecule i
Ψ_{nm}	UNIFAC group interaction parameter between groups n and m

Superscripts

C	Combinatorial
R	Residual

BIBLIOGRAPHY

Gmehling J, Li J, Schiller M. 1993. Modified UNIFAC model. 2. Present parameter matrix and results for different thermodynamic properties. Industrial & Engineering Chemistry Research 32(1):178-193.

C. CALCULATION OF THE DIFFUSION COEFFICIENTS BY THE WILKE-CHANG METHOD

The Wilke-Chang method (Reid et al., 1977) allows the estimation of binary diffusion coefficients at infinite dilution:

$$D_{AB}^{0} = 7.4 \times 10^{-8} \frac{(\phi M_B)^{1/2} T}{\eta_B V_A^{0.6}} \qquad \text{(C.1)}$$

where:

D_{AB}^{0} = Diffusion coefficient of solute A in solvent B at infinite dilution, cm^2/s

M_B = Molecular weight of the solvent (B)

T = Temperature, K

η_B = Viscosity of the solvent, cP

V_A = Molar volume of the solute, evaluated at $T_{b,\,normal}$, cm^3/mol

ϕ = Association factor of the solvent (1, for non-associated solvents such as hexane)

All properties used for the calculation of the diffusion coefficients were obtained in the DIPPR801 database and are presented in Table C. as well as the obtained diffusion coefficients.

Table C.1. Diffusion coefficients in hexane at infinite dilution at 30ºC and the physical properties used for their calculation.

Physical Property	Hexane	Vinyl acetate	Decanol
D_{AB}^{0} **(cm^2/s)**	-	4.6×10^{-5}	2.7×10^{-5}
M_i	86.1772	-	-
$T_{b,normal}$ **(K)**	341.88	497.65	497.65
ρ **(mol/dm^3)**	7.13	10	4.8
V_i **(dm^3/mol)**	0.140	0.0996	0.2394
η_B **(cP)**	0.2846	-	-

The diffusion coefficients calculated by the Wilke-Chang method are recommended to be used for molar fractions up to 0.1, which corresponds in this case to a concentration of around 1M. For more concentrated solutions, Vignes proposes the following correction (Reid et al., 1977):

$$D_{AB} = \left(D^0_{AB}\right)^{x_B} \left(D^0_{BA}\right)^{x_A} \qquad \text{(C.2)}$$

For the range of compositions that was experimentally used, the values of the diffusion coefficients for both vinyl acetate and decanol obtained with Equation (C.2) were not significantly different from the coefficients at infinite dilution and thus, the diffusion coefficients obtained by the Wilke-Chang method were used in all simulations.

NOMENCLATURE

D_{AB}	diffusion coefficient of component A in component B (cm^2/s)
Mi	Molecular weight of component I ($g.mol^{-1}$)
T	Temperature (K)
$T_{b,\ normal}$	Boiling temperature evaluated at normal pressure (K)
V	Molar volume evaluated at $T_{b,\ normal}$ (cm^3/mol)
x_i	mole fraction of component i

Greek Symbols

η	Viscosity (cP)
ρ	density (mol/dm^3)
ϕ	Association factor of the solvent

BIBLIOGRAPHY

Reid RC, Prausnitz JM, Sherwood TK. 1977. The Properties of Gases and Liquids. New York: McGraw-Hill.